AD NUMBER
AD333298
CLASSIFICATION CHANGES
TO: **UNCLASSIFIED**
FROM: **CONFIDENTIAL**
LIMITATION CHANGES
TO: **Approved for public release; distribution is unlimited.**
FROM: **Controlling DoD Organization: Army Biological Labs, Fort Detrick, Frederick, MD.**
AUTHORITY
OSD/WHS ltr dtd 1 Aug 2013; OSD/WHS ltr dtd 1 Aug 2013

#5

~~CONFIDENTIAL~~

AD 333 298

Reproduced by the

ARMED SERVICES TECHNICAL INFORMATION AGENCY
ARLINGTON HALL STATION
ARLINGTON 12, VIRGINIA

~~CONFIDENTIAL~~

12-1

12-M-3148

NOTICE: When government or other drawings, specifications or other data are used for any purpose other than in connection with a definitely related government procurement operation, the U. S. Government thereby incurs no responsibility, nor any obligation whatsoever; and the fact that the Government may have formulated, furnished, or in any way supplied the said drawings, specifications, or other data is not to be regarded by implication or otherwise as in any manner licensing the holder or any other person or corporation, or conveying any rights or permission to manufacture, use or sell any patented invention that may in any way be related thereto.

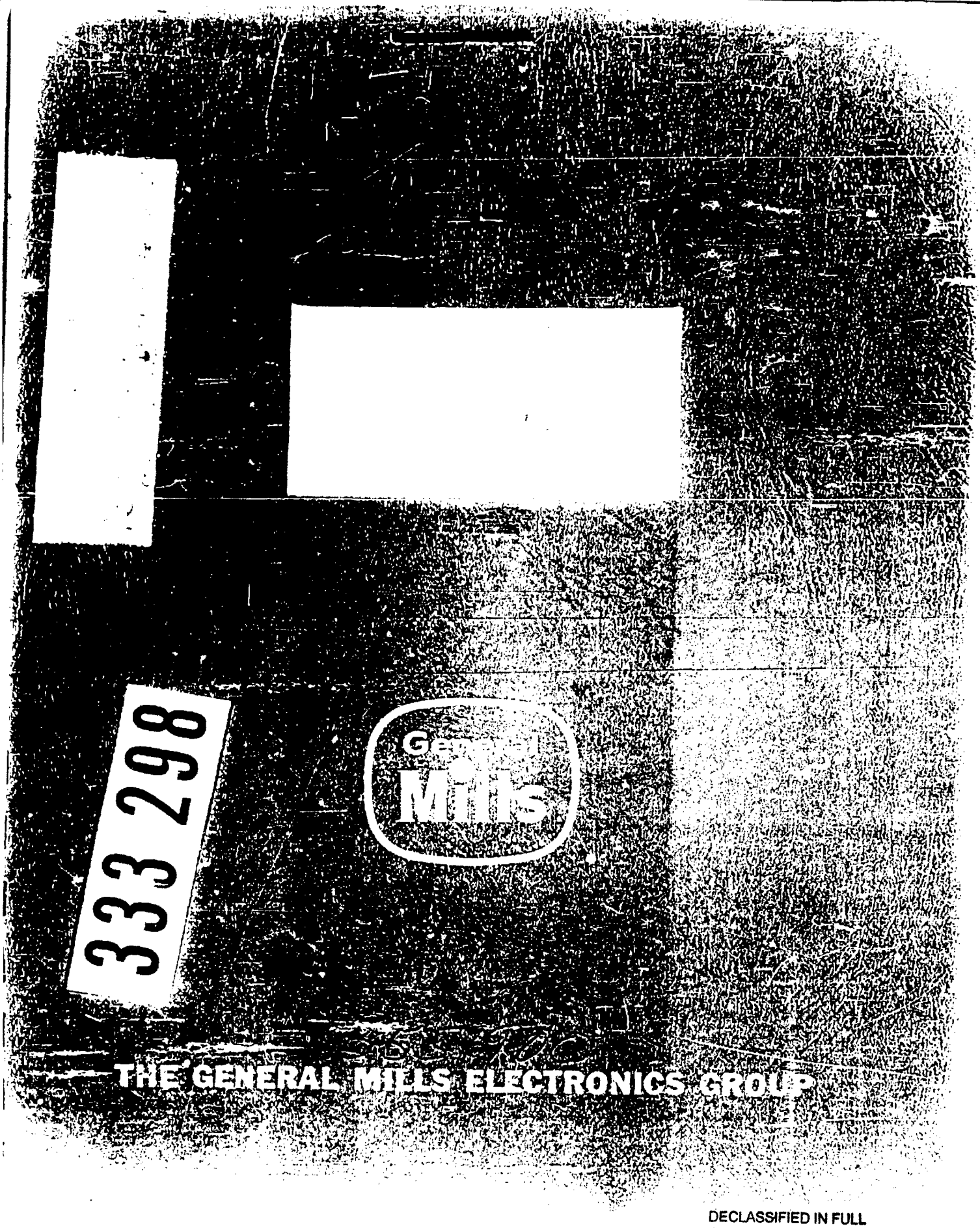

General Mills

[redacted]

ORIGINAL CONTAINS COLOR PLATES; ALL ASTIA REPRODUCTIONS WILL BE IN BLACK AND WHITE. ORIGINAL MAY BE SEEN IN ASTIA HEADQUARTERS.

[redacted]

This document consists of 100 pages and is number 1 of 40 copies, series A, and the following attachments.

NINTH QUARTERLY PROGRESS REPORT

ON

DISSEMINATION OF SOLID AND LIQUID BW AGENTS

(Unclassified Title)

For Period June 4, 1962 – September 4, 1962
Contract No. DA-18-064-CML-2745

Prepared for: [redacted]

U. S. Army Biological Laboratories
Fort Detrick, Maryland

Submitted by: G R Whitnah
G. R. Whitnah
Project Manager

Report No: 2344
Project No: 82408
Date: October 19, 1962

Approved by: S P Jones
S. P. Jones, Director
Aerospace Research

Engineering and Research
2003 East Hennepin Avenue
Minneapolis 13, Minnesota

[redacted]

FOREWORD

Staff members of the Aerospace Research Department and Engineering Department who have participated in directing and performing the work reported herein include Messrs. S. P. Jones, Jr., G. Whitnah, M. Sandgren, A. Anderson, R. Lindquist, J. McGillicuddy, J. Upton, C. Hagberg, W. L. Torgeson, S. Steinberg, P. Stroom, G. Morfitt, J. Walters, A. T. Bauman, T. Petersen, D. Harrington, R. Ackroyd, D. Kedl, B. Schmidt, G. Lunde, R. Dahlberg, R. Kendall, A. Kydd, E. Knutson, J. Ungs, D. Stender, H. Kuhlman, G. Granley, J. Pilney, A. Johnson, and O. Fackler.

ABSTRACT

This Ninth Quarterly Progress Report covers the period from June 4, 1962 to September 4, 1962. Accomplishments are reported in all phases of the research and development program pertaining to the line-source dissemination of BW agents.

Theoretical and experimental results relative to the studies of the mechanics of dry powders are presented for: 1) the applied stresses and energies required for the compaction of powders, 2) shear strength of compacted powders, and 3) bulk tensile strength and bulk density of compacted powders as a function of compressive load and distance from the face of the piston.

Data on aerosol decay as affected by relative humidity are reported for five powders. A statistical analysis of the behavior of aerosols is presented to explain the phenomena observed in the aerophilometer.

Tests on dissemination and deagglomeration, using the wind tunnel, are described which establish an upper limit of approximately 0.58 g/cm^3 density for compacted Sm which can be aerosolized efficiently by the aerodynamic breakup mechanism. A related discussion reports some preliminary data on the effects of storage on the aerodynamic breakup of compacted Sm.

Wind tunnel evaluation of a shroud for the discharge tube of the airborne dry agent disseminator is discussed.

Work with the full-scale experimental equipment for feeding and metering both compacted and uncompacted powder is reported.

Progress is reported on the design and fabrication of the first-generation airborne dry BW agent disseminating store.

An apparatus is described which is used for inserting charges of compacted powder into the experimental model of the dry agent disseminator. Other techniques for filling the disseminator are discussed.

Successful flight tests of the General Mills, Inc. liquid agent disseminating store on F-105 and F-100D airplanes at Eglin Air Force Base are reported.

TABLE OF CONTENTS

[redacted]

TABLE OF CONTENTS (Continued)

[redacted]

LIST OF ILLUSTRATIONS

LIST OF ILLUSTRATIONS (Continued)

[redacted]

LIST OF ILLUSTRATIONS (Continued)

[redacted]

LIST OF ILLUSTRATIONS (Continued)

NINTH QUARTERLY PROGRESS REPORT ON DISSEMINATION OF SOLID AND LIQUID BW AGENTS

1. INTRODUCTION

This Ninth Quarterly Progress Report covers the work accomplished during the three-month period ending approximately September 4, 1962. This work was done at General Mills, Inc. (GMI) under Contract DA-18-064-CML-2745 which is a comprehensive research and development program on the dissemination of solid and liquid BW agents.

This report presents some more of the results of the theoretical and experimental studies of the mechanics of dry powders. The objective of this part of the program is to obtain basic information for application in the engineering development of BW munitions and related support equipment. Progress is also reported on the development of an airborne munition for disseminating dry BW agent from a compacted state. This program has reached the stage where fabrication of the first-generation airborne unit is underway.

Also presented in this report is a brief summary of the results of flight testing the GMI liquid agent disseminating store on the F-105 and F-100D airplanes. These flight tests were conducted by the BW/CW Weapons Group at Eglin Air Force Base, Florida with GMI providing technical assistance. A test report is being prepared by the BW/CW Weapons Group.

2. THEORETICAL AND EXPERIMENTAL STUDIES OF THE MECHANICS OF DRY POWDERS

One of the basic goals of our investigation of the mechanics of powders is the development of means for measuring important physical properties of powdered materials. There are two main areas of interest in regard to the mechanical behavior of powders: 1) the bulk properties and characteristics of powders, which are particularly important with respect to the compaction process, and 2) the aerosolization behavior of compactible powders.

Considerable progress has been made in developing devices and techniques for measurement of the bulk properties of powders. A newly developed technique for precise experimental evaluation of the compaction characteristics of powders is described below. Also, further studies of the shear strength, bulk tensile strength, and bulk density of powders are reported in subsequent sections of this report.

Although the processes of breakup and aerosolization of compacted powders must be closely related to bulk properties, considerable difficulty has been experienced in establishing the nature of this relationship. For this reason, several new concepts are being studied in which pneumatic or hydrodynamic stresses would be employed in experiments to define the mechanical properties of powders. One such approach is discussed in Section 2.2 of this report.

2.1 Experimental Compaction Studies

2.1.1 Apparatus

A study of the compaction characteristics of various powders has been in progress during the past nine months as part of a comprehensive investigation of the mechanical behavior of dry powders. In the course of this work, several devices have been developed for measuring the applied stresses and energies required for compaction of powders; each of these

has been found to be deficient in one or more ways. An improved device for experimental study of the compaction characteristics of powders has been developed during the current report period and has been found to be completely satisfactory. This device is shown in Figure 2.1. It can be seen from the figure that the piston-cylinder configuration utilized in previous compaction devices has been retained in the new design. However, the new compaction unit is much more rigid than earlier models and, through use of an axial-circulating ball bearing for the piston, is less subject to frictional effects.

The material to be compacted is placed in a machined brass receptacle that fits into a recess in the base of the compaction unit, thus insuring proper alinement with the piston.

Tests are carried out by using the compaction unit shown in Figure 2.1 in conjunction with an Instron test machine. By utilizing the Instron machine for control of the sample deformation rate and for measurement and recording of the load applied to the powder, a very high degree of precision and reproducibility can be achieved in compaction experiments.

Compaction tests under controlled humidity conditions may be carried out by enclosing the compaction unit in a sealed plastic bag after prior conditioning of powder and apparatus in a dry box.

2.1.2 Experimental Results and Discussion

A number of experiments have been carried out with the apparatus described above. Because of the preliminary nature of these tests, which were carried out primarily for the purpose of evaluating the new compaction device, no attempt was made to control humidity. (Future tests will be conducted under controlled humidity conditions, as described above.)

A complete load-strain curve for cornstarch, as recorded on the Instron machine, is shown in Figure 2.2. This curve is quite typical of results obtained in tests of several powders. In this test, 0.72 grams of cornstarch

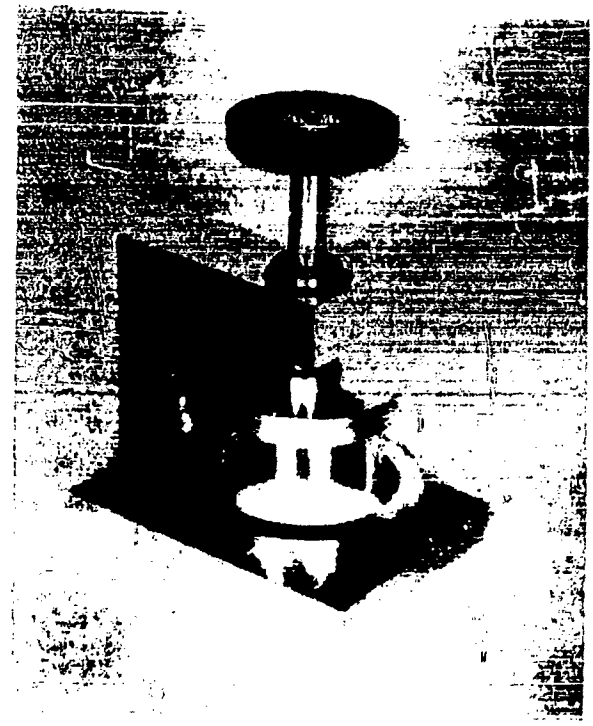

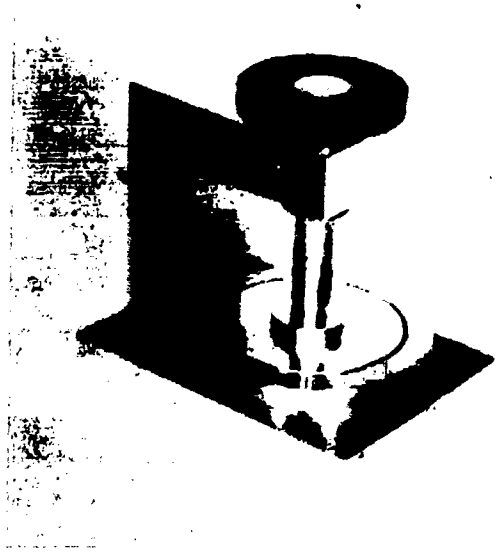

Figure 2.1 Compaction Apparatus

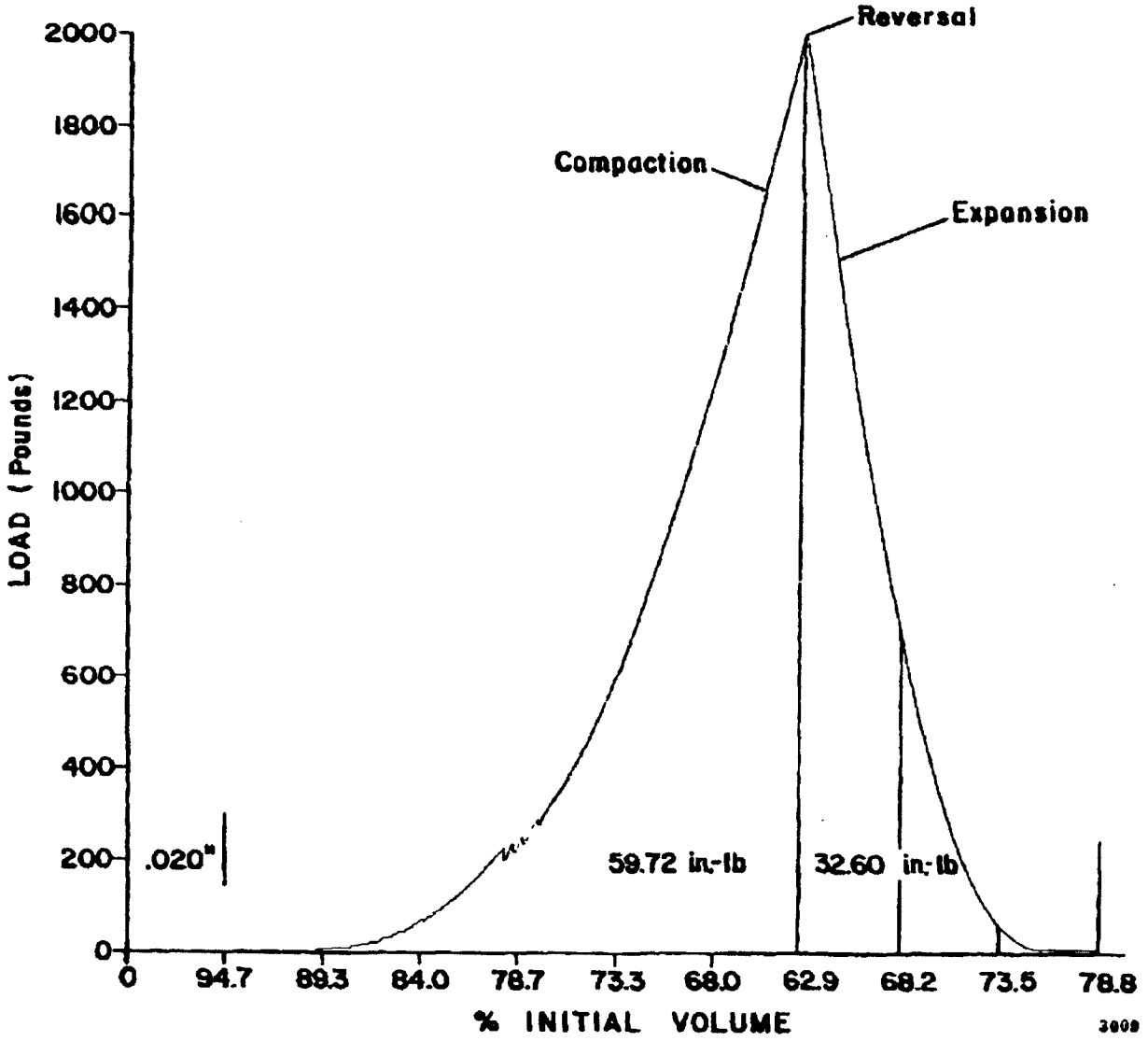

Figure 2.2 Compaction of Cornstarch – Compaction Rate 0.020 in./min, Initial Specific Volume 1.71 cm^3/g

with an initial density of 0.585 g/cm^3 were compacted at a rate of 0.02 in./min until the load reached 2000 pounds; then the cross-head direction was reversed and the elastic recovery of the sample was determined. The area under the compaction portion of the curve represents the total work (or energy) expended in an unidirectional compaction process. The net work absorbed by the powder is found by subtracting the area under the right-hand portion of the curve, which corresponds to the elastic energy stored in the compressed powder sample. In this case, the energy recovered was found to be about 55 percent of the total energy absorbed by the powder during compaction.

Compaction data for talc, saccharin, and cornstarch – as obtained with the new apparatus – are plotted versus specific volume in Figure 2.3. The data are in quite good agreement with previous results for these powders over the range of densities attainable in the earlier tests (see Table 2.1). It can be seen, however, that a considerable departure from the power-law relationship found in past tests occurs under high stresses. It should be emphasized that the high stresses applied to the samples in these tests are well beyond the practicable compaction range for viable materials. It is nevertheless desirable to establish the range of densities for which the empirical power-law relationship

$$\sigma = k \cdot \rho^m \qquad (1)$$

is a valid representation of the relationship between stress and density for compactible materials. The constants k and m in Equation (1), as determined with the new test technique, are presented in Table 2.1, together with constants from previous tests.

Previous experiments with cornstarch and powdered milk indicate that these powders exhibit a "stick-slip" behavior when compacted rapidly. Some evidence of this behavior can be seen in Figure 2.2 (cornstarch) at a load of about 200 pounds. For the most part, however, it is clear that the

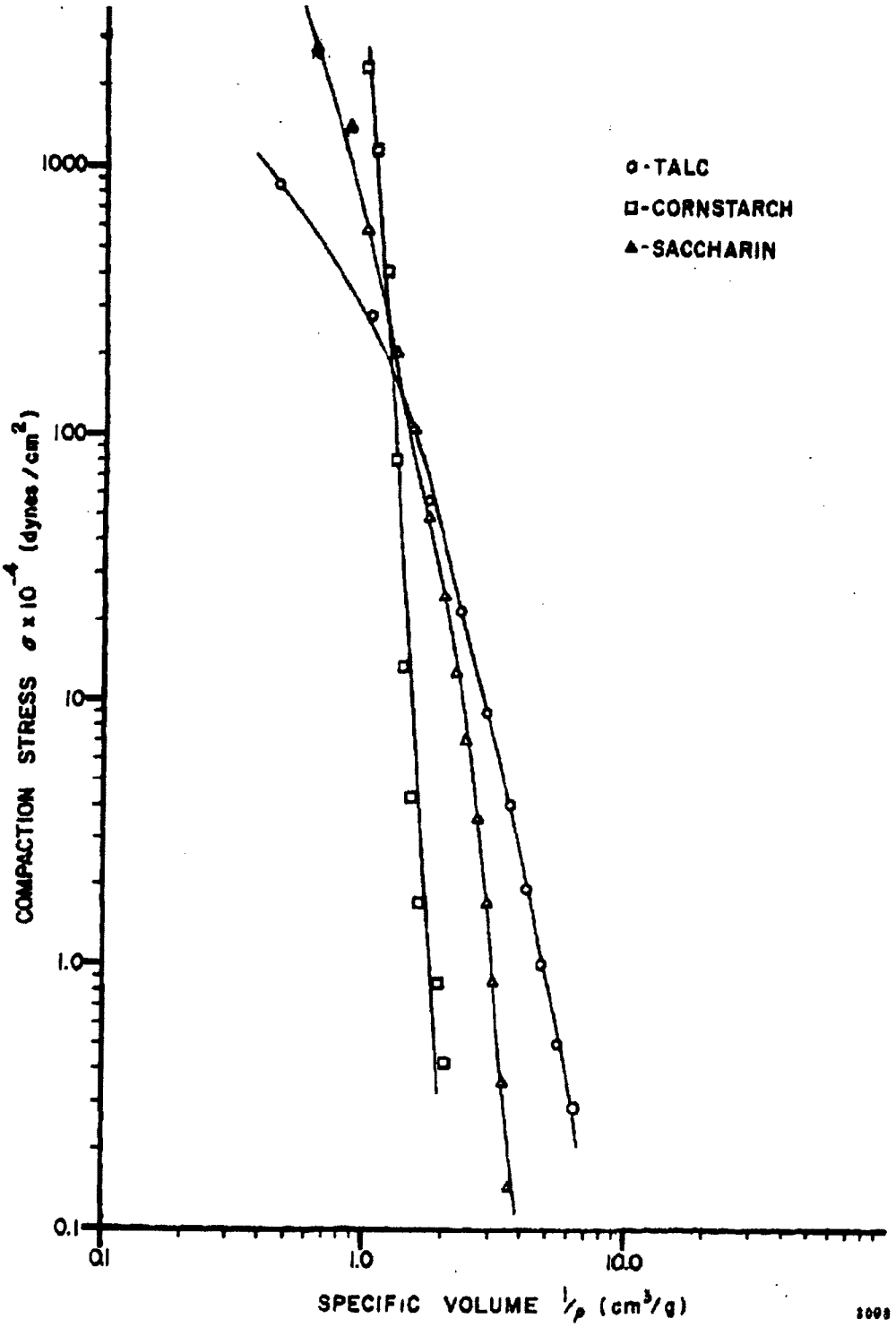

Figure 2.3 Compaction Stress as a Function of Powder Specific Volume-Compaction Rate 0.020 in./min

Table 2.1 Compaction Constants for Three Powders

Powder	m*	m	k*	k
Talc	- 6.50	- 6.75	4.42×10^7	2.35×10^7
Saccharin	- 7.70	- 6.50	2.21×10^7	1.72×10^7
Cornstarch	-20.8	-18.80	1.67×10^8	1.29×10^8

*Indicates previous results.

compaction process for cornstarch is free of irregularities at a compaction rate of 0.02 in./min. On the other hand, tests conducted at a compaction rate of 0.2 in./min for eight powders including cornstarch exhibited much less regular behavior (see Figure 2.4). In these tests, powdered milk and saccharin as well as cornstarch displayed "stick-slip" behavior as can be seen from the figures. These results are presented with reservations, however, since it is possible that the irregularities may in part be due to air entrapment in the samples as a result of the high compaction rate, plus the fact that the piston used in these tests was not vented. Effects of compaction rate will be investigated in future tests with suitable precautions to prevent air entrapment.

2.2 Triaxial Shear Tests

Considerable progress has been made in improving the triaxial technique for determining the shear strength of a compacted powder. As pointed out in the Eighth Quarterly Report[1], the conventional triaxial test method leads to experimental difficulties with compactible materials because the membrane used to seal the powder sample prevents a natural shear failure

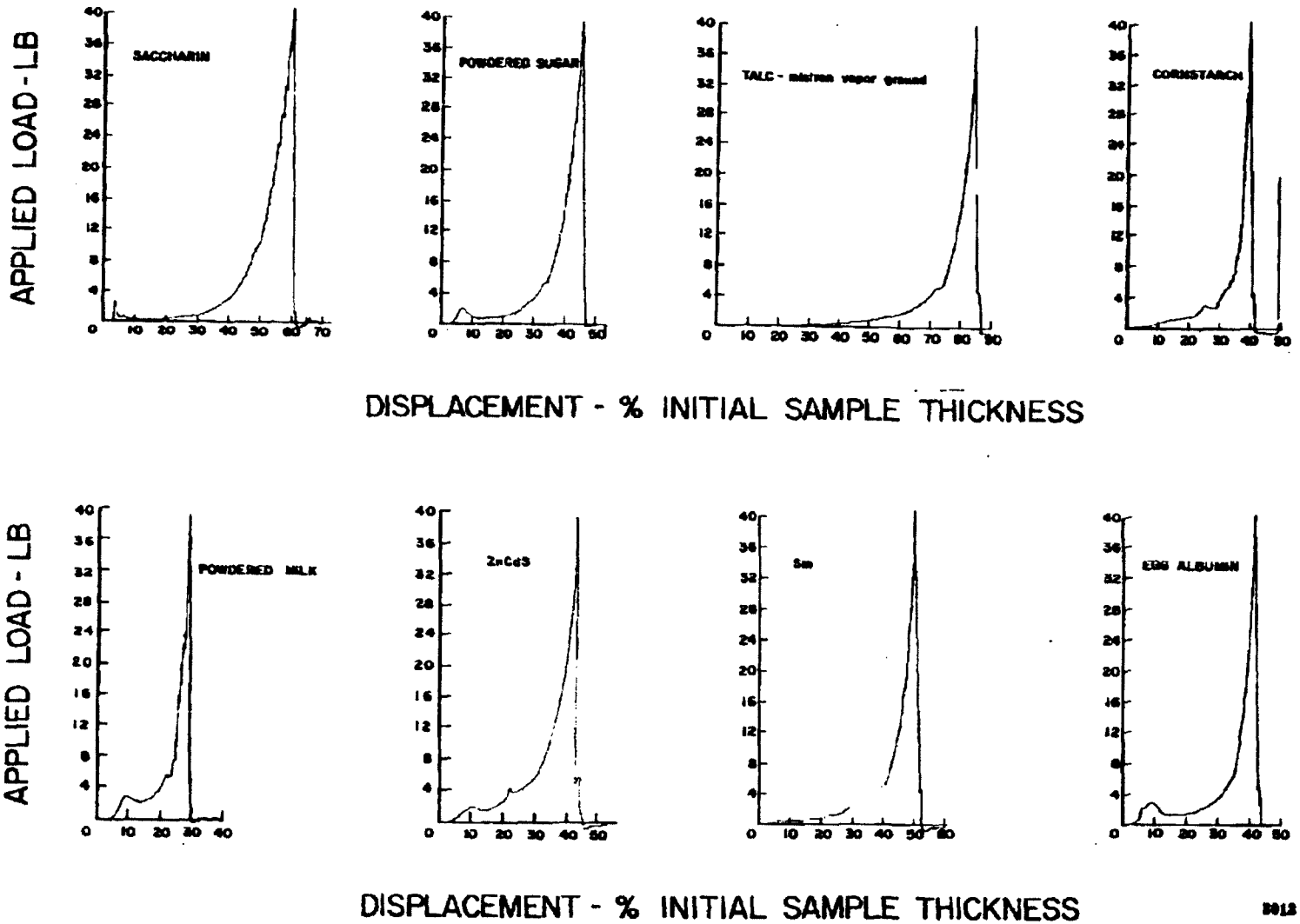

Figure 2.4 Compaction Characteristics of Various Powdered Materials at 0.200 in./min Compaction

of the sample. In order to eliminate this effect, a modified sample preparation procedure has been evolved that does not require use of a rubber membrane.

An exploded view of the assembly used for sample preparation is shown in Figure 2.5. The powder sample is compacted within a segmented cylindrical section, which is supported by means of an external housing as shown in the exploded view. The center segment is split into three 120-degree sections to facilitate removal after compaction of the sample. The test specimen is prepared by filling the cylinder with a known mass of powder which is then compacted by means of pistons forced into the cylindrical chamber from each end. Each piston is advanced at the same rate during compaction of the sample to center the compacted material in the cylinder. The final average density of the sample is fixed by accurately defining the distance between the pistons at the completion of the compaction process. For loose powders, extension units are placed at each end of the assembly shown in Figure 2.5 to permit initial compaction of the powder into the central section of the cylinder.

After compaction, the pistons are removed and threaded end plugs are installed in each end cylinder to give support to the compacted powder column. The entire assembly is then placed in the Instron test machine and a load of about 50 pounds is applied to the end plugs. (This load is not applied to the powder, but is carried by the central cylinder.) The housing may now be removed, after which the load is gradually released. Because of the elastic nature of the compacted powder, a small gap will generally appear between the center cylindrical segments and the upper-end cylinder, thus simplifying removal of the segmented center cylinder. (The center section is made of magnetic stainless steel; thus, the center-section segments can be readily removed with a weak magnet.) If this procedure is followed carefully, the exposed powder will be free of cracks or other imperfections.

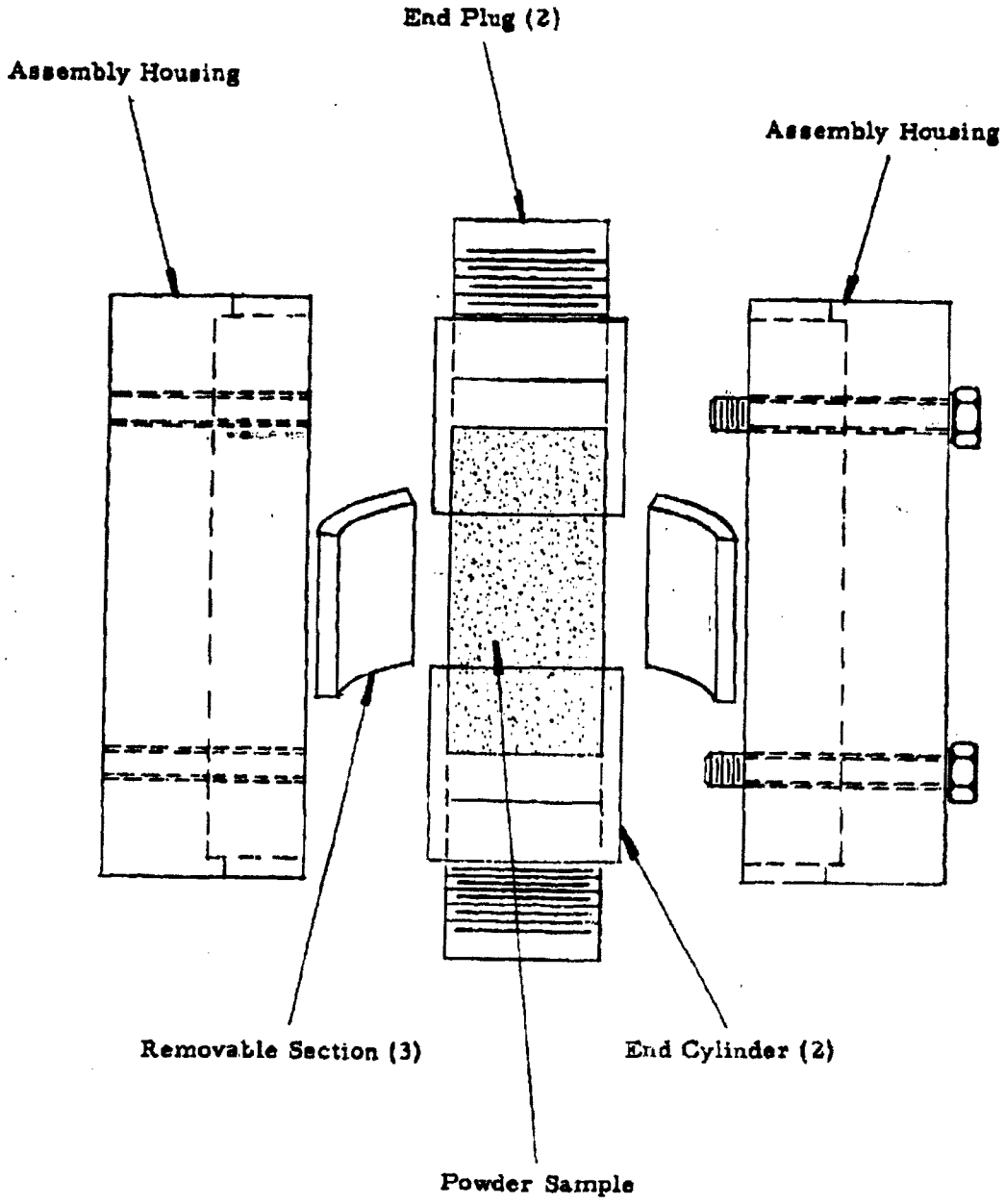

Figure 2.5 Exploded View of Triaxial Test Sample Preparation Assembly

The shear strength of saccharin compacted to an average density of 0.65 g/cm^3 by the above technique has been obtained by tests conducted in the Instron test machine. The load-strain diagram for a typical test is shown in Figure 2.6. It is apparent that the sample failure is very well defined, the load falling from about 6.7 to 0.5 pounds as the sample fails in shear. By stopping the machine at the instant of failure, it is possible to remove the fractured test sample intact. The typical appearance of a sheared sample is illustrated by Figure 2.7. The shear planes are clearly evident in the photograph.

This technique is currently being extended to permit triaxial tests in a pressurized chamber[1]. A thin loose-fitting membrane, enclosing the entire sample assembly, will be used in these tests. By venting the interior of the membrane to ambient pressure, the desired lateral stress on the sample will be achieved; however, the loose membrane will be free to deform as the sample shears. It is believed that this modification of the earlier test technique will result in clear-cut failure of the test specimens.

In order to fully define the shear strength of a compacted powder, it is necessary to examine the tensile shear strength of the powder as well as its compressive shear strength. The reason for this is evident from a study of Figure 2.8. Compressive shear tests are capable of establishing the portion of the shear locus B-C on the figure. However, the pure shear strength of the powder τ_c cannot be determined by the compressive triaxial technique, since a tensile stress must be applied to the sample in order to perform tests in the region A-B of Figure 2.8. In principle, the triaxial test can be performed in this region by applying a gradually increasing axial tension to the sample while maintaining a constant chamber pressure as before. Attempts to conduct such a test at zero chamber pressure have not succeeded, however, because sample failure invariably occurs in the plane of one of the end cylinders. Since sample failure in tension should occur as a result of combined tension and shear, it is to be expected that the sample

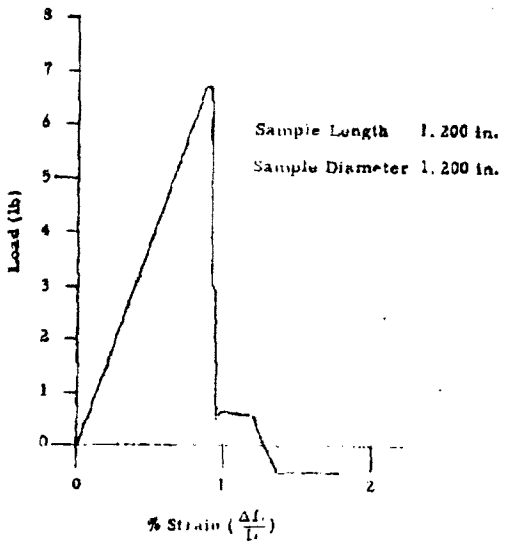

Figure 2.6 Load-Strain Curve for Compacted Saccharin (ρ_o = 0.65 g/cm^3)

Figure 2.7 Compacted Saccharin Failed in Compression (ρ_o = 0.65 g/cm^3)

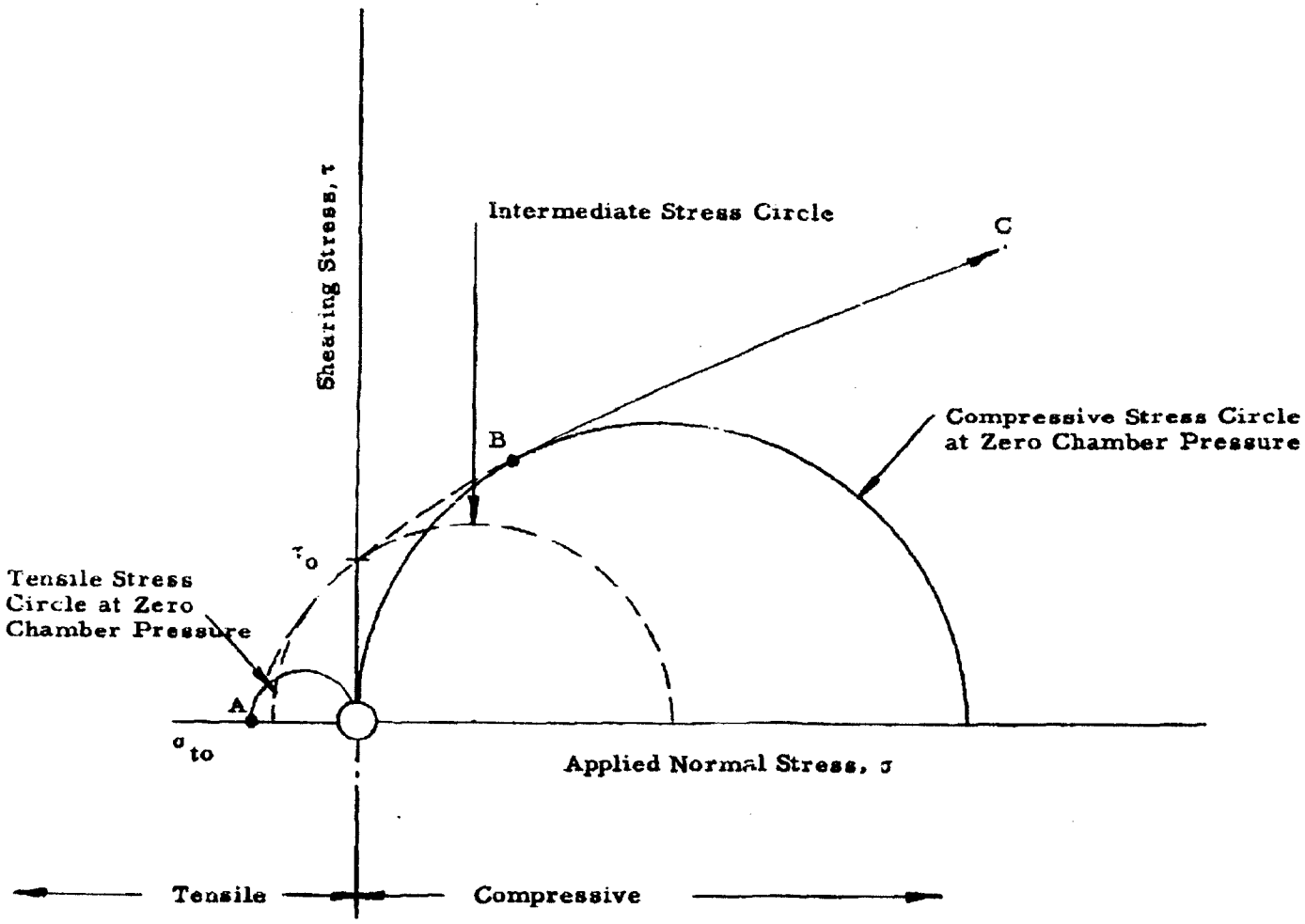

Figure 2.8 Shear Locus Curve Illustrating the Relationship between Bulk Shear Strength τ_o and Bulk Tensile Strength σ_{to}

should fail in the manner typified by Figure 2.7 for the compressive case. Presumably, the type of failure actually observed is due in part at least to the constraining effect of the end cylinder.

It is believed that measurements of bulk tensile strength should, if possible, be carried out in such a way that fracture occurs in the central region of the powder sample rather than at one end. A "natural" tensile failure may be possible if the test specimen is compacted so that the center section has a reduced cross-sectional area. Experiments with a reduced-area sample will be tried as soon as the modified center-section cylinder can be fabricated.

A completely different means of evaluating the tensile strength of a compacted powder is now under investigation. In the proposed test, a compacted powder sample is placed in a pressure chamber and the pressure in the chamber is gradually increased to a preselected value. After equilibrium is established, the chamber is depressurized at a controlled rate. The gas entrapped within the pores of the powder sample will flow toward the surface of the sample. The resulting viscous stresses at the powder surface will tend to break the relatively weak bonds holding the particles together. If properly carried out, this test should permit detection of a "threshold" condition at which erosion of the powder surface begins. From this information, it may be possible to compute the average strength of interparticle bonds.

This possible means of experimentally determining the tensile strength of compacted powders is based on the following observations: 1) Experience has shown that air entrapment occurs within a powder bed when compaction takes place rapidly. This is because time is required for the air contained in the void spaces to percolate through the powder. Also, experiments have shown that compacted powder samples subjected to a pressurized gas environment expand significantly when the pressure is suddenly released. 2) Even when compacted under high stresses most powders have void spaces amounting to 30 to 50 percent of the total volume of a powder sample.

Thus, it is clear that a very considerable mass of gas, capable of supplying a large amount of mechanical energy, can be stored in a powder sample at pressures of several atmospheres.

It is apparent that this concept may also provide a means for aerosollization of compacted powders. This possibility will be explored in the tests now being planned.

2.3 Bulk Tensile Strength of Compressed Powders

In the development of a method for the measurement of bulk tensile strengths of compressed powders[1,2], we have previously confined our study to zinc cadmium sulfide. In order to determine the effectiveness of our method in the measurement of the tensile strength of other powders, we have extended our study to include saccharin, cornstarch, powdered milk, Sm, and talc. Again we have confined our study to three compressive loads, 1454, 2130, and 2919 grams, and to a compression time of 1-1/2 hours. All measurements were made in a controlled environment of 15 percent relative humidity. The results obtained are presented in Figures 2.9 through 2.17. Diameter of the powder plug was 0.75 inches. Although talc was included in our study, no valid measurements were obtained. It was found that upon removal of the spring clips holding the column segments together, the release of elastic energy in the talc plug caused the column segments to spring apart fracturing the column of powder prior to measurement of the tensile strength. The present apparatus will have to be modified to overcome this problem. Figure 2.18 is a presentation of the variation of tensile strengths of various powders at the same compressive load. In this manner the powders can be characterized according to their relative tensile strengths fulfilling, in part, the purpose of the current study.

It is seen that the data do not follow the simple exponential relationship proposed earlier[1,2]:

$$\sigma = \sigma_o e^{-kL}$$

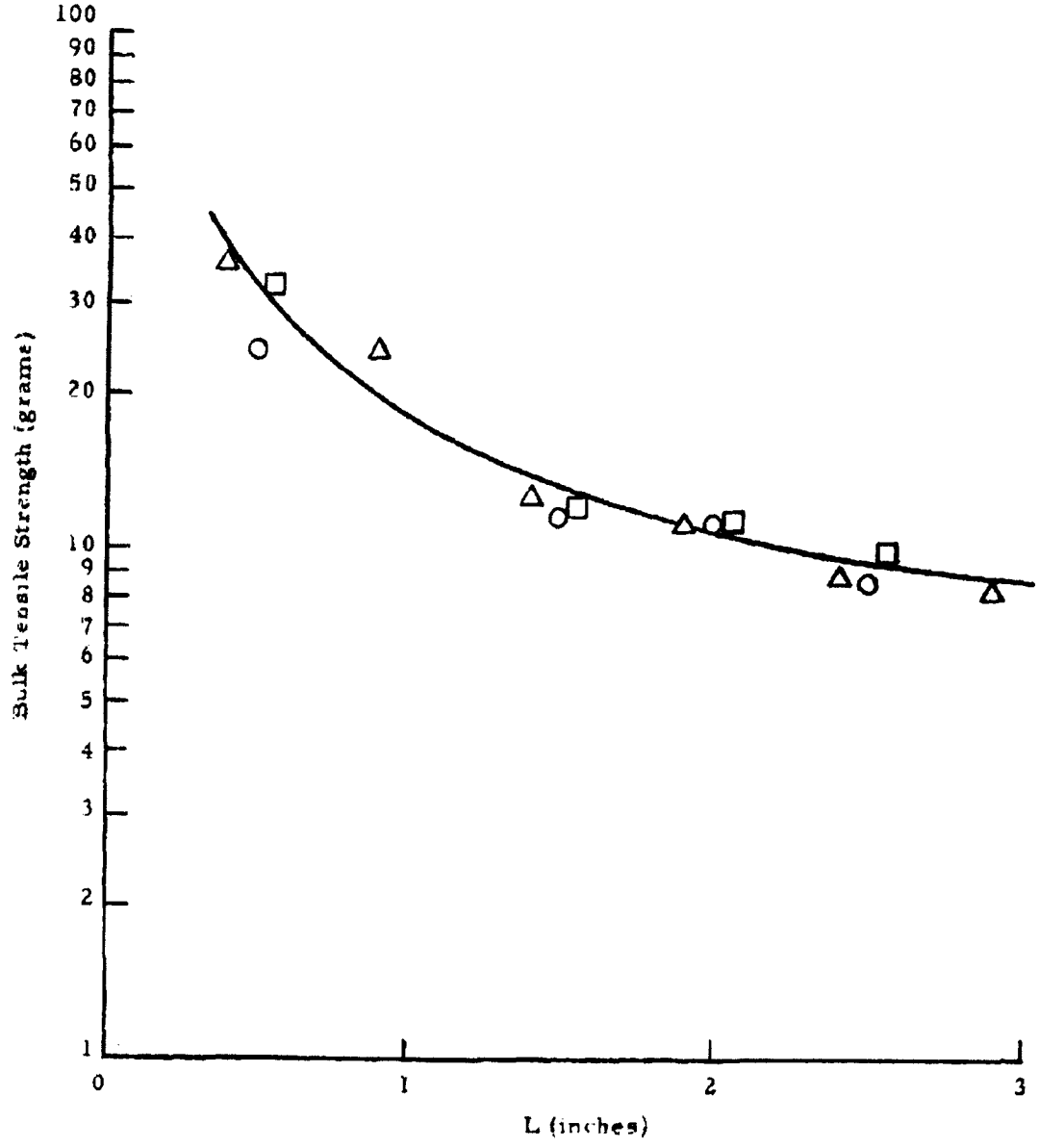

Figure 2.9 Bulk Tensile Strength for Saccharin as a Function of Distance "L" from Compressive Force at a Compressive Load of 1454 g

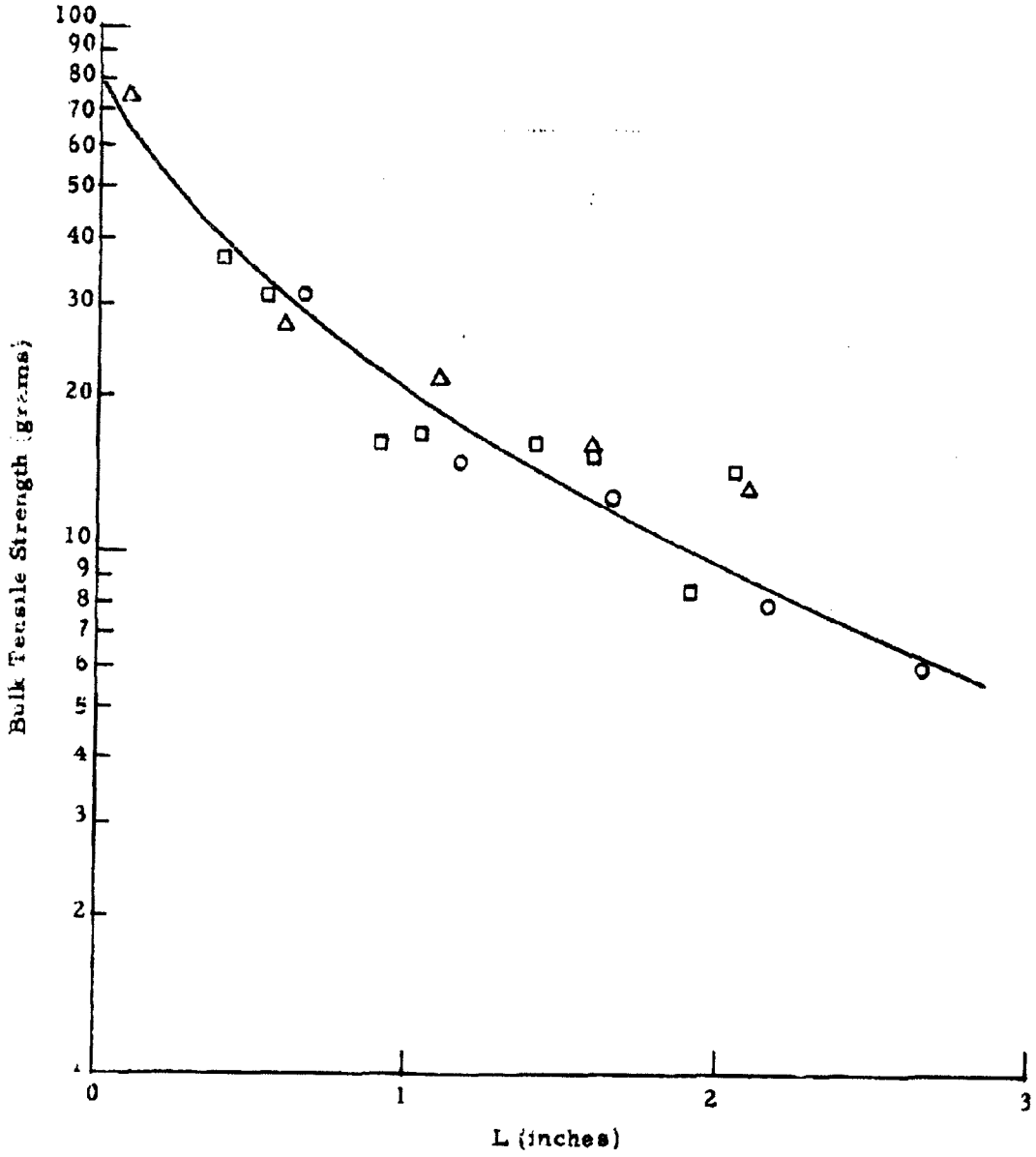

Figure 2.10 Bulk Tensile Strength for Saccharin as a Function of Distance "L" from Compressive Force at a Compressive Load of 2130 g

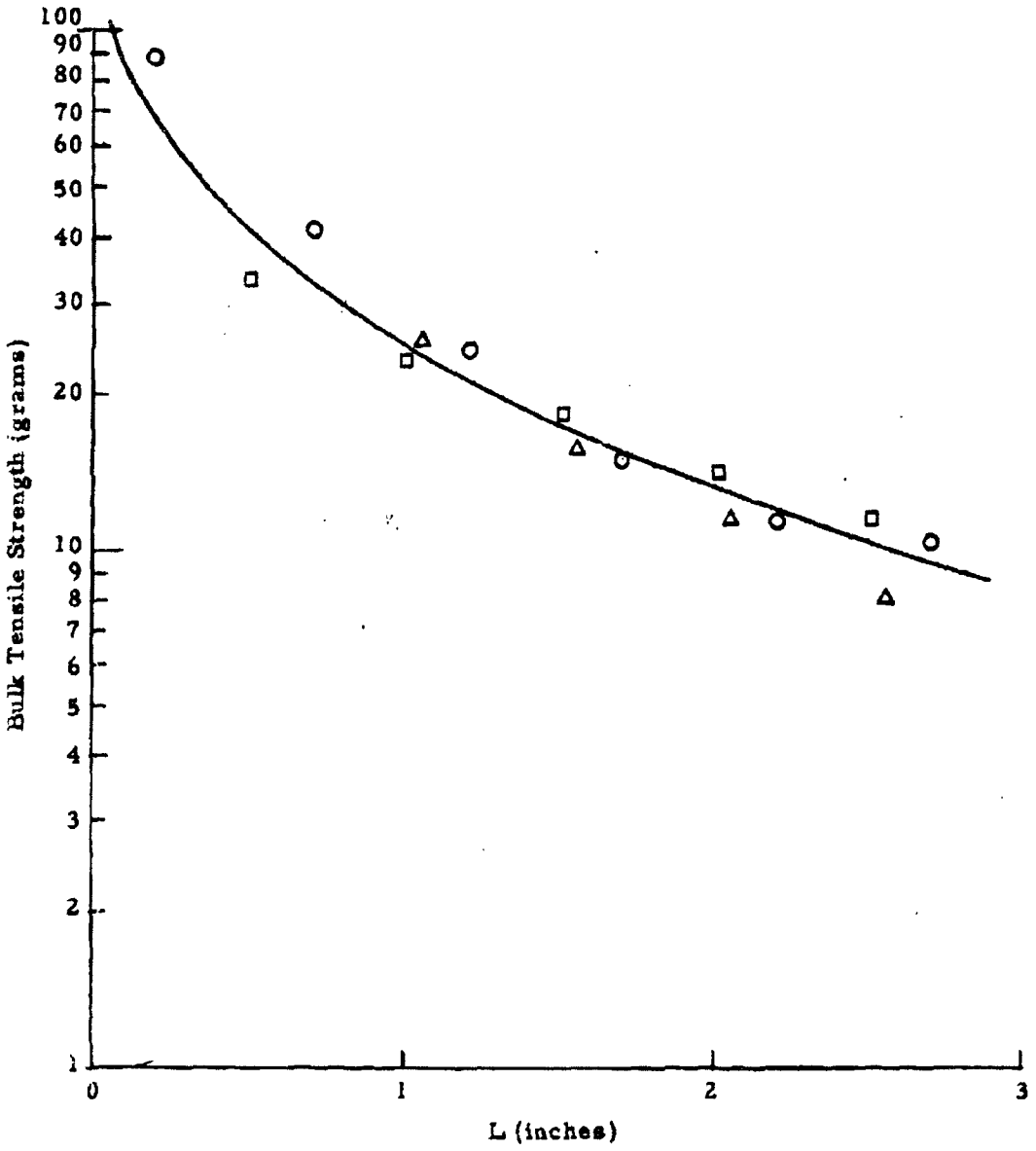

Figure 2.11 Bulk Tensile Strength for Saccharin as a Function of Distance "L" from Compressive Force at a Compressive Load of 2919 g

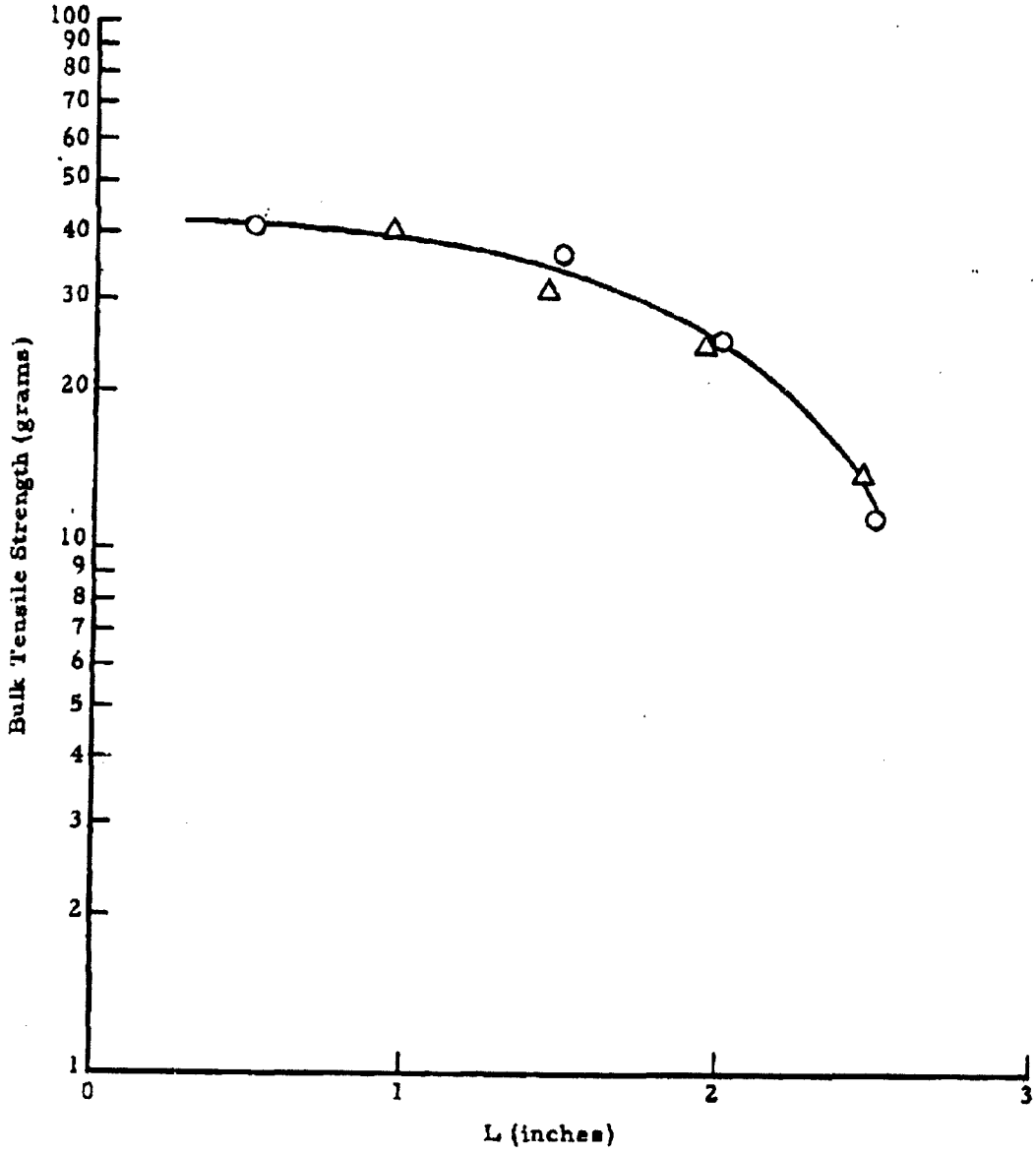

Figure 2.12 Bulk Tensile Strength for Cornstarch as a Function of Distance "L" from Compressive Force at a Compressive Load of 1454 g

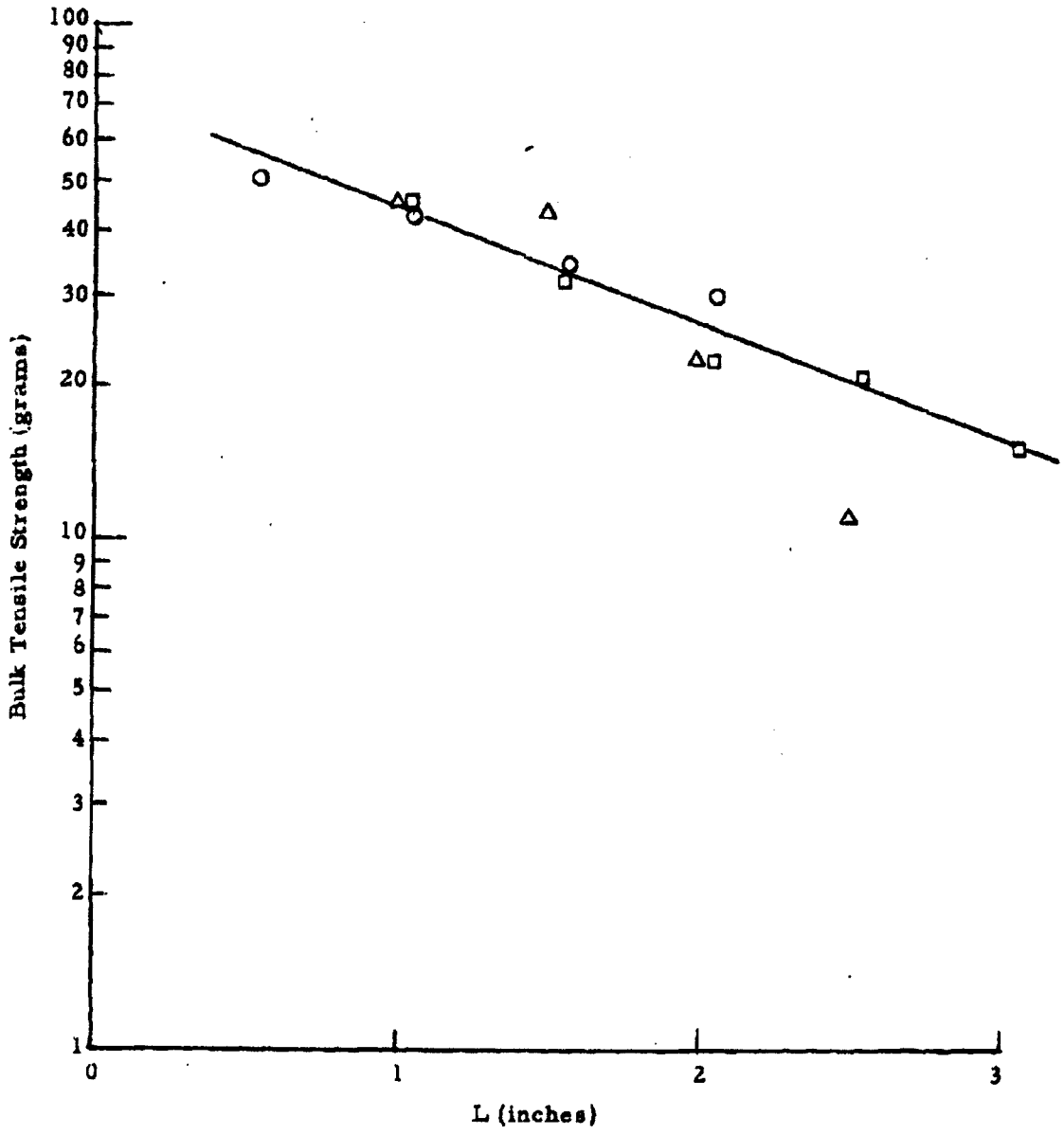

Figure 2.13 Bulk Tensile Strength for Cornstarch as a Function of Distance "L" from Compressive Force at a Compressive Load of 2130 g

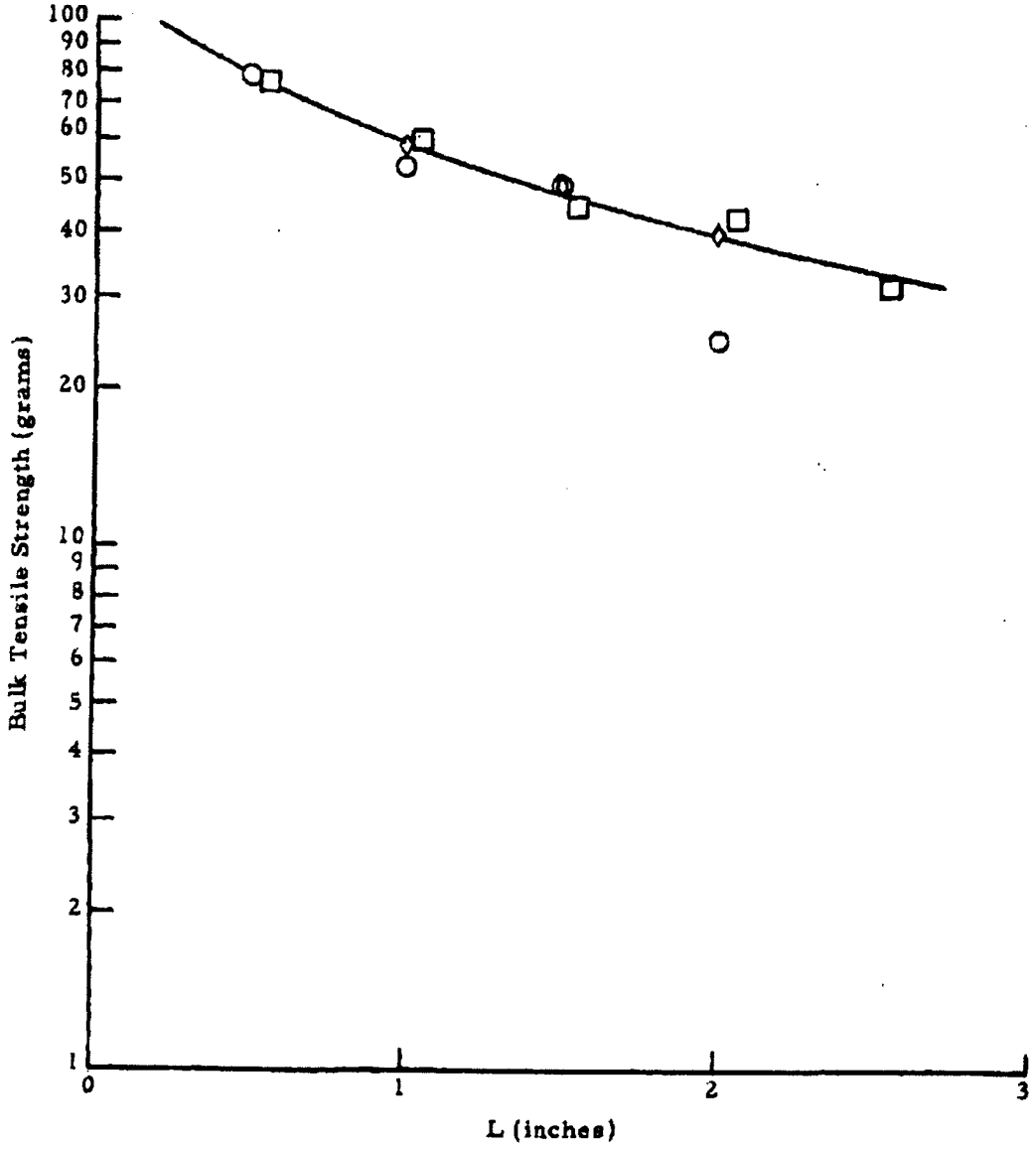

Figure 2.14 Bulk Tensile Strength for Cornstarch as a Function of Distance "L" from Compressive Force at a Compressive Load of 2919 g

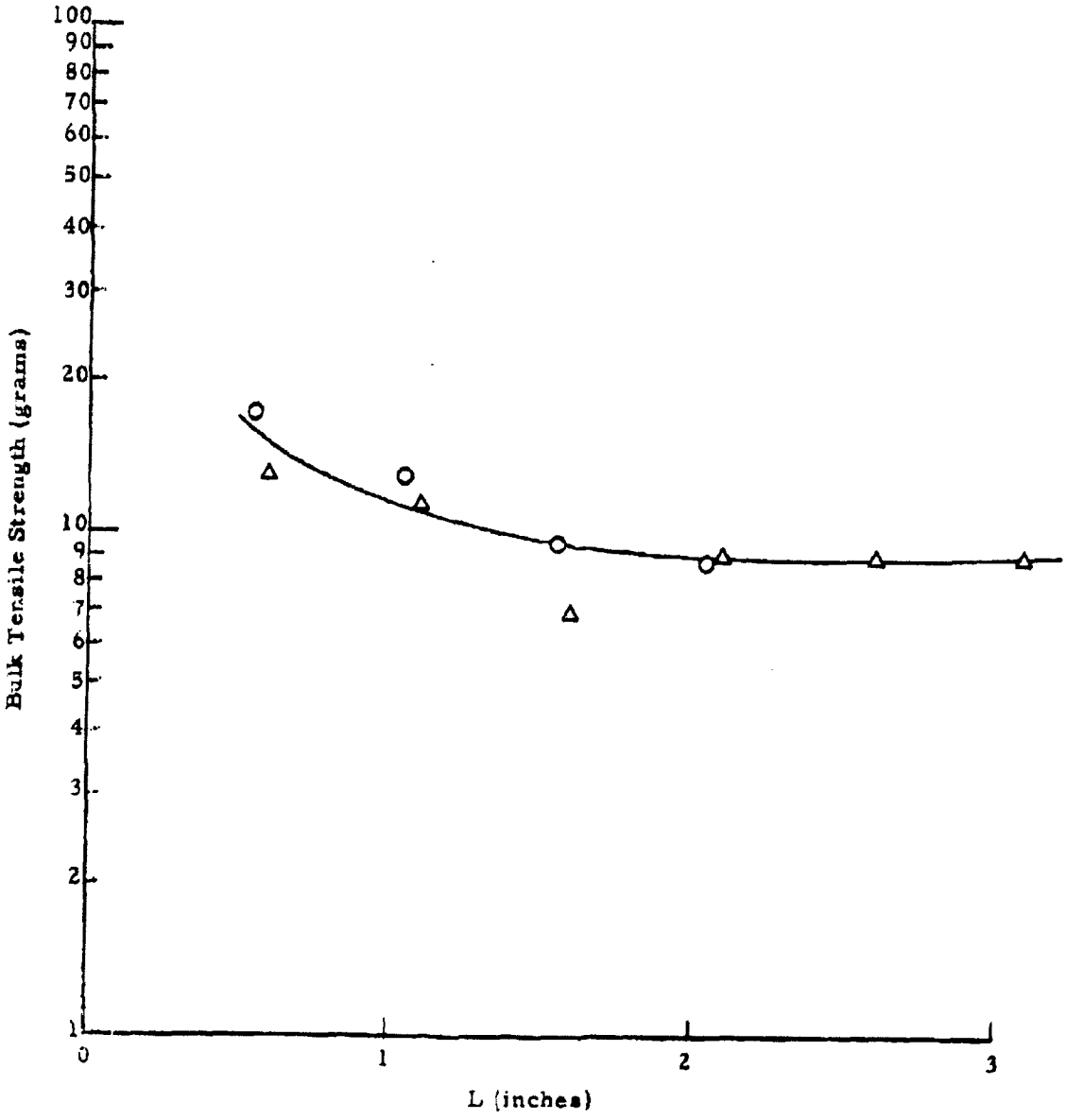

Figure 2.15 Bulk Tensile Strength for Sm as a Function of Distance "L" from Compressive Force at a Compressive Load of 2130 g

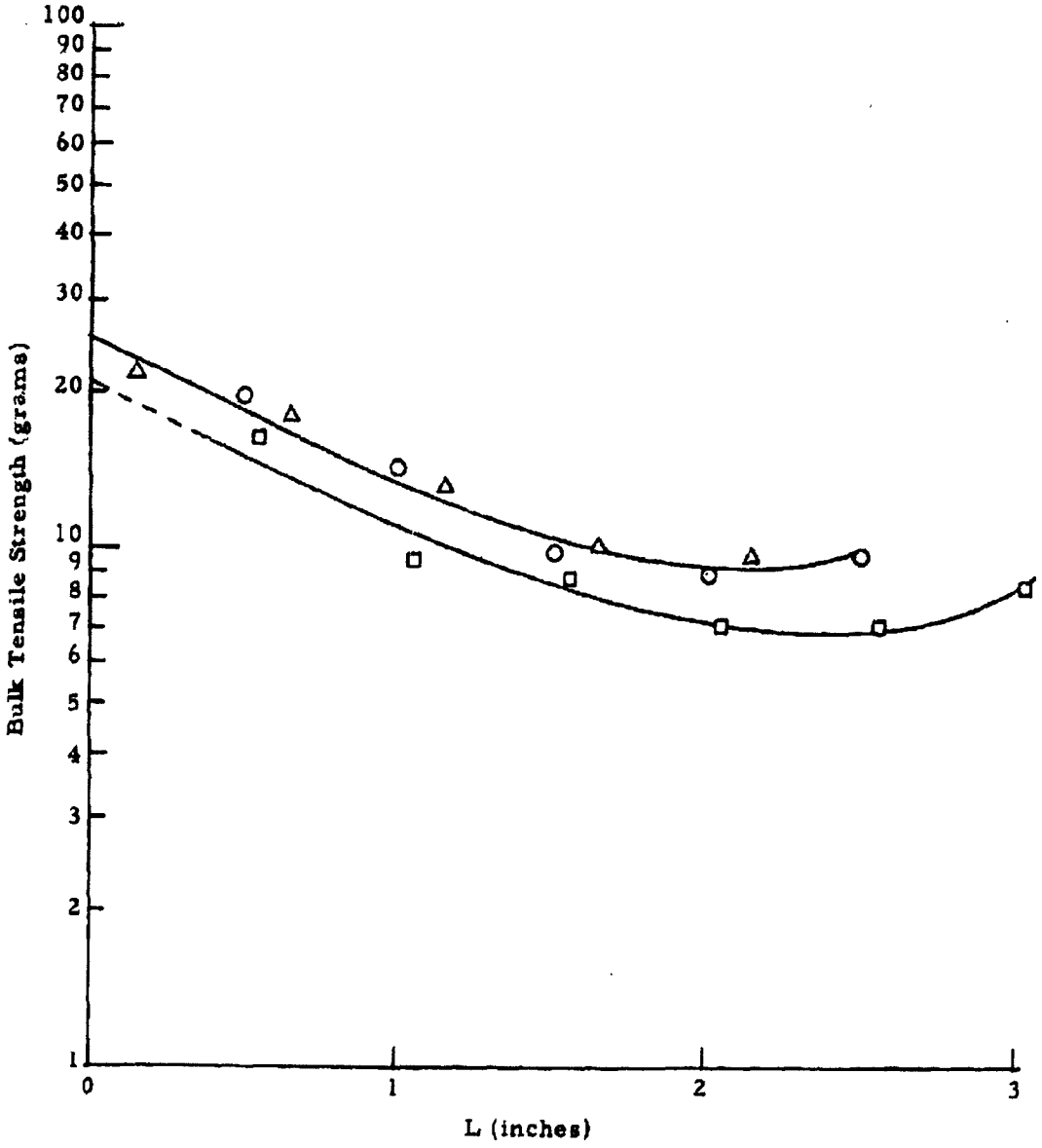

Figure 2.16 Bulk Tensile Strength for $\overline{Sm}$ as a Function of Distance "L" from Compressive Force at a Compressive Load of 2919 g

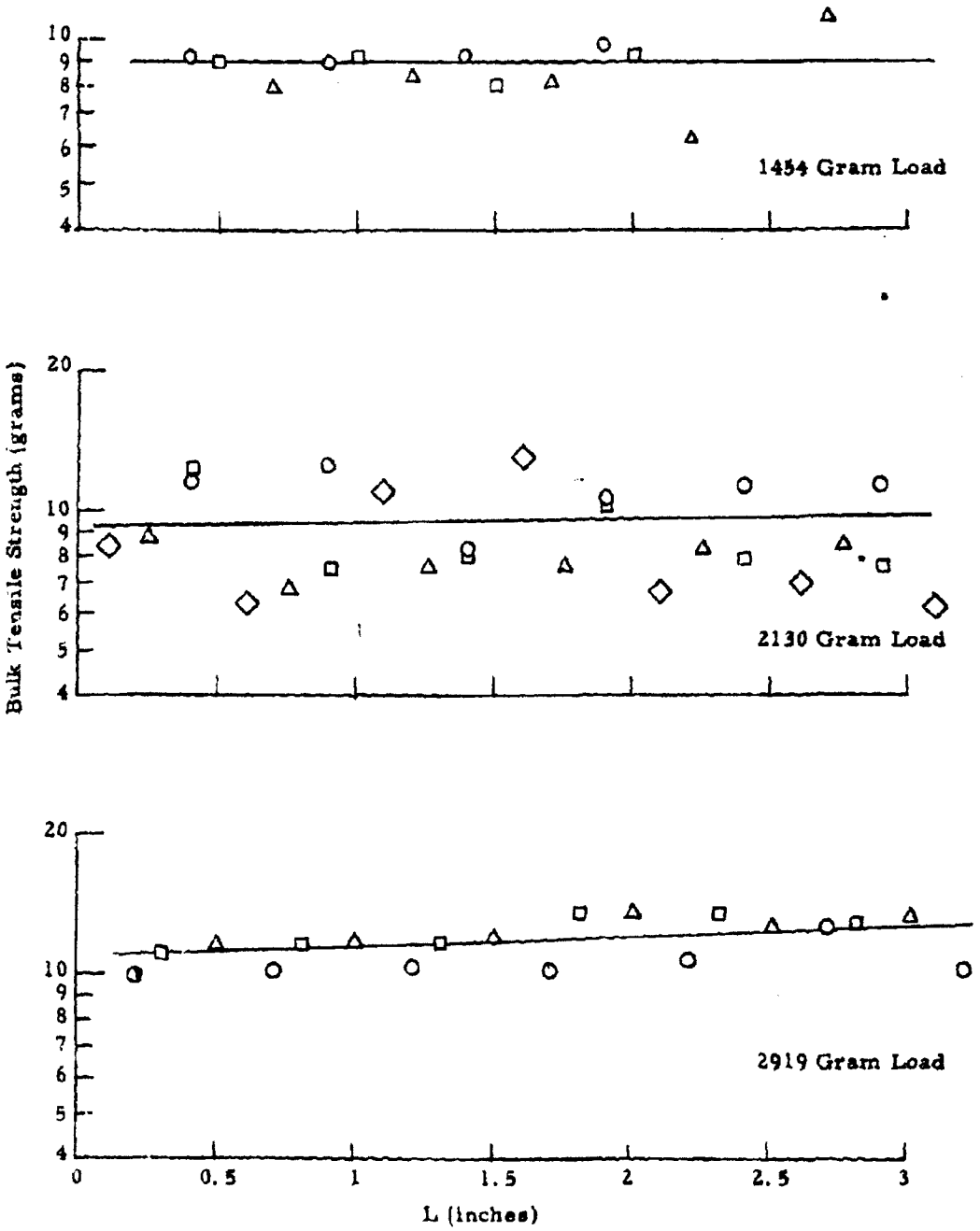

Figure 2.17 Bulk Tensile Strength for Powdered Milk as a Function of Distance "L" from Compressive Force at Three Compressive Loads

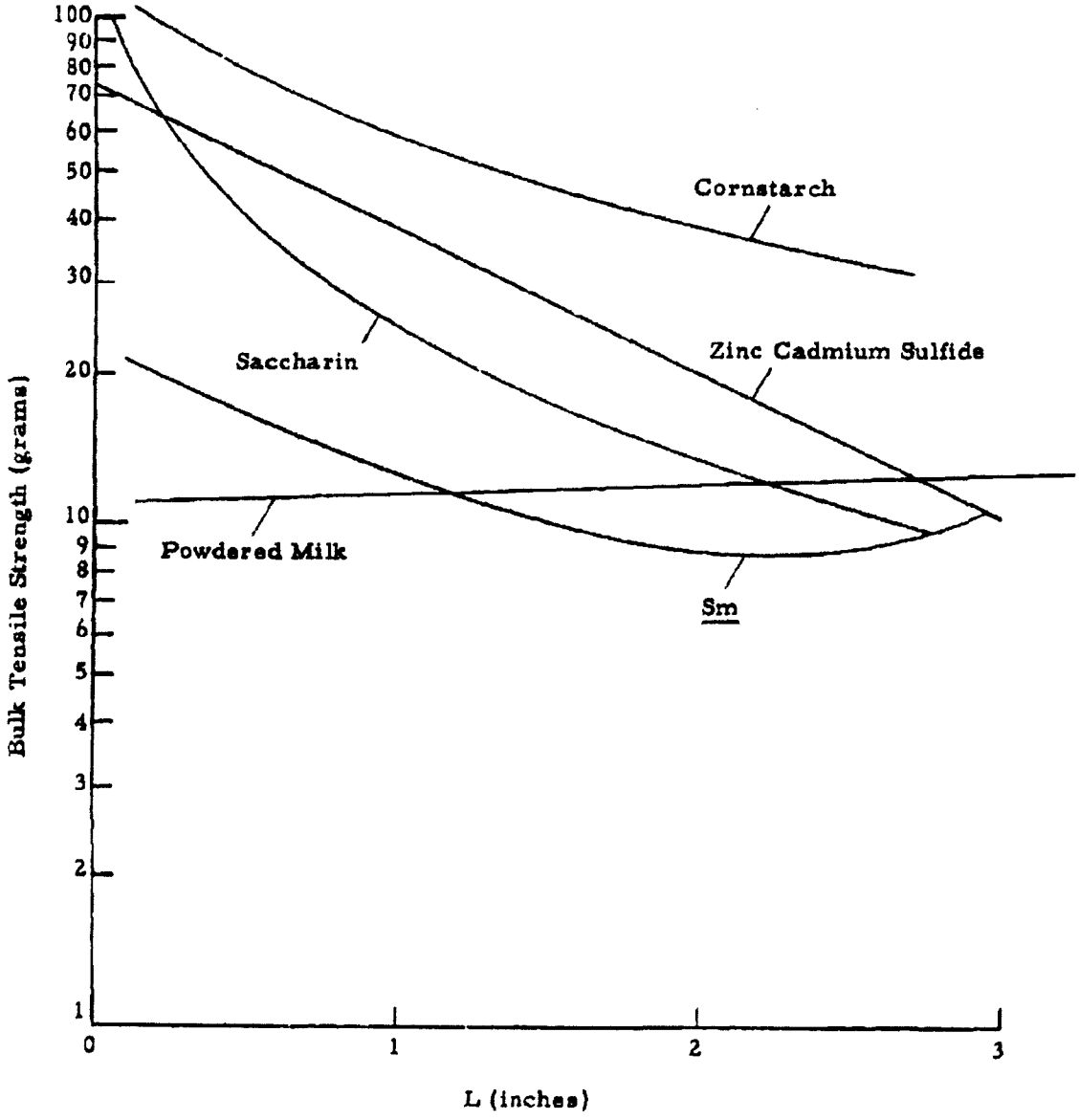

Figure 2.18 Comparison of Bulk Tensile Strength of Powders at the Same Compressive Load of 2919 g

where:

σ = bulk tensile strength of a column of compressed powder at a distance L from the piston

σ_o = bulk tensile strength of the compressed powder immediately below the piston

k = constant

L = distance from piston to fracture plane

If this deviation from current proposed theory continues throughout subsequent experimentation, it will be proposed that the bulk tensile strength may follow the relationship:

$$\sigma = \sigma_o e^{-kL} + \sigma_o e^{+kL}$$

indicating that the experimental values obtained are in reality the sum of two exponentials, with equal slopes but opposite in sign. This would represent a buildup of tensile strength from the bottom of the column of compressed powder as well as at the head of the compressive piston. Studies including variations in total column length as well as bulk density determinations will help to elaborate upon this.

2.4 Shear Strength of Compressed Powders by the Sliding Disk Method

An extensive test program is now in progress in which the shear strengths of a number of powders are being determined as a function of compressive load over a wide range of relative humidity environments. For reasons of continuity the reporting of these results will be delayed pending the completion of this study.

2.5 Bulk Density of Compressed Powders

During the previous quarter[1], a study of the bulk density variation in a compressed column of saccharin was made at various compressive loads. This study has been extended, for comparative purposes, to talc. The apparatus and techniques are identical to those previously described[1] in which the loose bulk powder is used to fill a segmented column 5-3/32 inch ID which, following compression of the powder, is then cut into one-inch segments to determine the density variation throughout the column. In the apparatus described the total column length of uncompacted powder was 20 inches. A few preliminary experiments indicated that the talc was sufficiently more compressible than saccharin to necessitate a 5-inch extension of the fill tube in order to obtain column lengths of the compressed powder comparable to those obtained for saccharin. With this revision in the apparatus the column of uncompacted talc is now 25 inches in length. The data obtained are presented in Figures 2.19 and 2.20. Figure 2.19 shows the effect of increasing the powder column length. The broken lines represent results obtained using a 20-inch column length prior to compaction, whereas the solid lines represent results with a 25-inch column length. Figure 2.20 represents the completed study for talc. The plot for each compressive load represents the average of two independent determinations.

The behavior of talc differed from that of saccharin in two distinct ways: 1) the decrease in density down the column is significantly greater for talc than for saccharin, and 2) talc displays a considerable release of elastic energy following the removal of the compressive force. This difference was also noted in the bulk tensile strength measurements discussed earlier in this report.

Our continued study of the radial variation of the bulk density in a column of compressed powder indicates that the differences in density previously reported[1] between the inner core and the outer annular segment were due to experimental error. Refined experimental techniques show the absence of significant variations in the radial distribution of bulk densities of compressed powders.

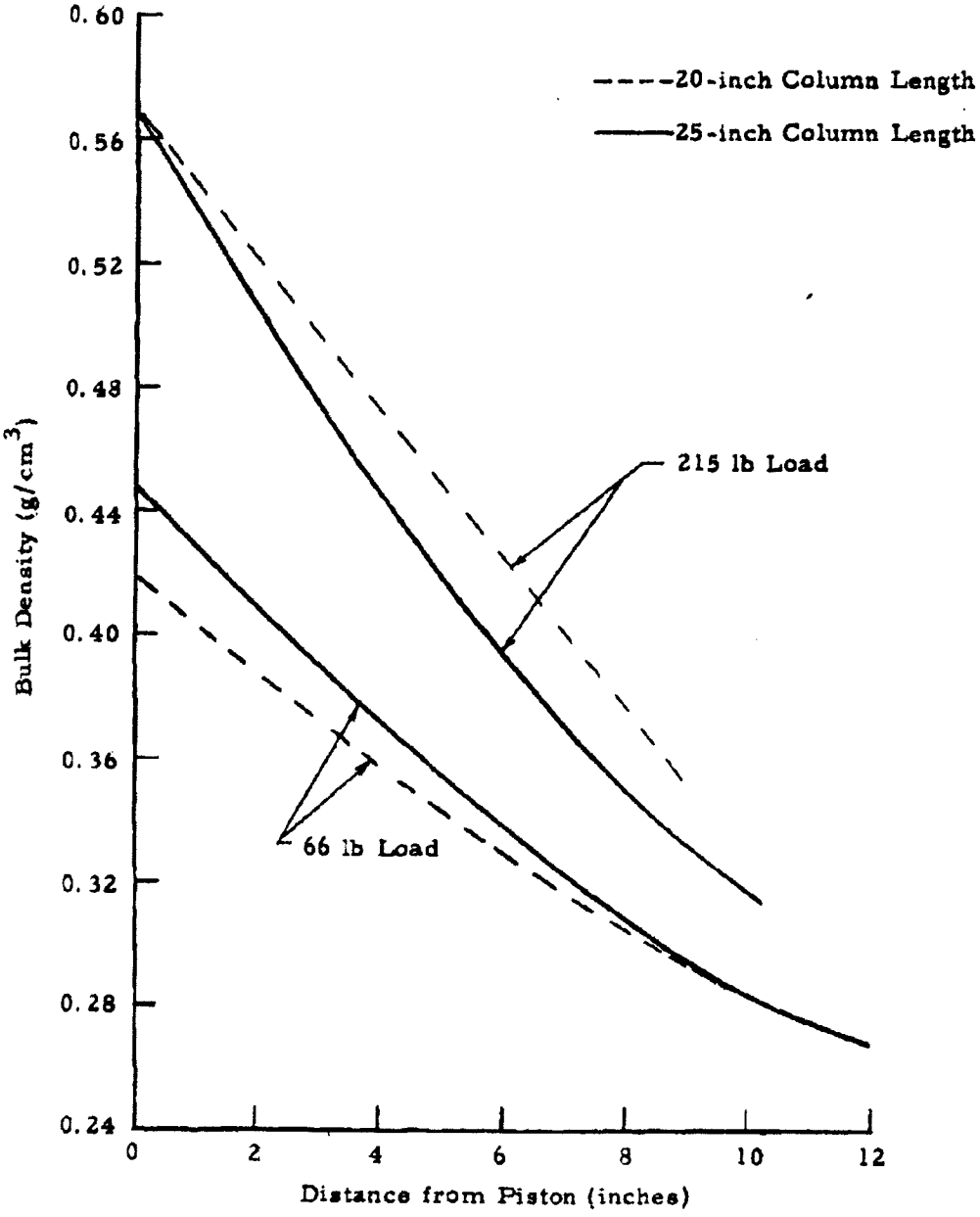

Figure 2.19 Variation of Bulk Density of Talc with Total Plug Length

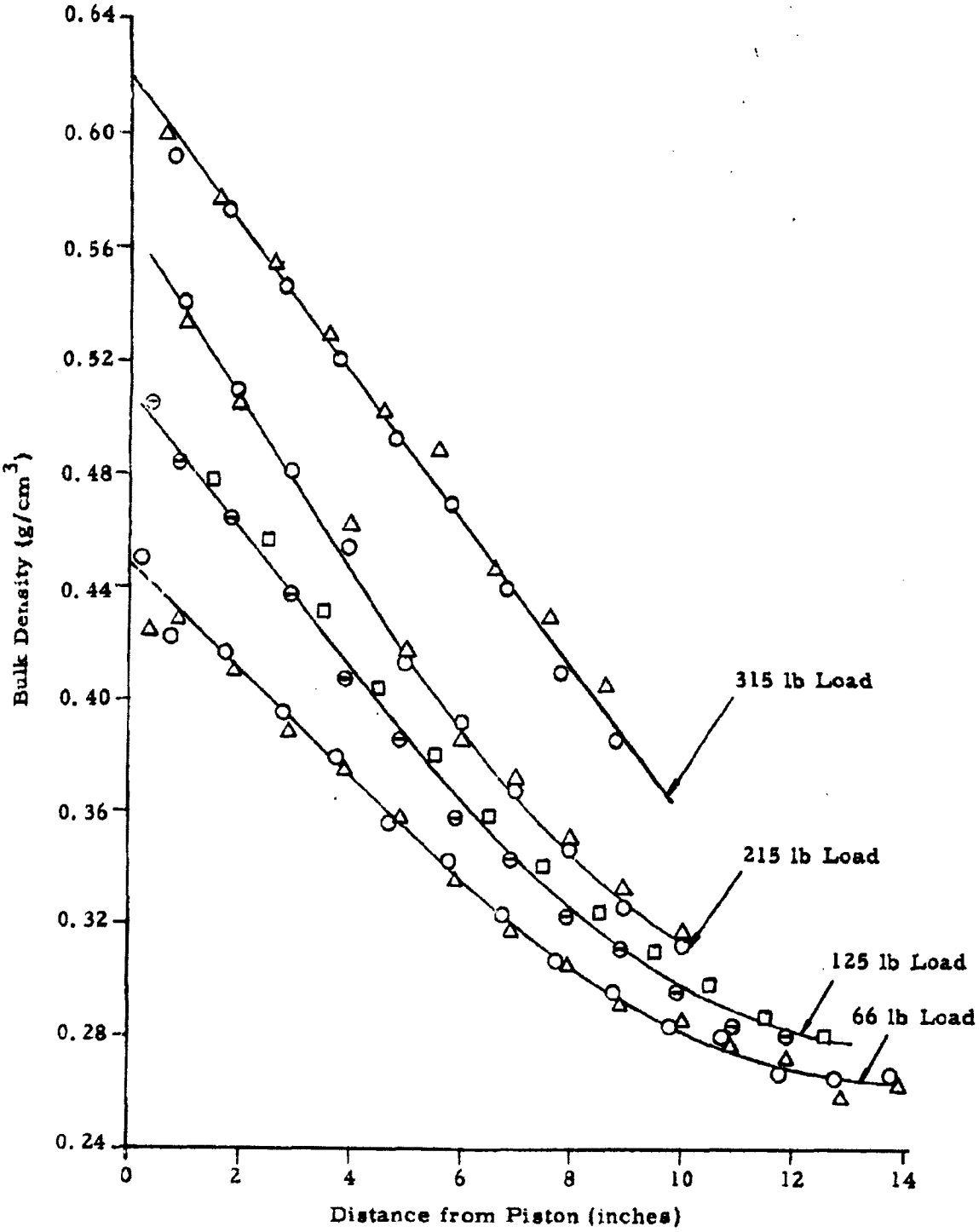

Figure 2.20 Bulk Density of Talc (Mistron Vapor) as a Function of Distance from Piston at Various Compressive Loads

3. AEROSOL STUDIES

The aerosol studies of the present quarter have proceeded along those mentioned at the conclusion of the last report[1]. A number of runs have been made at three humidity conditions – less than 5 percent, about 50 percent, and greater than 95 percent – for each of five different powders. The possibility of obtaining more direct information on the aerosol condition by analysis of the noise level on the light-scattering signals has been investigated, with positive results. Some time was devoted to the problem of obtaining an initially well-dispersed aerosol, resulting in the development of an alternate method of dispersing powders. Further work, chiefly involving ion injection, is outlined in the concluding section.

3.1 Study of the Effects of Environmental Humidity on Aerosol Decay

As a preliminary step in the study of humidity effects on the decay of aerosols, runs have been made at three humidity conditions. One series of runs made use of normal room humidity conditions that were in the range of 45 to 50 percent during the period covered. In a second series of runs, a low humidity condition was obtained by placing a pan containing molecular sieve desiccant on the floor of the chamber near the fan. After the chamber was closed and the fan turned on, a check with an infrared hygrometer showed that the humidity was reduced to less than 5 percent after 1-1/2 hours. A third series of runs was made with a pan of water in place of the pan of desiccant. The hygrometer showed that the chamber humidity rose to greater than 95 percent 1-1/2 hours after closing the chamber.

Five powders – talc, saccharin, cornstarch, powdered sugar, and powdered milk – were run at each of the three humidity conditions. The stirring fan, with the small (4-inch) blade, was operated at 35 volts throughout each run so that the decay observed was in each case "turbulent" decay. The powder dispersing system was operated as described in the last report.

No attempt was made to precondition the powder samples prior to dispersing. Only one of the two light-scattering units was used in this work, since it was shown in the last report that the two signals were identical for the stirred settling case.

The light-scattering data from the humidity runs are shown in Figures 3.1 through 3.5. The runs for talc and saccharin were repeated; these showed generally good reproducibility. It will be noted that the five powders fall into two categories as regards the effect of humidity on aerosol decay.

Saccharin is the prototype for the powders of the first category. The decay rate for saccharin was about the same in the 5 and 50 percent relative humidity environments, but was somewhat larger at 95 percent relative humidity. Cornstarch and powdered milk behaved similarly.

Powders of the second category, talc and powdered sugar, exhibited a different behavior. For talc the decay rates were about equal for the two extreme humidity conditions and less for the intermediate humidity condition. In summary, the decay rate for powders of the second category first decreased, then increased with increasing humidity; whereas powders of the first category exhibited decay rates that increased monotonically with increasing humidity.

The behavior of aerosols exposed to various humidities is difficult to interpret in terms of fundamental decay processes. The behavior of powders of the first category seems quite reasonable, i.e., increased humidity increases either or both the agglomeration rate and rate of loss to walls. However, the behavior of powders of the second category is more difficult to explain. For the latter category, the eminent possibility would seem to be that increasing humidity enhances one of the rates and retards the other, one rate dominating at one extreme humidity condition with the other rate dominating at the other extreme. Thus, if a hypothetical decay rate parameter λ is comprised of two parts, $\lambda_{settling} + \lambda_{agglomeration}$, the observed behavior could be accounted for as indicated in Figure 3.6. For the present,

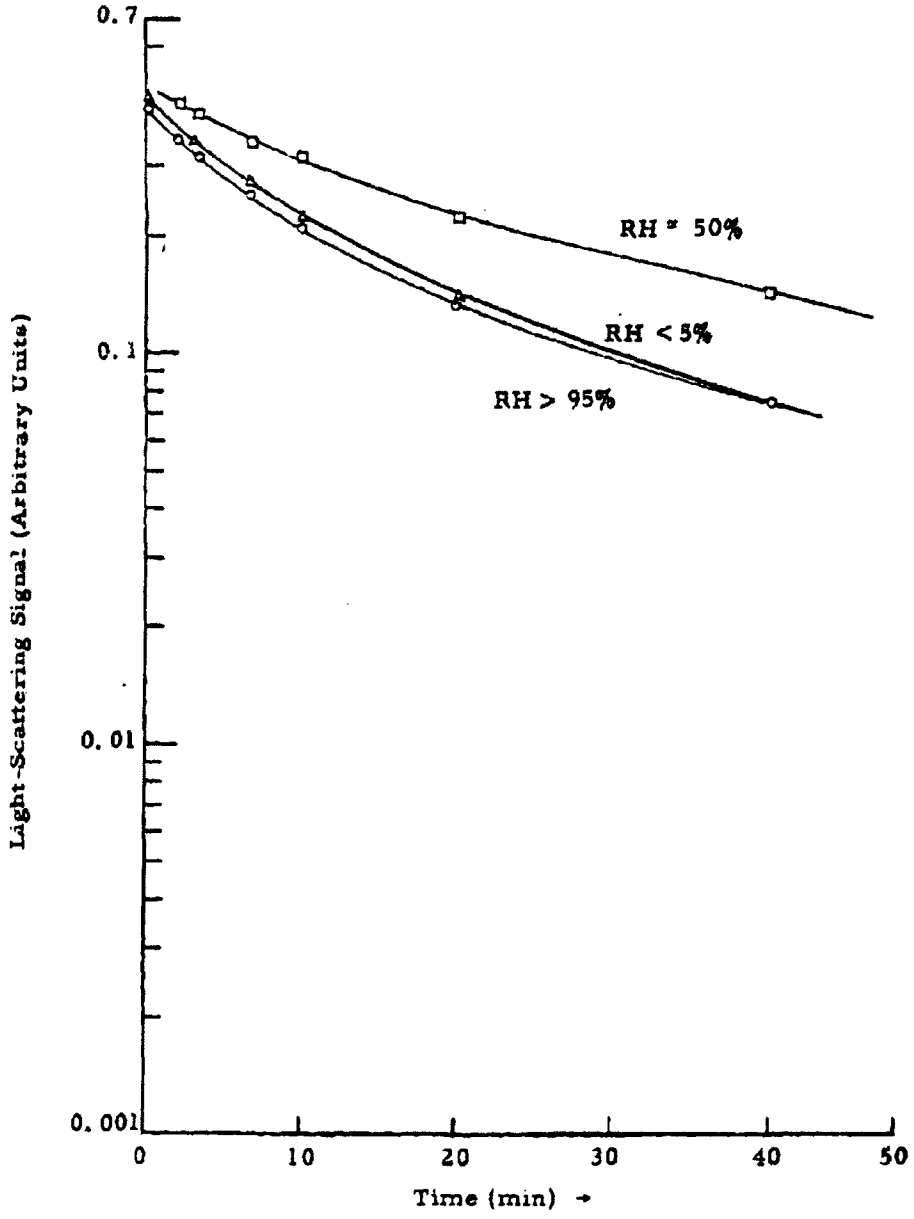

Figure 3.1 Effect of Humidity on Decay of Talc Aerosols (= 52 mg Samples)

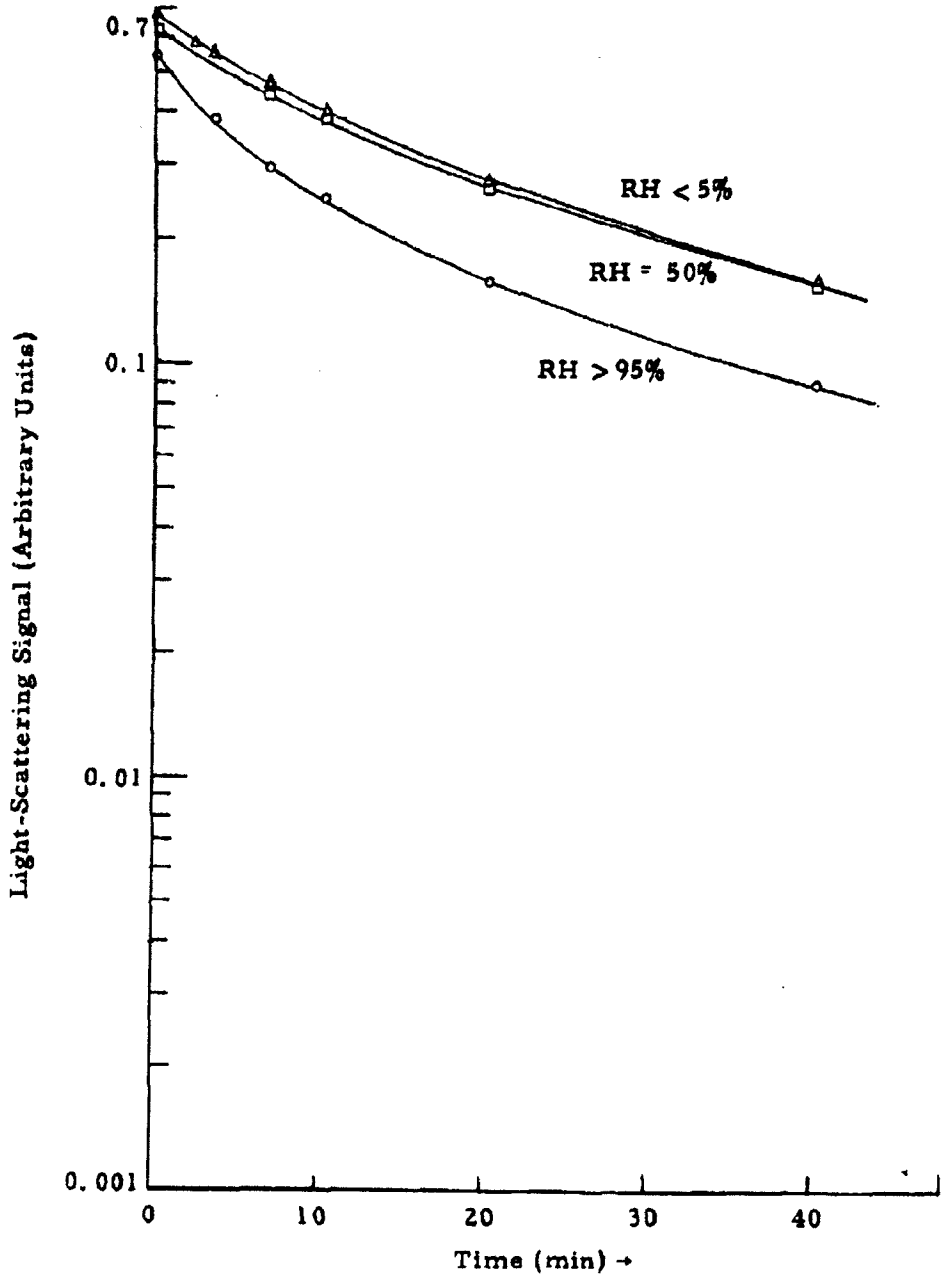

Figure 3.2 Effect of Humidity on Decay of Saccharin Aerosols (* 57 mg Samples)

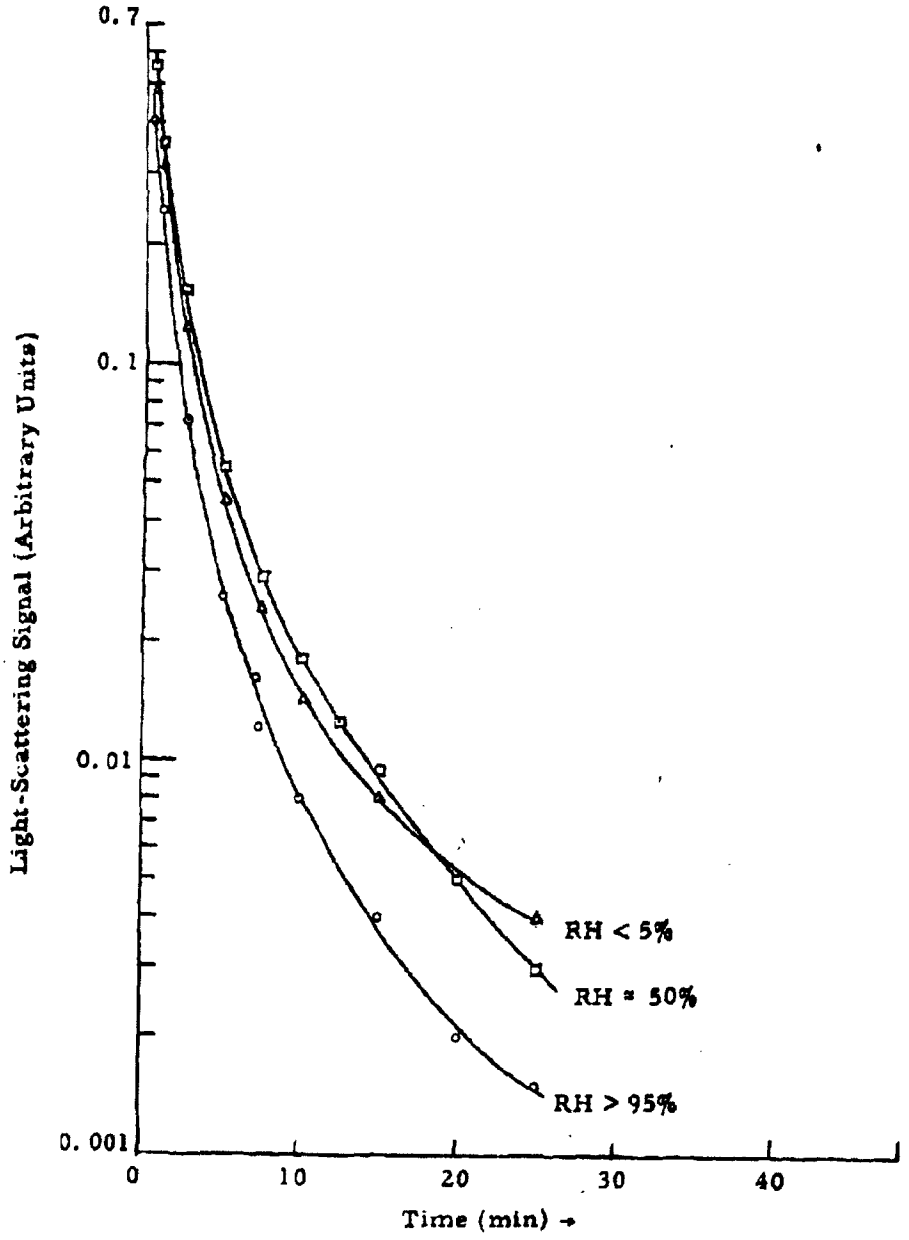

Figure 3.3 Effect of Humidity on Decay of Cornstarch Aerosols (≈550 mg Samples)

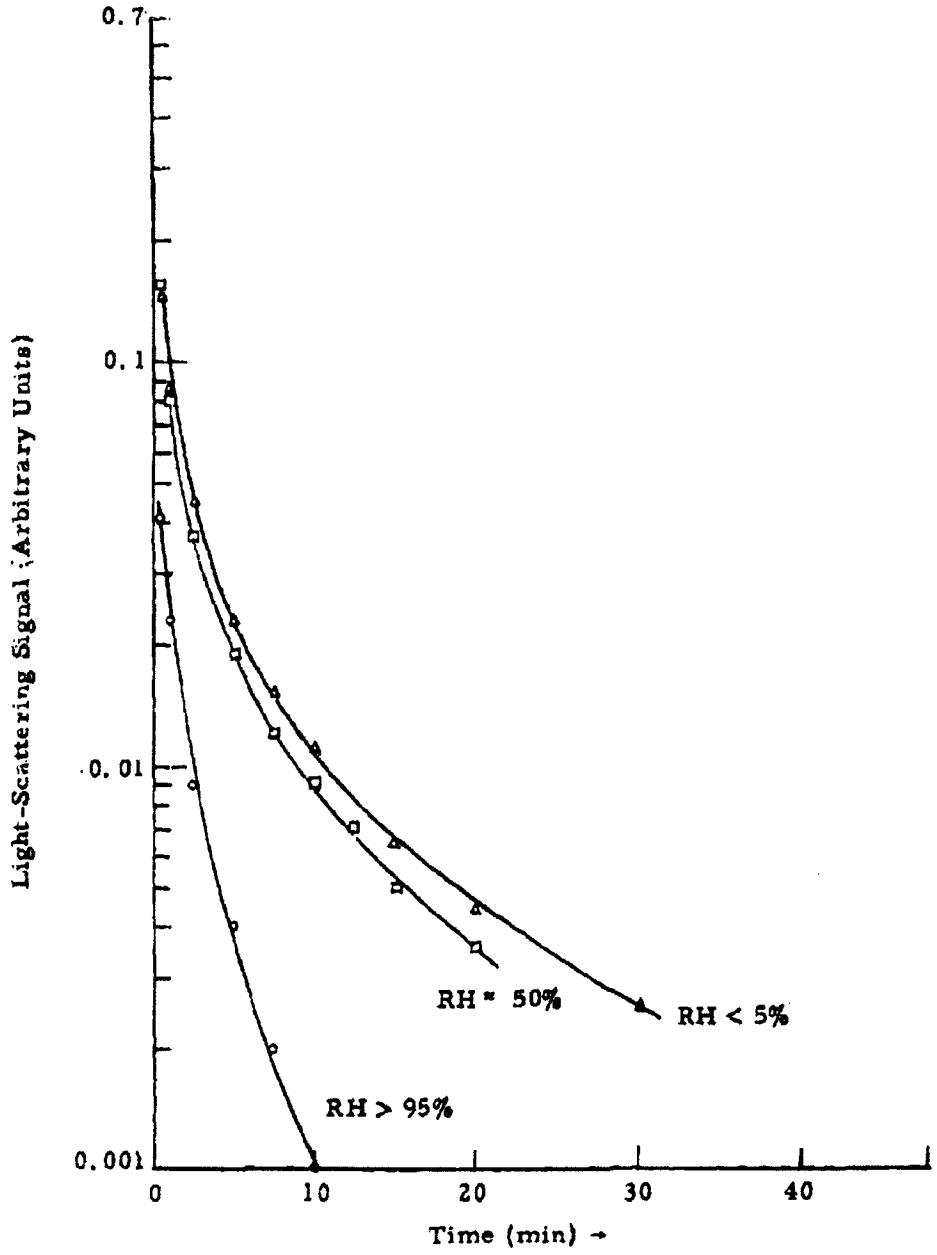

Figure 3.4 Effect of Humidity on Decay of Powdered Milk Aerosols (~550 mg Samples)

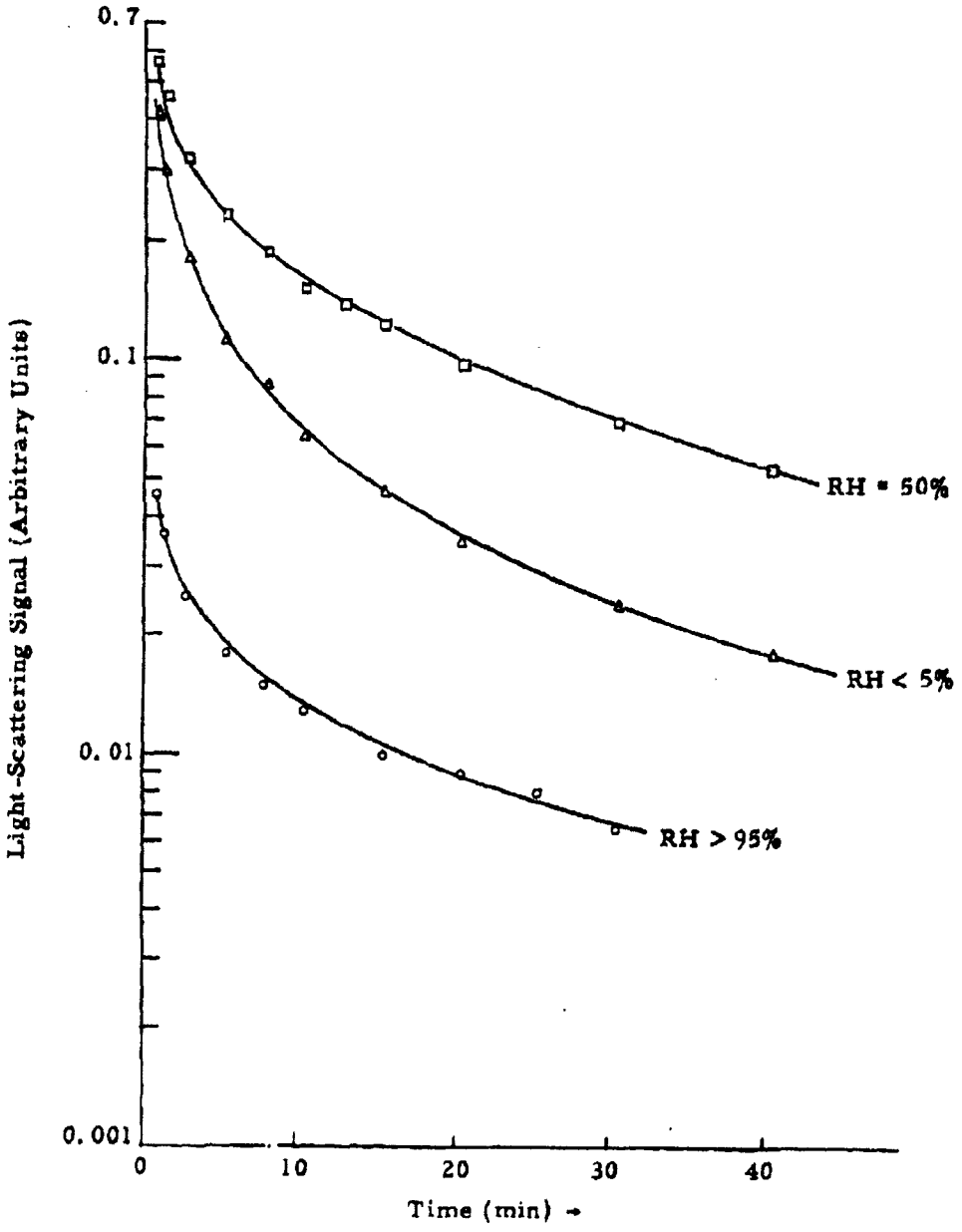

Figure 3.5 Effect of Humidity on Decay of Powdered Sugar Aerosols (~ 530 mg Samples)

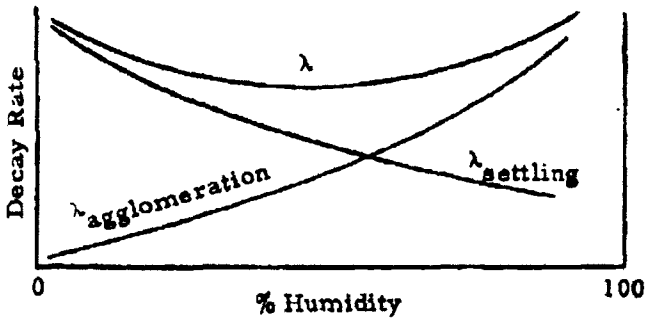

Figure 3.6 Proposed Mechanism for Anomalous Humidity Effect

we shall not speculate further on the mechanisms behind the humidity effects. Certain theoretical considerations that may be pertinent are forthcoming and further experimental work is planned in this area.

3.2 Considerations on Light-Scattering Noise Levels

It was noticed during the work of the last quarter that the noise levels on the light-scattering records were consistently higher for talc aerosols than for saccharin aerosols. Some of the work of this quarter was devoted to investigating this phenomenon. Actual copies of typical records are shown in Figure 3.7. The important point to be noted is that for a given scattering signal, the noise level (breadth of trace) for talc is about twice that for saccharin.

The noise observed may have one or more origins. Fluctuations may arise from the light source, from the aerosol within the scattering volume, from the photomultiplier tube, or from various points in the amplification system. In order to study these points, two systems of illumination other

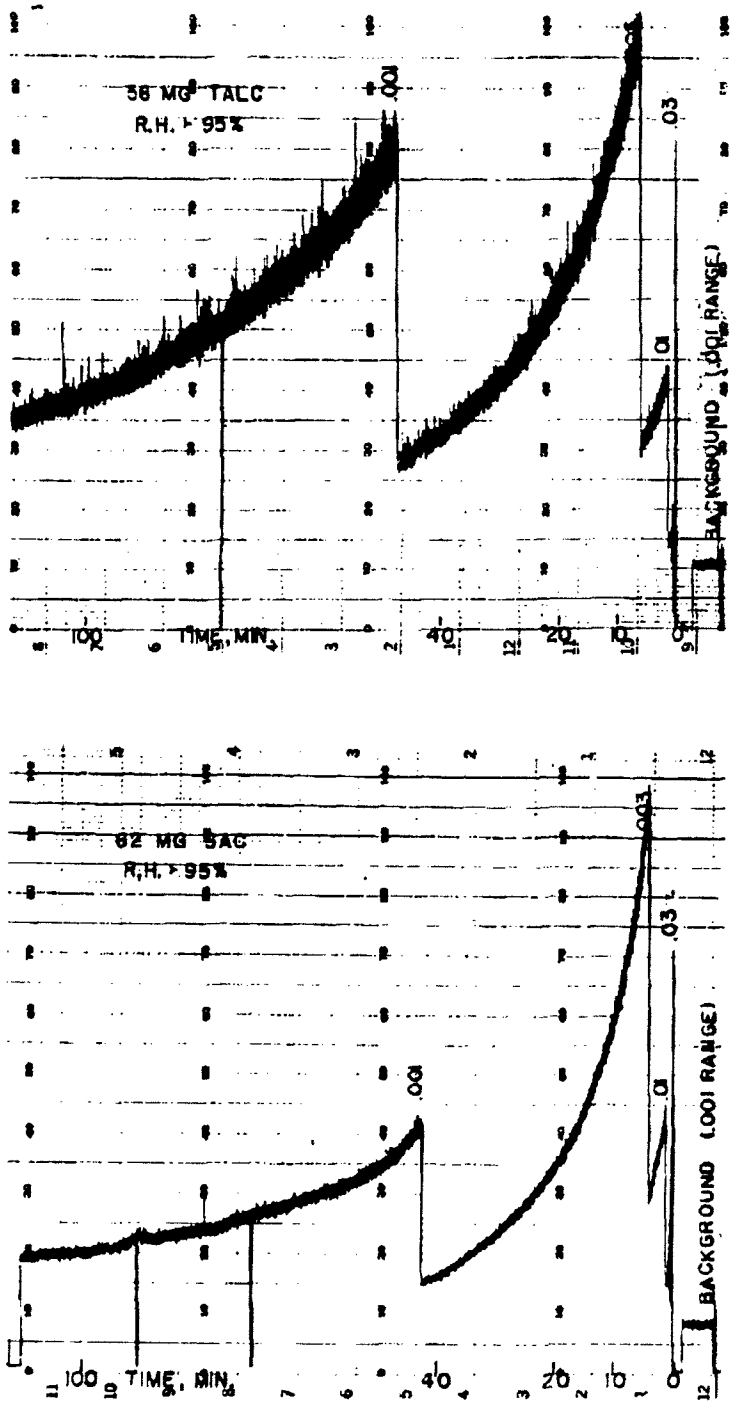

Figure 3.7 Copies of Light-Scattering Records: Top-Talc Aerosol, Bottom-Saccharin Aerosol

than the usual light scattered from an aerosol were tried. The first made use of a radicactive standard light source that was taped inside the chamber to the window facing the photomultiplier tube. Masks were used to control illumination. The second method of illumination consisted of light scattered from a bottle of distilled water placed in the chamber at the scattering volume. Illumination was controlled by adjusting the voltage of the light source. The noise resulting from these two methods of illumination, together with noise levels from talc and saccharin aerosols, are shown in Figure 3.8.

Figure 3.8 shows that the noise levels from the two auxiliary methods of illumination, the radioactive light source and scattering from distilled water, are very nearly equal up to about 1 mv signal. Both aerosol noise levels are somewhat higher. Since the fluctuations in the scattered light are independent of those fluctuations operative without the aerosol*, we have

$$(\text{observed fluctuation})^2 = \begin{pmatrix}\text{fluctuation}\\ \text{due to aerosol}\end{pmatrix}^2 + \begin{pmatrix}\text{intrinsic}\\ \text{fluctuations}\end{pmatrix}^2 .$$

3.3 Mathematical Analysis of Fluctuations in the Light-Scattering Signal

The experimentally discovered phenomena of fluctuations in the light-scattering signal have motivated further theoretical analysis which will be presented in this section. In the process we shall rephrase certain parts of the work presented in the last quarterly report[1] and extend certain definitions given there.

* The fact that the two auxiliary methods of illumination yield the same noise level indicates that this "intrinsic noise" arises in the photomultiplier tube or the subsequent electronics. A simple calculation based on the theory of the shot effect indicates that the origin is in fact shot noise in the photomultiplier tube.

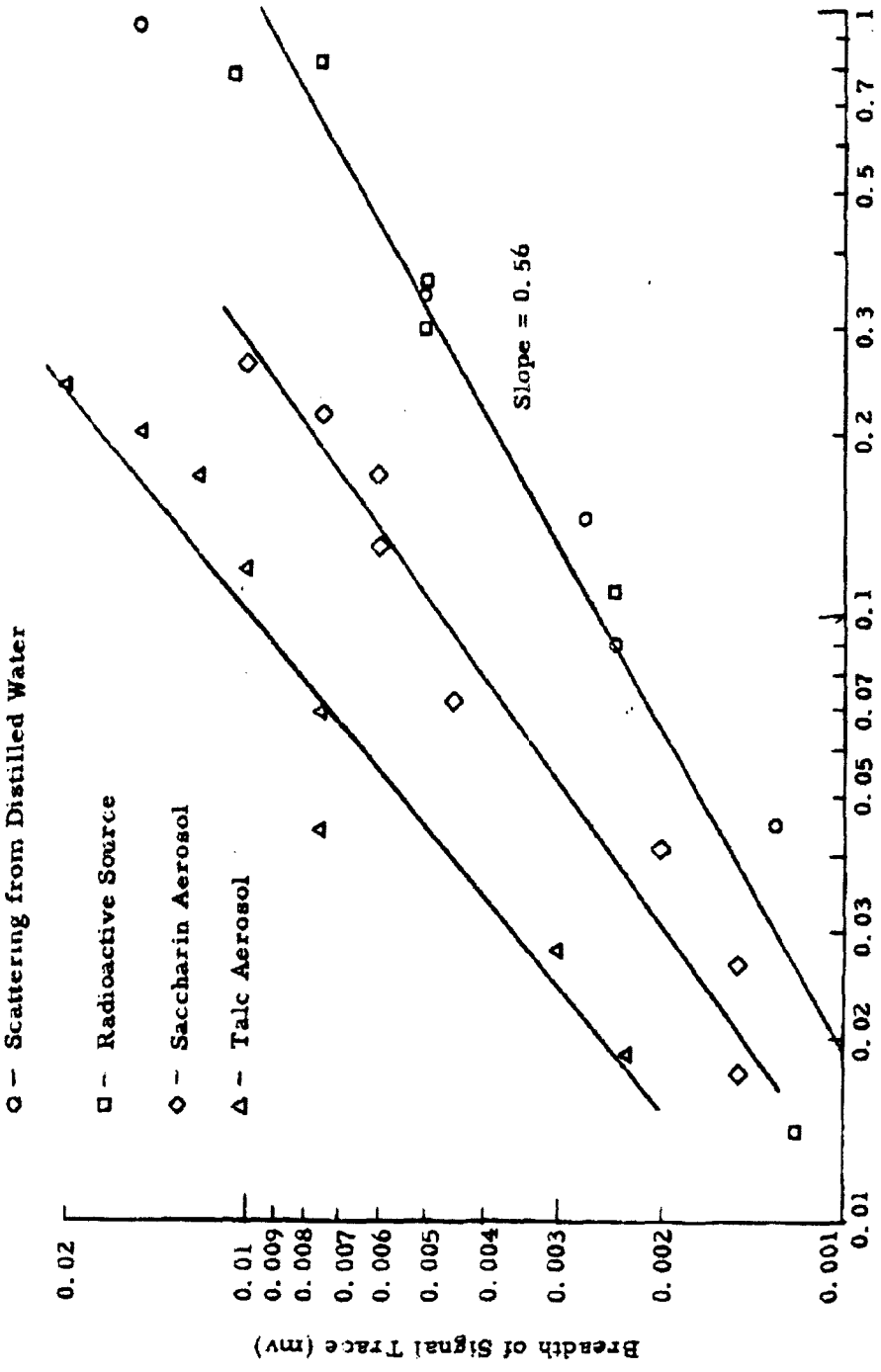

Figure 3.8 Noise Levels for Various Scattering Agencies

Let N(t) be the number of particles in the aerosol at time t. The corresponding cumulative particle size distribution N(d, t) and particle size distribution N'(d, t) are defined as before[3], as are the fractional distributions n(d, t) and n'(d, t).

The analysis that follows will emphasize the randomness associated with aerosols, a point of view which in light of experience is more in accord with facts than an analysis emphasizing the regularities of aerosols. We assume that at any particular instant t, the N(t) particles are distributed randomly throughout the chamber, the distribution being in a constant state of flux because of air currents. At any particular time t certain particles find themselves in the light-scattering volume[4] δV, while at some later time other particles are so located. We assume that this constant exchange of light-scattering samples is equivalent to random sampling of the aerosol. The following analysis also requires that many samples be taken over an interval of time during which N(t) is approximately constant. An oscilloscope study has shown that this requirement is probably satisfied for the aerosols under study.

Under the assumptions just made, the aerosol sampling process obeys Poisson statistics*, wherein the probability p(m) that exactly m particles are located in a sample of volume δV picked at random is

$$p(m) = \frac{1}{m!} \left[N(t) \frac{\delta V}{V} \right]^m \cdot \exp \left[-N(t) \frac{\delta V}{V} \right] . \qquad (2)$$

If many independent samples of size δV are taken, the expected average $\overline{m}$ of m is

$$\overline{m} \equiv \sum_{m=0}^{\infty} mp(m) = N(t) \frac{\delta V}{V} , \qquad (3)$$

*See, for example, the discussion of Poisson's distribution in Feller, An introduction to the theory of probability and its application, Vol. I, 2nd edition, John Wiley & Sons.

while the expected mean square fluctuation $\overline{(m - \overline{m})^2}$ is

$$\overline{(m - \overline{m})^2} \equiv \overline{m^2} - \overline{m}^2 = \sum_{m=0}^{\infty} m^2 p(m) - \overline{m}^2 \qquad (4)$$

$$= (\overline{m} + \overline{m}^2) - \overline{m}^2 = \overline{m} \ .$$

The light scattered may now be calculated on a statistical basis*. Suppose that at time t it is known that there are exactly m particles in δV. The light scattered is[4]

$$(I_s)_m = I \cdot \delta\Omega \cdot \sum_{i=1}^{m} \sigma(d_i) \ , \qquad (5)$$

where d_i is the diameter of the i^{th} particle and $\sigma(d_i)$ is the corresponding scattering cross-section. The d_i, however, must be predicted by statistics. If the i^{th} of the m particles is regarded as picked at random, the probability that its diameter is in the range $(d_i, d_i + \delta d_i)$ is just $n'(d_i, t)$. The average value $\overline{(I_s)}_m$ of $(I_s)_m$ is found by averaging $(I_s)_m$ over all possible values of each d_i. Thus

$$\overline{(I_s)}_m = \underbrace{\int\int \ldots \int}_{m \text{ integrals}} (I_s)_m \cdot n'(d_1, t)\, n'(d_2 t) \ldots n'(d_m, t)\, \delta d_1\, \delta d_2 \ldots \delta d_m$$

$$= I\, \delta\Omega \int\int \ldots \int \left[\sum_{i=1}^{m} \sigma(d_i) \right] n'(d_1, t)\, n'(d_2, t) \ldots n'(d_m, t)\, \delta d_1 \delta d_2 \ldots \delta d_m$$

* The analysis given here is modeled on the analysis of the shot effect by S. O. Rice, Mathematical analysis of noise, Bell System Technical Journal, Vol. 23 & 24; The reasoning is further elucidated in Lindsey and Margonau, Foundations of physics, Dover Press.

$$= I\delta\Omega \cdot \sum_{i=1}^{m} \left[\int \sigma(d_1)\, n'(d_1, t)\, \delta d_1 \right] \cdot \underbrace{\int n'(d_1, t)\, \delta d_1 \ldots \int n'(d_m, t)\, \delta d_m}_{i^{th} \text{ integral missing}}$$

$$= I\,\delta\Omega \sum_{i=1}^{m} \int \sigma(d_1)\, n'(d_1, t)\, \delta d_i \,. \tag{6}$$

The latter step makes use of

$$\int n'(d_1, t)\, \delta d_1 = \int n'(d_2, t)\, \delta d_2 = \ldots = 1.$$

Similarly, the m integrals in the sum differ only in integration variable, so that

$$\overline{(I_s)}_m = m \int \sigma(d)\, n'(d, t)\, \delta d$$

$$= m\, \bar{\sigma} \quad , \tag{7}$$

where use has been made of the definition of the average cross-section $\bar{\sigma}$.

At this point the restriction to m particles may be lifted. The average scattered light $\overline{I_s}$ is given by

$$\overline{I_s} = \sum_{m=0}^{\infty} p(m) \cdot \overline{(I_s)}_m$$

$$= I\,\delta\Omega\, \bar{\sigma} \sum_{m=0}^{\infty} m p(m)$$

$$= I\,\delta\Omega\, \overline{m}\, \bar{\sigma} \,. \tag{8}$$

The calculation scheme used is somewhat overpowerful for this problem, the result of which could have been seen directly. The same method, however, may be used for the more subtle problem of calculating the fluctuation of I_s.

The fluctuation of I_s is found by calculating $\overline{I_s^2}$ and making use of the identity:

$$\overline{(I_s - \bar{I}_s)^2} = \overline{I_s^2} - \bar{I}_s^2 \quad . \tag{9}$$

The expression for I_s^2 for the case where m particles are assumed is

$$(I_s^2)_m = (I_s)_m \cdot (I_s)_m = \left[I\delta\Omega \sum_{i=1}^{m} \sigma(d_i) \right] \cdot \left[I\delta\Omega \sum_{j=1}^{m} \sigma(d_j) \right] . \tag{10}$$

Averaging over the variety of particle sizes gives:

$$\overline{(I_s^2)_m} = (I\,\delta\Omega)^2 \sum_{i=1}^{m} \sum_{j=1}^{m} \int\int \ldots \int \sigma(d_i)\, \sigma(d_j)\, n'(d_1, t)\, n'(d_2, t) \ldots$$

$$n'(d_m, t)\, \delta d_1\, \delta d_2 \ldots \delta d_m \quad . \tag{11}$$

The double sum contains two distinct types of terms, as seen in

$$\overline{(I_s^2)_m} = (I\,\delta\Omega)^2 \sum_{i=1}^{m} \int \left[\sigma(d_i)\right]^2 n'(d_i, t)\, \delta d_i$$

$$+ (I\,\delta\Omega)^2 \sum_{\substack{i=1 \\ i \neq j}}^{m} \sum_{j=1}^{m} \left[\int \sigma(d_i)\, n'(d_i, t)\, \delta d_i\right] \cdot \left[\int \sigma(d_j)\, n'(d_j, t)\, \delta d_j\right] . \tag{12}$$

There are m terms of the first type, whereas the remaining $m^2 - m$ terms are of the second type. Thus

$$\overline{(I_s^2)}_m = (I\delta\Omega)^2 \, m \, \overline{\sigma^2} + (I\delta\Omega)^2 \, m(m-1) \, \bar{\sigma}^2 \, . \tag{13}$$

Again lifting the restriction to m particles:

$$\overline{I_s^2} = \sum_{m=0}^{\infty} p(m) \cdot \overline{(I_s^2)}_m$$

$$= (I\delta\Omega)^2 \, \overline{\sigma^2} \sum_{m=0}^{\infty} m \, p(m) + (I\delta\Omega)^2 \, \bar{\sigma}^2 \sum_{m=0}^{\infty} m(m-1) \, p(m)$$

$$= (I\delta\Omega)^2 \left[\bar{m} \, \overline{\sigma^2} + \bar{m}^2 \, \bar{\sigma}^2 \right] \, . \tag{14}$$

The mean square fluctuation $\overline{(I_s - \bar{I}_s)^2}$ is therefore

$$\overline{(I_s - \bar{I}_s)^2} = (I\delta\Omega)^2 \, \bar{m} \, \overline{\sigma^2} \, , \tag{15}$$

and the fractional root mean square fluctuation is

$$\frac{1}{\bar{I}_s} \left[\overline{(I_s - \bar{I}_s)^2} \right]^{\frac{1}{2}} = \frac{1}{\sqrt{\bar{m}}} \frac{\sqrt{\overline{\sigma^2}}}{\bar{\sigma}} \, . \tag{16}$$

This completes the calculation of the fluctuation. It is to be noted that in the case of a monodisperse aerosol, $\bar{\sigma}^2 = \overline{\sigma^2}$ so that the fluctuation provides a direct measure of

$$\bar{m} = N(t) \, \frac{\delta V}{V} \, . \tag{17}$$

If the aerosol is polydisperse, we have $\overline{\sigma^2} \geq \bar{\sigma}^2$ so that polydispersity increases the fluctuation, as one might expect. The formula shows the form of the dependence.

The formula for the fluctuation is general in that the distribution $n'(d,t)$ from which it is derived has been left quite arbitrary. More specific results are available if a specific form for $n'(d,t)$ is assumed. Before taking the full step, assuming $n'(d, t=o)$ is logarithmic normal, we digress slightly to arrive at an unexpected result. It will now be assumed[5] that

$$\sigma(d) = \frac{d^2}{6\pi} \tag{18}$$

and that

$$N'(d,t) = N'(d,o) \cdot \exp\left[- \frac{v(d)}{H} t \right] . \tag{19}$$

In consequence

$$N(t) = \int N'(d,t)\, \delta d$$

$$= \int N'(d,o) \exp\left[- \frac{v(d)}{H} t \right] \delta d, \tag{20}$$

and

$$n'(d,t) = \frac{N'(d,t)}{N(t)}$$

$$= \frac{N'(d,o) \cdot \exp\left[- \frac{v(d)}{H} t \right]}{\int N'(d,o) \cdot \exp\left[- \frac{v(d)}{H} t \right] \delta d} . \tag{21}$$

The expression for the average scattered light, Equation (8), is

$$\overline{I_s} = I\delta\Omega\ \overline{m}\ \overline{\sigma} = I\delta\Omega\ N(t)\ \frac{\delta V}{V} \int \sigma(d)\, n'(d,t)\, \delta d$$

$$= I\delta\Omega\ \frac{\delta V}{V} \int \sigma(d)\, N'(d,t)\, \delta d \quad . \tag{22}$$

The rate of change of I_s is

$$\frac{d\overline{I_s}}{dt} = I\delta\Omega\ \frac{\delta V}{V} \int \sigma(d)\ \frac{\partial}{\partial t}\ N'(d,t)\, \delta d \quad . \tag{23}$$

Now,

$$\frac{\partial}{\partial t}\ N'(d,t) = N'(d,o)\ \frac{\partial}{\partial t}\ \exp\left[-\frac{v(d)}{H}\, t\right]$$

$$= -N'(d,o)\ \frac{v(d)}{H} \exp\left[-\frac{v(d)}{H}\, t\right]$$

$$= -\frac{v(d)}{H} \cdot N'(d,t) \quad . \tag{24}$$

It may be noted, however, that

$$\frac{v(d)}{H} = \frac{\rho g d^2}{18\eta H} = \frac{\pi\rho g}{3\eta H} \cdot \frac{d^2}{6\pi} = \frac{\pi\rho g}{3\eta H}\, \sigma(d) \quad , \tag{25}$$

so that

$$\frac{d\bar{I}_s}{dt} = -\frac{\pi\rho g}{3\eta H} I\delta\Omega \frac{\delta V}{V} \int [\sigma(d)]^2 N'(d,t)\,\delta d$$

$$= -\frac{\pi\rho g}{3\eta H} I\delta\Omega \frac{\delta V}{V} N(t) \int [\sigma(d)]^2 n'(d,t)\,\delta d$$

$$= \frac{\pi\rho g}{3\eta H} \bar{m}\,\overline{\sigma^2}\, I\delta\Omega \quad . \tag{26}$$

But $(I\delta\Omega)^2 \bar{m}\ \overline{\sigma^2}$ is the mean square fluctuation. Thus

$$\frac{d\bar{I}_s}{dt} = -\frac{\pi\rho g}{3\eta H} \frac{1}{I\delta\Omega} \overline{(I_s - \bar{I}_s)^2} \quad . \tag{27}$$

In other words, the rate of change of the light scattering is proportional to the fluctuation. The remarkable point is that the expression is quite independent of the initial particle size distribution $N'(d, o)$. This relation may afford a means of directly checking the degree of validity of the assumed relations:

$$\sigma(d) = \frac{d^2}{6\pi}$$

and

$$N'(d,t) = N'(d,o) \cdot \exp\left[-\frac{v(d)}{H} t\right] \quad . \tag{28}$$

It may also be noted that, under the hypotheses introduced:

$$\frac{d}{dt} \ln \bar{I}_s = -\frac{\pi\rho g}{3\eta H} \frac{\overline{\sigma^2}}{\bar{\sigma}} \tag{29}$$

which may help to clarify the significance of the logarithmic derivative. It is independent of $\overline{m}$ as, of course, it should be for nonagglomerative decay.

If it is assumed that the initial particle size distribution is logarithmic normal, it may be seen that the various expressions take on the form of the turbulent settling integral discussed in the last report. This point will be reported on at a later date.

3.4 A Swirl Powder Disperser

It was mentioned previously[6] that the present method of dispersing powders in the aerosol decay chamber leaves something to be desired. During the present report period, a new dispersing system was designed. The new dispersing system differs from the old system in that 1) it is intended to introduce the powder over a period of several seconds rather than in a sudden burst as did the old disperser; and 2) the new disperser is designed to partially aerosolize the powder before injection.

The swirl disperser, shown schematically in Figure 3.9, consists of a shallow cylindrical chamber which is mounted edgewise on the aerosol chamber wall. Dry nitrogen is admitted into the cylindrical disperser chamber (which is two inches in diameter and about one-half inch deep) through two tangential jets (711 microns in diameter) in such a way that the powder is made to swirl. There are two exit ports, each 1016 microns in diameter, that form a 45-degree angle with the tangent to the powder chamber. Therefore, powder particles must negotiate a sharp 45-degree turn in order to leave the disperser. The ratio of outlet port area to inlet port area is about 2:1; therefore, at equilibrium flow conditions, the pressure in the dispersing chamber is one-half the supply pressure. Both inlet and exit flow are sonic, provided the supply pressure is greater than 45 psi. Flow rate is of the order of liters of free gas per second.

An experimental model of the new disperser-produced aerosols that in general were considerably more stable than those produced by the old disperser. The major drawback of the swirl disperser is that a powder residue

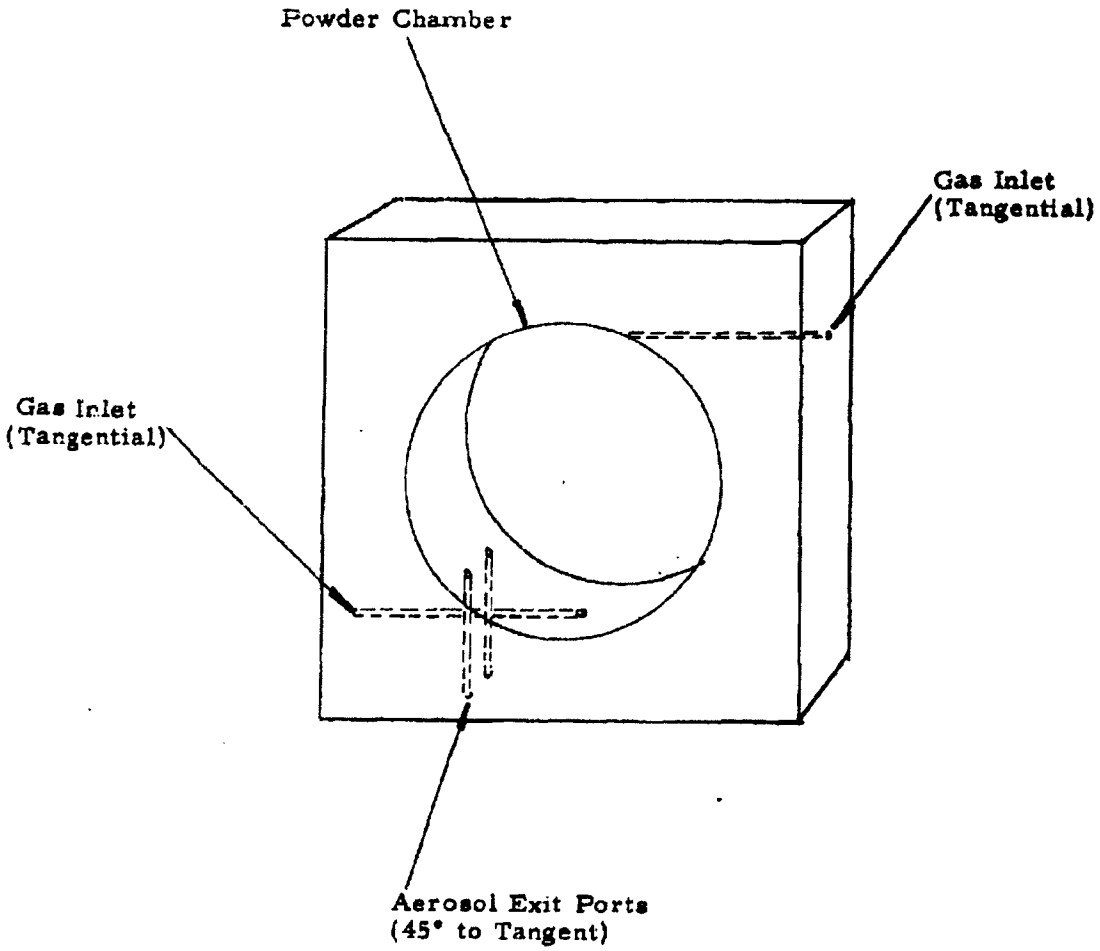

Figure 3.9 Swirl Powder Disperser

coats, or in the case of some powders, actually cakes up the inside of the disperser. A carefully made model with polished internal surfaces may alleviate these difficulties. While the swirl disperser may not be the ultimate dispersing system, it at least provides an alternative method of dispersing powders.

3.5 Conclusions and Plans for Future Work

The experimental work of this quarter has revealed some pronounced effects of humidity on the stability of aerosols. One surprising feature is that for some powders the decay rate does not vary monotonically for increasing humidity. Some of the humidity runs will be repeated using the new dispersing technique described in Section 4.

Investigations up to this point have involved injecting particles into an atmosphere containing a background level of about 10^3 ions/cm^3. Future work is planned where this ion concentration may be pushed up to 10^6/cm^3 by means of a Whitby-type ion generator. This device produces either positive, negative, or equal amounts of positive and negative ions.

One may expect that work with different ion concentrations will add considerably to our knowledge of aerosol stability. Ion injection may prove a useful experimental tool in determining the relative importance of decay processes, since injection of ions of one sign only will clearly favor aerosol decay by precipitation on walls, whereas injection of ions of both signs would favor agglomeration. The literature on charged aerosols is rather extensive and should prove helpful in interpreting experimental results.

4. DISSEMINATION AND DEAGGLOMERATION STUDIES

4.1 General

During this period the blow-down wind tunnel was utilized in three separate investigations related to the dissemination of dry, finely-divided materials. Major emphasis was devoted to defining the maximum bulk density of Sm which could be efficiently aerosolized by the aerodynamic break-up mechanism. For these tests the concentration of the fine aerosol cloud was determined over a range of bulk densities. When used in conjunction with our other methods of assessing the aerosol, i.e., filter and impactor samples for observation of small and large agglomerates respectively, this method serves to establish the point where dissemination becomes inefficient as bulk density is increased. Secondly, an investigation was conducted to determine the aerodynamic performance of the ejector shroud component of the prototype dry agent disseminator, so as to minimize the contamination of the store. Thirdly, a study was made of the effect of storing Sm in a compacted state.

4.2 Aerosol Concentration Measurements

In studying the performance of the GMI-3 disseminator in the wind tunnel at a flow rate of 30 lb/min by use of the full-flow impactor, it was found that the quantity of Sm in the form of large agglomerates (100 to 500 microns) increased rapidly when the bulk density was increased above 0.60 g/cm^3. However, at these high densities it was impossible to determine directly the quantity of material comprising these agglomerates, since many of them were impacted on the tunnel wall opposite the point of ejection. Therefore, it was found advantageous to sample the fine aerosol, which was essentially deagglomerated, to determine its change in concentration.

Impactor tests have shown that the large agglomerates were heavily concentrated in the top half of the tunnel, opposite the point of dissemination. Also, it was found that the fine deagglomerated aerosol cloud was located along the bottom wall. In order to sample the fine aerosol, the high-velocity sampling probe was located at 0.5 inch from the bottom wall and samples were collected on Millipore filters. The quantity of Sm collected was determined by measuring the turbidity of the samples with a calibrated Bausch and Lomb spectrophotometer (light extinction method).

In Figure 4.1 the results of this work are given for free stream Mach numbers 0.5 and 0.8. The measurements indicate that the concentration of the fine, deagglomerated aerosol is essentially independent of the bulk density in the range 0.33 to 0.57 g/cm^3. However, above this range the quantity of material in the fine aerosol cloud decreases with increasing bulk density. Conversely, the results indicate that as the bulk density exceeds 0.57 g/cm^3, a greater quantity of the material is comprised of large agglomerates which do not readily break up.

Notice that the two curves break at approximately the same bulk density. This was a rather unexpected result since the maximum aerodynamic force exerted on agglomerates during dissemination is proportional to the square of the free stream velocity. At Mach number 0.8 the deagglomeration force is about 2.5 times that at Mach number 0.5. An explanation for this behavior is that the strength of the large agglomerates increases rapidly with bulk density in the region of the break point. Figure 4.2 shows the force required to compact this lot of Sm to bulk densities up to 0.61 g/cm^3. The curve is an exponential that increases rapidly with increasing bulk densities above the 0.55 g/cm^3 level.

The experimental technique employed in this study, measurement of the deagglomerated aerosol concentration, depends on the classification of material into large agglomerates and a fine aerosol. In order to determine whether the samples collected were representative of the fine aerosol concentration and to determine the effect of sampling probe position, the

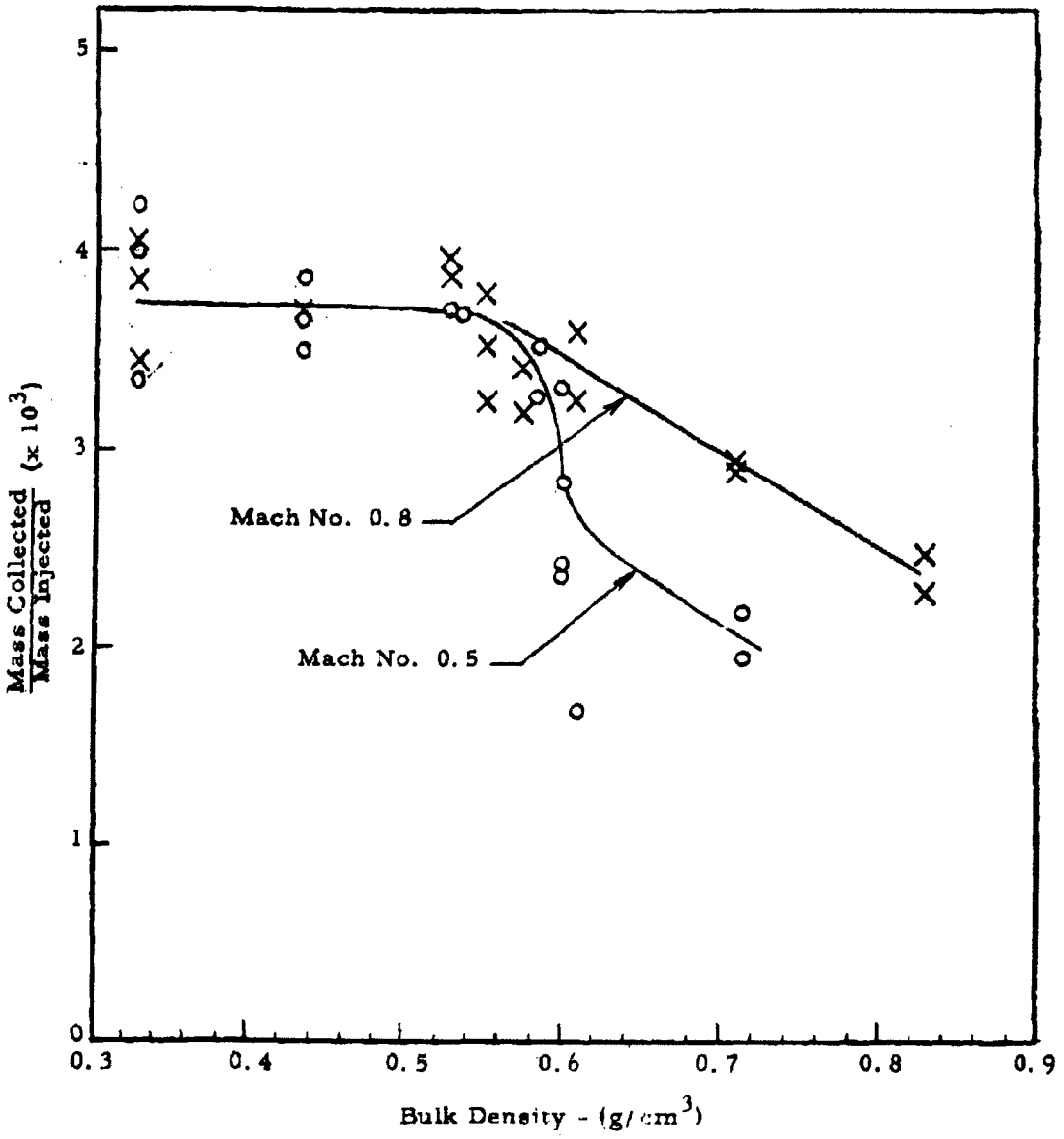

Figure 4.1 Concentration of Fine Sm Aerosol Cloud in Wind Tunnel as a Function of Bulk Density – Sampling Probe at 0.5 inches from Wall

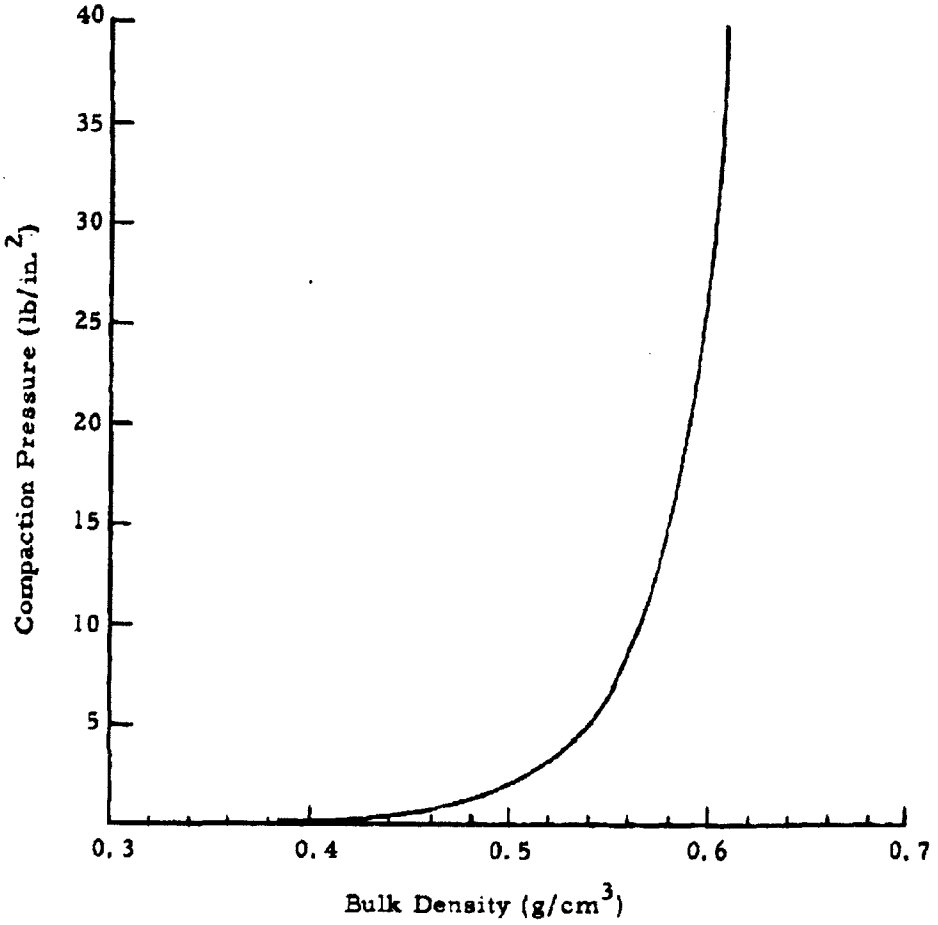

Figure 4.2 Pressure Required to Compact Sm having a Mass Median Diameter of 6.2 Microns

concentration gradient within the fine aerosol cloud was measured for the two bulk densities 0.33 and 0.57 g/cm^3. The results are shown in Figure 4.3. The concentration of the aerosol cloud was essentially the same for the two cases, indicating that the quantity of material that was deagglomerated during dissemination was similar. There appears to be some difference in the gradient at the 0.75-inch distance; however, this should have only a small effect on the whole fine aerosol cloud. The difference in the absolute values shown in Figures 4.1 and 4.3 is due to an essentially systematic error in the data of Figure 4.1. Since this study is concerned with relative changes in concentration, such an error does not affect the interpretation of the data.

It can be concluded from this study that the maximum Sm bulk density which is feasible for dissemination is about 0.58 g/cm^3. It is important to realize that the Sm simulant was not stored in the compacted state for this work. Recent data indicate that storage of the compacted material will somewhat reduce this value (see Section 4.5).

4.3 Shroud Investigation - Prototype Dry Agent Disseminator

In planning the prototype dry agent disseminator, it was decided that the agent should be injected into the air stream at a substantial distance outward from the disseminator store to prevent excessive contamination of the unit. Wind tunnel studies have shown that the agent aerosol cloud will flow along the skin of the store if the orifice is positioned flush with the surface.

The original shroud design is shown in our previous report[7]. It projects outward five inches from the store. Because the requirements that the shroud must contain a valve mechanism and that the cord length could not exceed ten inches, an elliptical cylinder configuration was chosen. This shape is not the most satisfactory from the aerodynamic standpoint, and therefore, a plate was designed for the end of the shroud which would prevent the aerosol from flowing into the low-pressure separation region along the trailing edge.

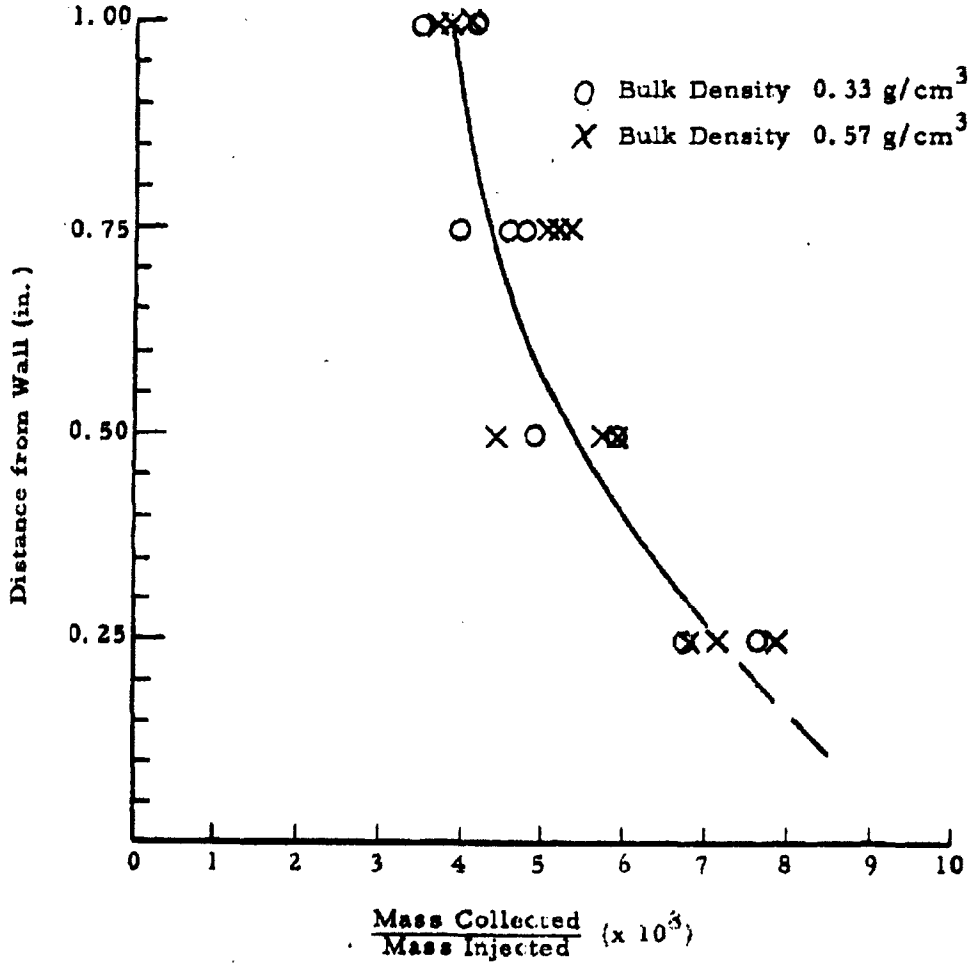

Figure 4.3 Concentration Profile of Fine Aerosol Cloud Generated in Wind Tunnel with Mach Number 0.5 Air Stream

Very little information on such an application is available in the literature. Consequently, it was necessary to investigate its performance in the blow-down wind tunnel. A model of the shroud was constructed to a scale of one-fifth the actual size. The cross-sectional area of the model was approximately 11 percent of that of the tunnel, allowing a free stream Mach number of 0.65 to be investigated without choking the flow at the model. To simulate the prototype unit, the ratio of the wall boundary-layer thickness to model length was made similar to the actual case. The boundary-layer thickness was measured and found to be in agreement with our previously calculated values. The Reynolds number of the shroud is another important parameter. However, it was impossible to simulate the prototype in this respect. The Reynolds number based on the length of the shroud from the leading edge will be about 36.7×10^6 for the prototype unit, while the maximum we could obtain from the model was 2.1×10^6. Since flow separation is retarded with increased Reynolds number, the results from the wind tunnel study can be considered conservative, i.e., the prototype should perform better than the model.

The investigation was primarily based on photographic observations of the aerosol flow pattern and powder deposits on the tunnel wall and model. Aerosols were generated from four materials: talc, zinc cadmium sulfide, iron oxide pigment, and Sm. The pigment was most helpful when studying the powder deposits, while Sm and talc were especially suitable for observing the aerosol flow pattern during the tests.

The first runs were conducted without the end plate mounted on the shroud. The resulting flow pattern was unsatisfactory as a portion of the aerosol flowed downward along the back of the shroud before moving in the downstream direction. There was a large amount of powder deposited on the tunnel wall with this configuration.

By adding the end plate to the shroud the amount of material deposited on the back of the model and tunnel was significantly reduced, although this arrangement was still considered unsatisfactory. Figure 4.4 shows the

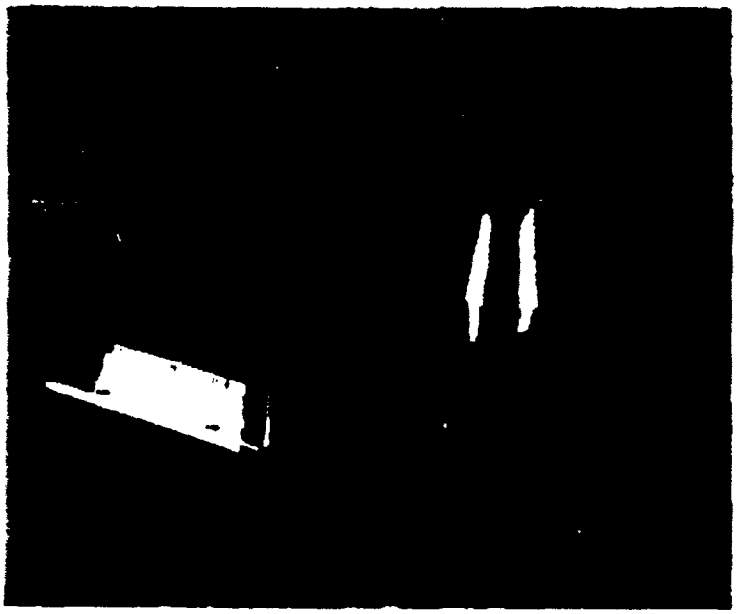

Figure 4.4 Deposition of Iron Oxide on Trailing Edge of Shroud and on Tunnel Wall

model and tunnel wall deposits. Note that on the wall there appears to be two deposit areas. One is located at the back of the shroud while the second begins about three inches downstream of the shroud and continues downward along the tunnel. The explanation for this pattern is that the material was collected on the model because a portion of the aerosol flowed directly into the separation region along the back of the shroud, while the wall deposit resulted from turbulent mixing downstream of the shroud.

Modifications were made to the original model to reduce the effect of flow separation. Roughness elements such as fine emory cloth and wires were secured to the forward surface of the model to generate a turbulent boundary layer on the model and thereby retard the separation point on the model. However when these tests were made, much more material was deposited on the base wall. In actuality these turbulence generators caused more severe separation because they were too thick for the existing boundary layer.

In another case, air was injected into the separation region behind the shroud to increase the pressure. These tests showed that by this technique all material deposits on back of the shroud and on the wall directly behind the shroud could be eliminated. However, the only solution for reducing the downstream wall deposit was to add a faring to the back of the shroud which would reduce turbulent mixing.

Figure 4.5 shows the model faring modification that was tested. The length was increased by 50 percent. Observations and motion pictures such as shown in Figure 4.6 indicated this configuration was a substantial improvement over the original one.

As a result of this wind tunnel study, the shroud design for the prototype unit was modified. The dimensions for the new shroud are given in GMI drawing SK 29100-795 in Appendix A.

To estimate the amount of material that might collect on the disseminator store using the improved shroud design, a known quantity of viable Sm was injected into the wind tunnel. Three areas of the tunnel were washed

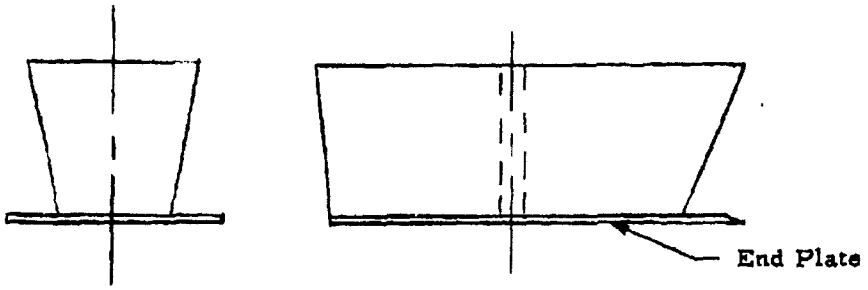

Front View Side View

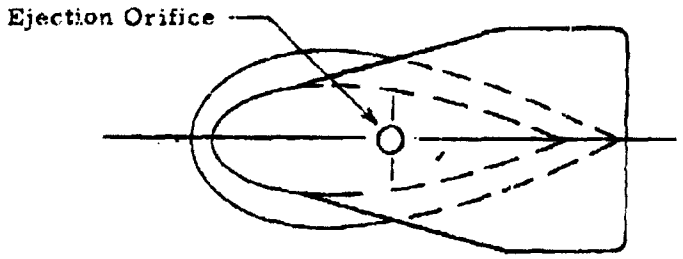

Bottom View

Figure 4.5 Modified Model Disseminator Shroud

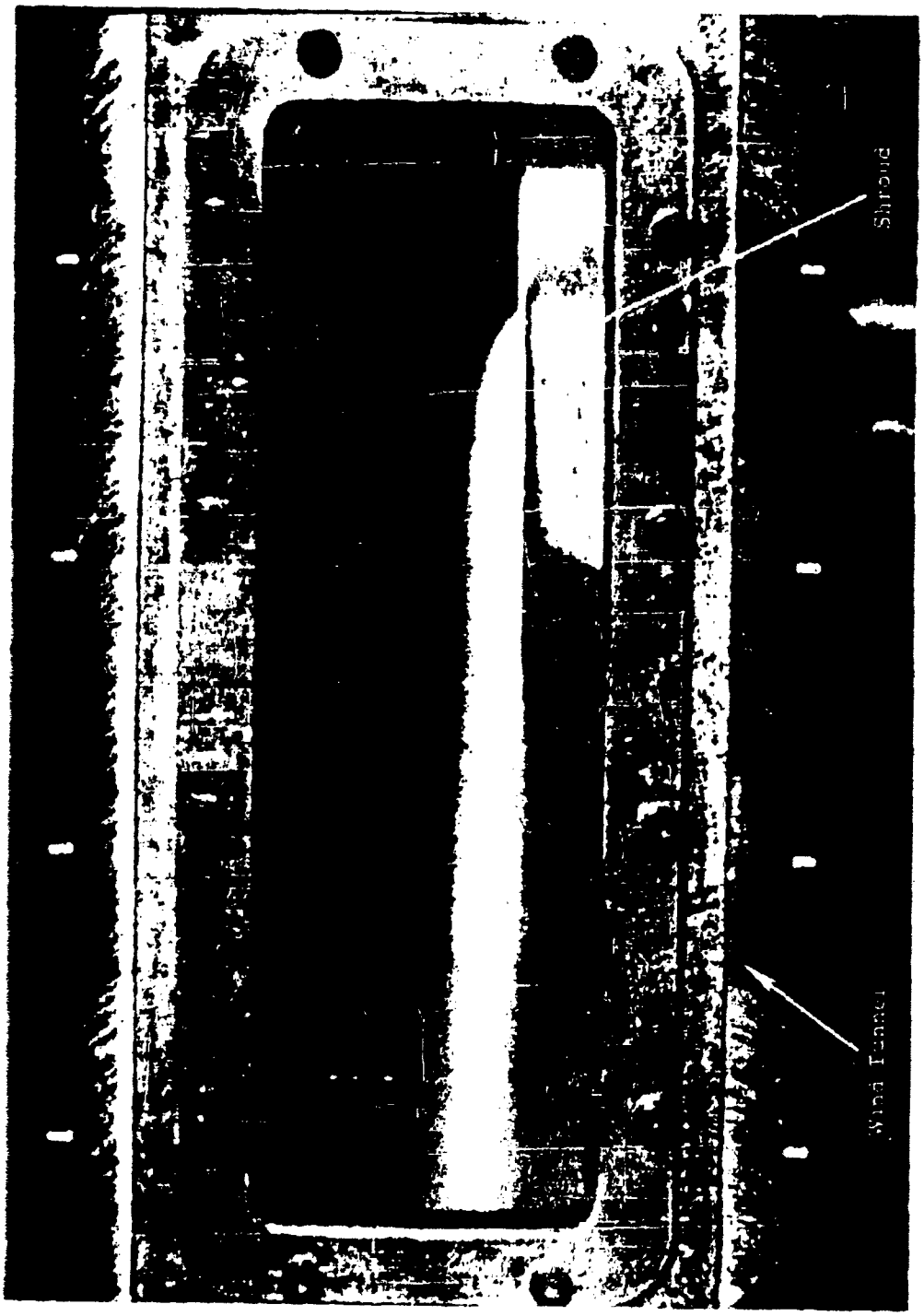

Figure 4.6 Dissemination Flow Pattern of Modified Shroud

down and the samples were assayed using standard techniques. Figure 4.7 shows the concentration of viable organisms on the wall as a function of distance from the injection point. The contamination increase, beginning about nine inches downstream of the ejection point, indicates that turbulent mixing becomes important in this region. If the scale model had been made with a portion of the under side of the store, the tapered tail section would begin at about six inches downstream of the point of dissemination. Since the store begins to taper well ahead of the region where contamination increase was observed, it is believed that the condition will be much more favorable on the prototype unit. The total organism count on the tunnel wall over the 0 to 8-inch length was found to be 5×10^{3} organisms when the wind tunnel was operated at Mach number 0.5. Since 15.1×10^{11} organisms were aerosolized during this run, about 3.3×10^{-7} percent of the material disseminated may collect on the store. It should be emphasized that this is only a rough prediction of the contamination that could be expected on the actual store. It is extremely difficult to simulate the actual flow conditions around such a store with a sealed-down model. However, we believe that if any difference exists between the prototype and the model, the prototype store will have the better performance.

4.4 Wind Tunnel Boundary Layer

In the above shroud investigation it was pointed out that the ratio of boundary-layer thickness to shroud length was important in scaling the model. Therefore, the boundary-layer profile was measured at Mach numbers 0.5 and 0.8 and compared with a theoretical calculation similar to that discussed in our earlier report[8].

The velocity profile was determined by measuring the stagnation pressure at numerous points in the air stream and the static pressure at the tunnel wall. The temperature within the boundary layer was assumed constant. A double impact probe was made from 0.032-inch outside diameter tubing such that for each run two stagnation pressures were measured, one in the free stream and the other within the boundary layer.

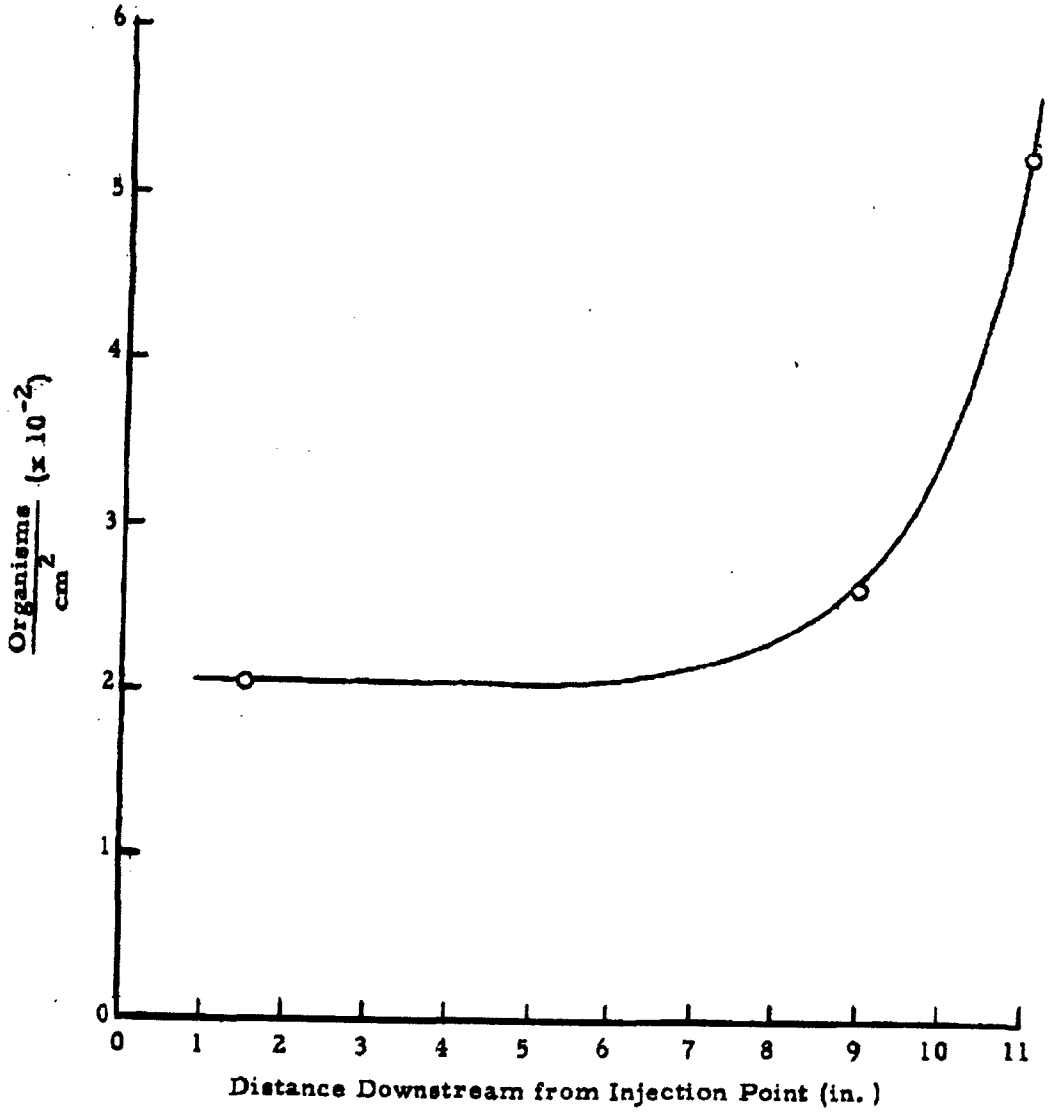

Figure 4.7 Concentration of Viable Organisms on Wind Tunnel Wall

The resulting boundary-layer profiles are shown in Figures 4.8 and 4.9 for free stream Mach numbers 0.5 and 0.8, respectively. The velocity, plotted on the abscissa, is normalized to the free stream velocity. Notice that the measured boundary-layer thickness is similar to the calculated value in both cases and that the free stream velocity is quite uniform. Within the boundary layer, a difference between the theoretical and measured profile may be due to stagnation probe errors or the fact that the boundary layer is in transition from the laminar to the turbulent boundary condition. Correction factors were calculated to determine the probe error, which was found negligible. Using the Reynolds number based on tunnel length (Reynolds number = 1.77×10^6 for Mach number 0.5; Reynolds number = 2.82×10^6 for Mach number 0.8) as the criterion for judgment, it is thought that the boundary layer is in transition between the purely laminar and turbulent conditions.

4.5 Sm Storage Test

The influence of storage on the physical properties of compacted powders is considered an important parameter in dissemination. In the case of noncompacted Sm, storage periods on the order of one year have very little detrimental effect on the aerosolization of the material. In our dissemination tests, only small amounts of strong agglomerates have been observed in material that has been stored at a temperature of 0°F for long periods.

A study was conducted to determine whether storage of Sm in the compacted form would reduce the aerosolization efficiency during dissemination. Therefore Sm was compacted to densities ranging from 0.52 to 0.60 g/cm^3 in a dry box and stored in a deep freeze. After ten weeks the material was disseminated with the GMI-3 fixture at a flow rate of about 30 lb/min into the wind tunnel at Mach number 0.5.

Our standard methods of assessing the aerosol were used which included the full-flow impactor and the sampling probe. There was a definite change in the characteristics of the material – over the full density range covered

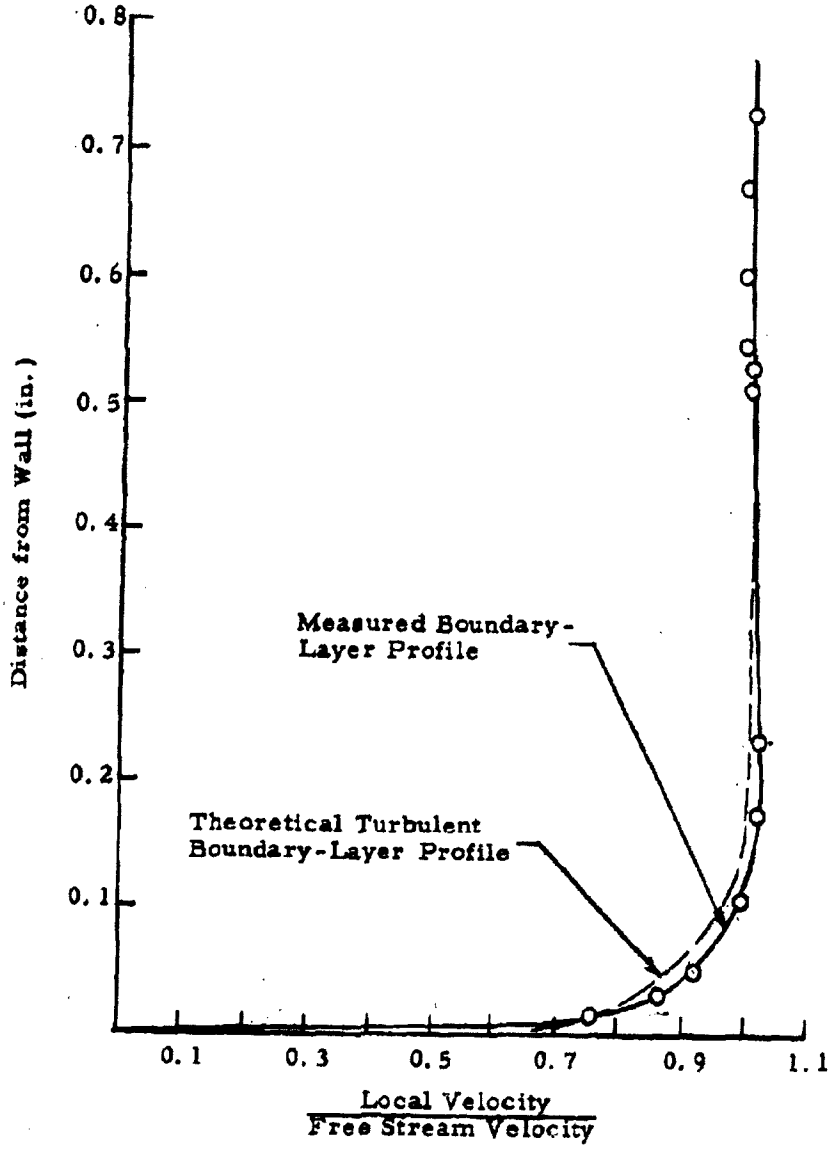

Figure 4.8 Wind Tunnel Boundary-Layer Profile with Mach Number 0.5 Free Stream

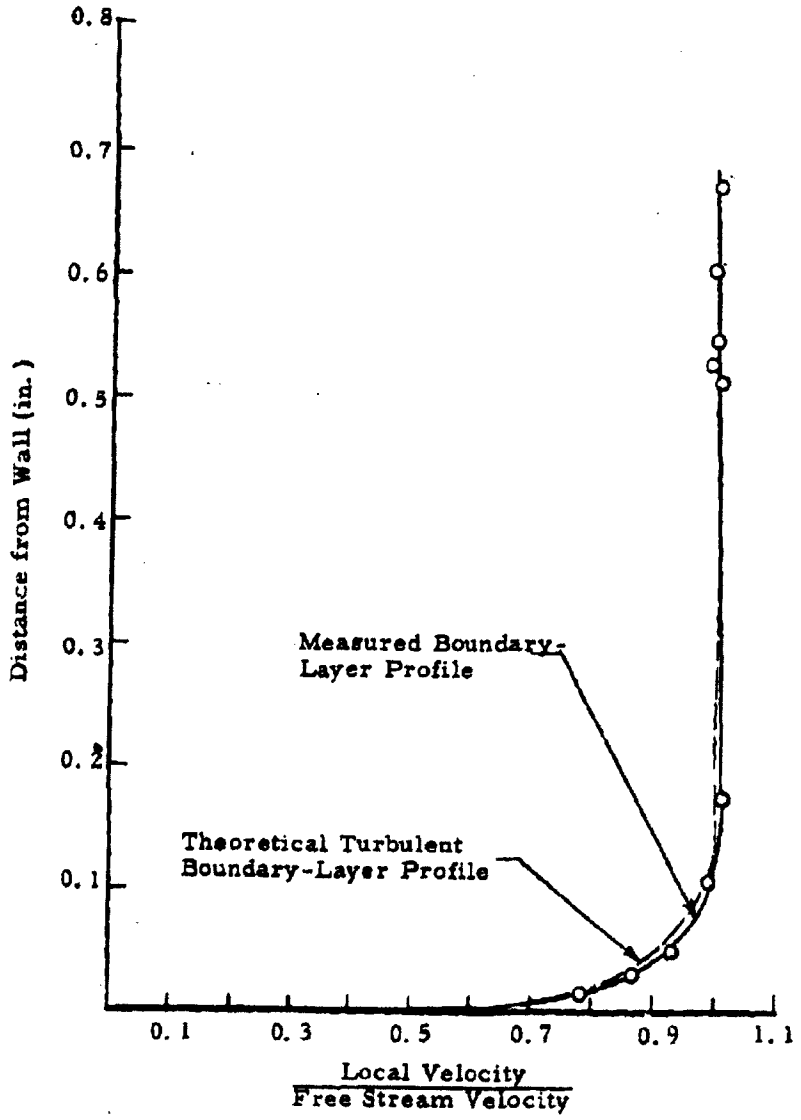

Figure 4.9 Wind Tunnel Boundary-Layer Profile with Mach Number 0.8 Free Stream

there was an increase in agglomerates present in the aerosols. Material stored at density 0.60 g/cm^3 did not aerosolize satisfactorily. An excessive amount of large agglomerates (100 to 500 microns) were observed on the impactor plate. Results with this particular material were similar to those obtained at 0.65 g/cm^3 when the material was not stored in the compacted condition.

Material stored at 0.54 g/cm^3 aerosolized satisfactorily. In analyzing the filters for small scale agglomeration (5 to 20 microns), it was found that because of agglomeration in the 5 to 20-micron range an estimated 14 percent of the useful 1 to 5-micron material was lost[9].

Based on these storage investigations, it appears that the maximum bulk density that can be stored for relatively long periods and subsequently disseminated satisfactorily is about 0.55 g/cm^3. Thus, the effect of storage will tend to reduce the maximum density that can be feasibly disseminated as shown in Figure 4.1.

A larger and more detailed study of the effects of storage on the characteristics of compacted Sm has been planned for the future. It will continue for a year so as to provide data for a relatively long-storage period. In the investigation, information will also be obtained on the viability of the stored Sm.

5. CONTINUATION OF EXPERIMENTS WITH THE FULL-SCALE FEEDER FOR COMPACTED DRY AGENT SIMULANT MATERIALS

5.1 Tests at 0.65 g/cm^3 Density

During the period covered by this report, the full-scale experimental feeder was operated successfully with a load of talc compacted to a density of 0.65 g/cm^3. The schedule permitted only one series of runs to be made at this density. The feeder was then removed from the test stand so preparations could be made for testing the second experimental unit[10], which is similar in design to the first-generation airborne dry agent disseminator.

The arrangement used in conducting this series of runs at 0.65 g/cm^3 density was the same as was used in the work that has been reported previously[11,12]. In a series of 16 runs with the feeder driven at 24 rpm, the average feed rate was determined to be 53 lb/min. Approximately 320 pounds of talc were fed during these runs. Air was supplied to the feeder at rates ranging from 4 to 10 std cfm. The pressure as measured inside the feeder varied from 3 cm Hg at 4 std cfm air rate to 8 cm Hg at 10 std cfm.

The driving torque was observed to vary between 18 and 27 ft-lb. At a speed of 24 rpm, the 27 ft-lb torque requirement results in an input of 0.12 hp to drive the feeder.

5.2 Wind-Tunnel Dissemination of Talc Discharged from Feeder

This series of runs was also used to provide a sample of talc that was disseminated in the high-speed wind tunnel to observe subsequent breakup into basic particles. Virgin talc at an initial compacted density of 0.5 g/cm^3 was desired for this sample, whereas a higher density was to be used for the actual test runs. The virgin material was loaded so as to discharge first when the feeder was operated.

The material sampled from the feeder discharge was disseminated in the wind tunnel using the GMI-3 disseminator and standard techniques. The tunnel was operated at Mach 0.5, and aerosol samples were obtained with the full-discharge impactor on one run and the high velocity sampling probe on the other.

The impactor has a cutoff point at about 6 microns. Essentially no large agglomerated material was found on the impactor, indicating that the talc was deagglomerated very well. The material collected on the filter in the sampling probe was examined under the microscope. There was no significant agglomeration. A majority of the material was collected in the form of basic particles, and the agglomerates that were observed consisted mainly of doublets and triplets.

5.3 Operation with Uncompacted Talc

Because of the emphasis which has been placed on disseminating compacted agents, all of the experiments with the first full-scale experimental feeder were conducted with compacted powder. When the second experimental feeder was completed, a few days were devoted to operating the unit with uncompacted talc. The loose bulk powder was loaded into the disseminator with the unit standing on end. It was possible to put 150 pounds of talc into the unit for each of two test series. The average density was calculated to be approximately 0.25 g/cm^3.

The observations made during these tests with uncompacted talc are not sufficient to justify detailed discussion of the results. However, the unit was capable of feeding the powder in a fairly uniform manner and for this reason the data are presented here to document the tests.

The results are summarized in Table 5.1 and in Figures 5.1 and 5.2. Only the first run with the first loading is documented because the remainder of the material was expended in miscellaneous experimental operation of the unit. Attempts to get high powder flow rates by operating at 37 rpm

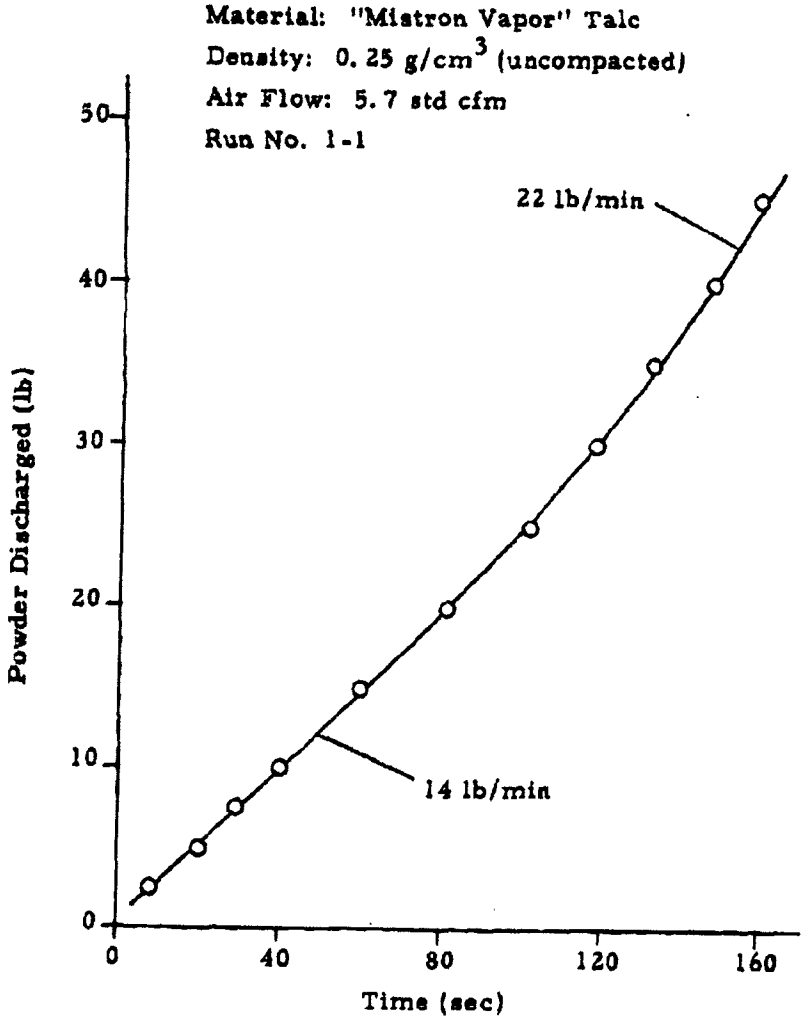

Figure 5.1 Powder Flow Rate Curve for Second Experimental Unit

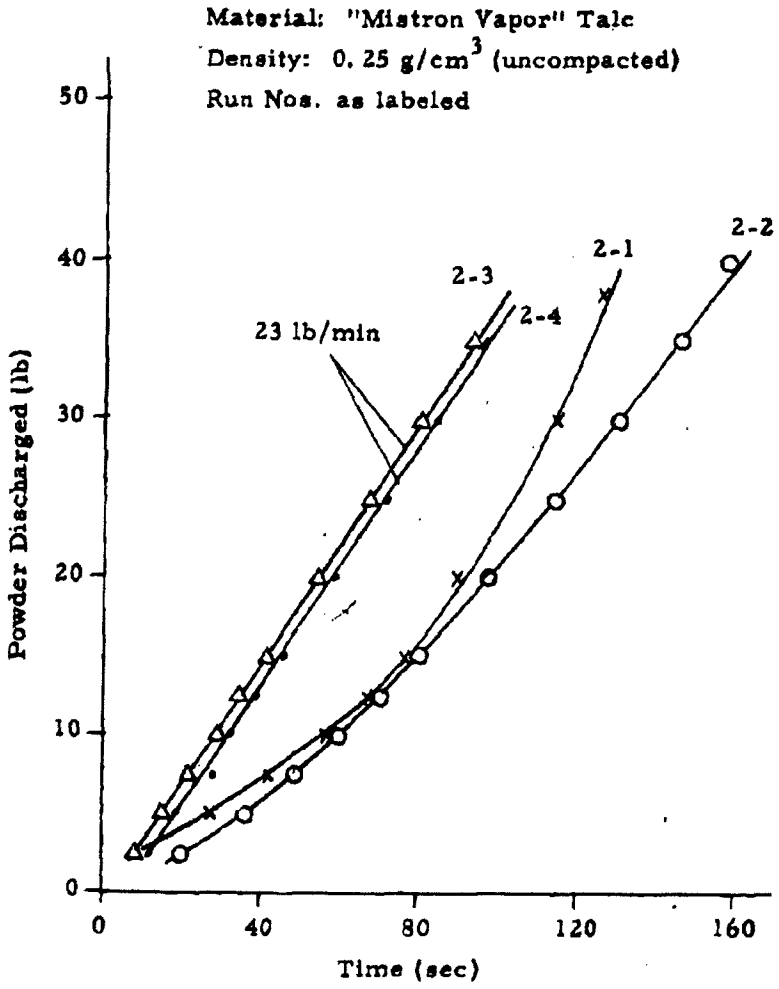

Figure 5.2 Powder Flow Rate Curves for Second Experimental Unit

in runs 2-1 and 2-2 were not successful; the drive belt used to drive the disseminator slipped on the input pulley to the gear reduction unit in the test stand. Operation at 25 rpm resulted in a fairly uniform discharge rate for run 1-2 and identical rates for runs 2-3 and 2-4. The rate of 23 lb/min for runs 2-3 and 2-4 agreed well with the rate at the end of run 1-1.

The maximum torque observed during these trials was approximately 30 ft-lb.

Table 5.1 Summary of Data Obtained While Operating the Second Experimental Unit with Uncompacted Talc

Run No.	Q	Speed (rpm)	Rate (lb/min)
1-1	5.7	25	14-22
2-1	3.1	37*	8.5-34.5
2-2	4.0	37*	10-19.5
2-3	3.5	25	23
2-4	3.1	25	23

* The rpm was not constant because of belt slippage on drive pulley.

6. DESIGN AND FABRICATION OF THE FIRST-GENERATION PROTOTYPE DRY AGENT DISSEMINATING STORE

The general configuration for the first-generation airborne dry agent disseminating store was described in the Eighth Quarterly Progress Report[13]. During the period covered by this report, work has progressed on the design, fabrication, and procurement of all parts of the disseminator.

6.1 Store Structure

During the reporting period, a purchase order was placed with Fletcher Aviation Company of El Monte, California for fabrication of the outer and inner tank structures. Parts being fabricated by Fletcher include:

1) The outer tank skin
2) The strong back casting
3) Tank reinforcement rings
4) Bayonet attachment rings
5) Inner tank

Fletcher Aviation Company will also install the foam insulation between the inner and outer tank.

Figures 6.1 through 6.4 show fabrication in process at Fletcher Aviation Company. In Figure 6.1, an end ring is being welded on an outer tank center section. The four holes in the tank section are for the lug attachments. Figure 6.2 shows an outer tank center section and a strong back casting. Bayonet rings on tank center and tail sections can be seen in Figure 6.3. Figure 6.4 shows an end ring being welded on an inner tank.

Three store structures have been ordered -- one for the airborne store for flight tests, and two for laboratory structural tests. The structural tests are scheduled for the latter part of October, 1962.

Figure 6.1 Welding an End Ring on Outer Shell at Center Section

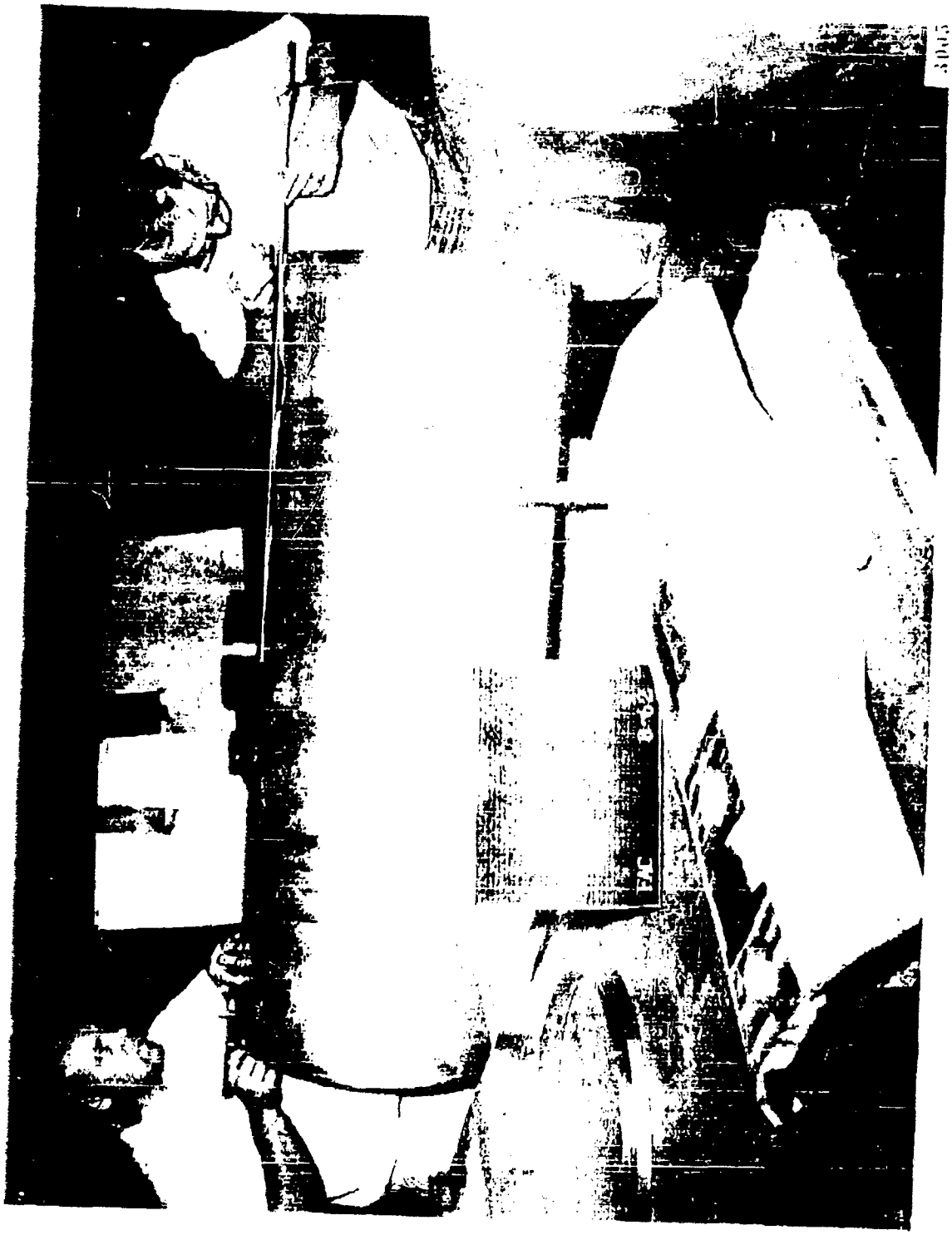

Figure 6.2 Strong Back Casting and Outer Shell of Center Section

Figure 6.3 Bayonet Rings on Center and Tail Sections

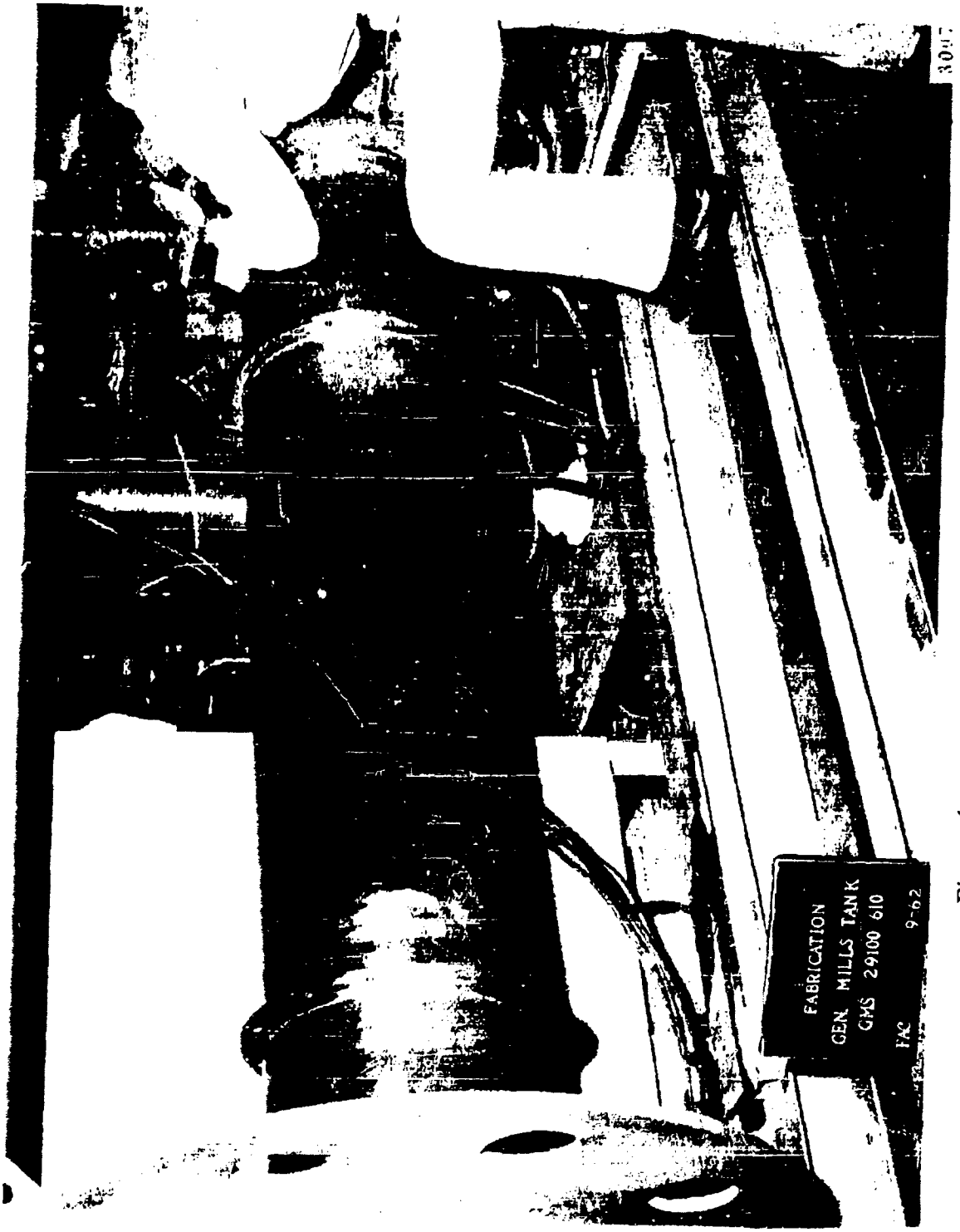

Figure 6.4 Welding an End Ring on Inner Tank

6.2 Rotary Actuator Assembly

During the reporting period, the design of the rotary actuator was completed and all parts were released for fabrication. At the close of the period about 75 percent of the designed parts had been fabricated and all of the purchased items, including the drive motor, had been received.

A method of mounting the motor leads within the actuator housing was developed. This permits the motor shell and support to rotate with respect to the outer shell during the change of gears for speed selection.

During the shifting of drive speeds, the motor pinion becomes completely disengaged from one driven gear before engaging the next. Since all gears are in a completely random rotational position, there is a possibility of interference when attempting a new gear mesh. To overcome the problem, if it should occur, a system was developed to "jog" the motor armature (and shaft and gear) when in the disengaged position. By means of a switch and set of relays, a short electrical impulse is delivered to the drive motor producing the jog.

Two types of dry lubricants have been tested on the motor pinion and gears in the speed change unit. Teflon coating provided adequate lubrication but tended to flake off during operation. A mixture composed of molybdenum disulfide and graphite in a resin binder also provided adequate lubrication.

Special effort has gone into the design of the coupling required between the actuator output and the drive screw of the tank feed mechanism. The coupling must be very compact because of the limited space and must have a relatively large torque and horsepower capacity. The evolved design is a segmented type coupling with elastomeric inserts and permits some angular and radial misalinement as well as axial motion.

6.3 Cockpit Control Panel

Since the solid agent disseminator functions in a manner quite differently from the liquid agent unit, it has been necessary to design a new control panel for the airplane cockpit. An assembly drawing of this control box is presented in Appendix B. The panel contains two toggle switches and three indicator lights.

When operated, the master switch connects 28 volt d-c airplane power to the disseminator electrical system. This is accomplished by energizing a relay with the switch action; the closing of the relay contacts connects the generator output to the system. The relay and generator are in the disseminator store. The second toggle switch, the arming switch, is provided with a guard. It is impossible to disseminate until this switch is operated. In addition to arming the circuit, closing this switch also fires the squibs that blow out the safety seal in the discharge tube through which the agent is disseminated. The arming switch is wired in series with the master switch.

The top indicator light becomes illuminated when the store generator malfunctions. The center indicator light shows when the discharge valve is open, and the bottom indicator light comes on when dissemination occurs. These indicators are the "push-to-test" type and can be tested after the master switch is closed.

The control box is also used as a junction box through which the disseminator is connected to the armament circuit used to initiate dissemination. The "pickle" switch on the control stick is used for dissemination.

At the end of the reporting period, approximately 50 percent of the components for the control box had been received.

6.4 Aft Actuator Control Panel

This control panel is located within the store just aft of the actuator assembly and is reached through an access door. Its purpose is to provide extra-cockpit control of the actuator and tank drive mechanism positions during servicing. The unit contains a toggle switch to cut out the normal automatic operation of the drive system and permit local manual control. Two pushbutton switches initiate the inward and outward motions of the drive pistons – essentially forward and reverse controls. Two indicator lights signal when the pistons have reached either extreme position. A separate pushbutton switch is used to stop the actuator. Provision is also made for the switch to jog the motor armature for gear meshing if this feature proves to be necessary.

6.5 Dry Nitrogen System

The dry nitrogen system was described in the Eighth Quarterly Progress Report[14]. During the past quarter, effort was devoted to fabrication and procurement of the various components in the gas system. An order was placed with Tavco, Inc. of Santa Monica, California to furnish the pressure vessel with electrical heater and an integral valve and pressure regulator assembly containing the following: high-pressure relief valve, charging valve, manual shutoff valve, solenoid valve, ground checkout valve, pressure regulator, low-pressure relief valve, ground checkout discharge port, and high and low-pressure gages.

Two methods of filling the system with high-pressure nitrogen were investigated: 1) using a compressor to pump nitrogen from 2200 or 2400-psi cylinders into the pressure vessel, and 2) using 6000-psi cylinders to top off after partial filling with standard cylinders. The method of cascading high-pressure nitrogen vessels into the system vessel was considered most practical for filling the first-generation flying model. Two ground carts will

be employed, one cart carrying three manifolded 2400-psi bottles, and the other transporting a 6000-psi bottle. The 2400-psi bottles will be used to fill the system vessel part way and to check out the system. The 6000-psi bottle will be used to top off the system vessel. The combination of the three 2400-psi bottles and the 6000-psi bottle will fully charge three system vessels to 3000 psi, while allowing one minute flow for calibration and checkout of the system.

7. FILLING THE DRY AGENT DISSEMINATING STORE

7.1 Introduction

Ever since the conception of an airborne store for disseminating dry agent material from a compacted state, it has been recognized that filling such a disseminator would present problems quite different from those associated with filling a material that could be handled in a fluid state. As work has progressed on the development of the disseminator itself, a concurrent effort has been devoted to developing a suitable filling procedure. Early in the program it was evident that a method employing an auxiliary loading tube would very likely work. Consequently, a suitable device was designed and fabrication of this loader was completed during this reporting period. Effort has also been expended in an attempt to devise a suitable method of encapsulating the compacted dry agent in a manner that would permit manual loading of the disseminator without requiring the use of auxiliary loading equipment.

At a meeting at Fort Detrick on June 20-21, 1962, the subject of filling the dry agent disseminator was discussed with personnel from the Process Development Division. These people felt that the disseminator design was compatible with the general requirements for filling dry agents. However, they expressed the view that the use of the auxiliary loading device, which was described for them by the GMI engineers, would require rather elaborate plant loading facilities. They recommended compacting the agent in sealed packages that could be loaded into the disseminator by one man. The use of sealed packages would eliminate the need for decontaminating the unit after filling. They already have experience with filling similar packages for other applications. Consequently, an increased effort has been devoted to the search for a packaging material that will provide a sealed container and yet will break up and pass through the disseminator along with the agent without clogging the disaggregator or plugging the discharge orifice.

7.2 Loading Fixture

The loading tube, which has been fabricated for the purpose of placing a charge of compacted dry powder material in the dry agent disseminating store, is shown schematically in Figure 7.1. A photograph of the complete loading fixture comprised of the loading tube, pneumatic controls, and portable, adjustable mount is shown in Figure 7.2. The loading fixture is described in the following paragraphs.

The basic components of the loading device are the outer tube, the inner tube, the piston, and the gas supply system. The piston and the charge of compacted powder are contained within the inner tube. This tube, in turn, is contained by the outer tube. Means are provided for admitting gas under pressure to either the space behind the piston or the space behind the inner tube.

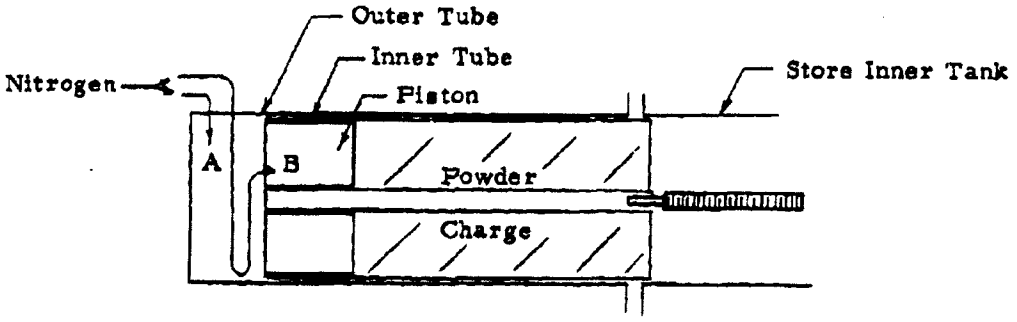

Figure 7.1 Loading Tube Assembly

In operation the loading tube assembly is alined with the store, and the outer tube of the loader is attached to the flange of the store inner tank (Figure 7.1). The inner tube, with powder charge and piston, is pushed into the store by applying gas pressure in space "A" (Figure 7.1). The small central tube is fastened to the inner tube and serves to guide the store drive screw as the powder charge is inserted. The inner tube hits a stop block when the powder face comes within 1/8 inch of the disaggregator blades. Space "A" is then vented to the atmosphere and space "B" is pressurized. Pressure in space "B" forces the piston and consequently the powder charge out of the inner tube, but since the powder face is against the disaggregator disk the powder cannot move and the inner tube retracts into the outer tube leaving the powder charge in the store inner tank.

The tubes and piston are made entirely of aluminum. The outer surfaces of the inner tube, central tube, and piston are Teflon-coated to prevent aluminum from rubbing against aluminum.

Seals are incorporated to prevent gas leakage past the inner tube and the piston. In order to obtain a seal with the required flexibility, rubber tubing of 35 durometer hardness was used in making the large diameter seals. Conventional O-rings are used in the piston to seal on the central tube. Since less than 1 psi pressure is required to move the inner tube into the store, a single seal has proven adequate on the inner tube. However, the 35 psi pressure required to force the powder out of the inner tube necessitated using two seals on the piston. The piston is shown in Figure 7.3. The flat on the piston matches a corresponding surface on the inner tube and provides clearance for a guide mounted on the inside wall of the store.

The pressure line to feed the space behind the piston is a flexible coil of 3/8 inch nylon tubing. The connection inside the outer tube is a swivel so the tubing can swing from a tangential to an axial direction as the inner tube is forced out of the outer tube. The other end of the nylon tube is attached to the back of the inner tube by a quick connect coupling. This coupling is readily accessible when the inner tube is completely withdrawn from the outer tube for the purpose of changing inner tubes.

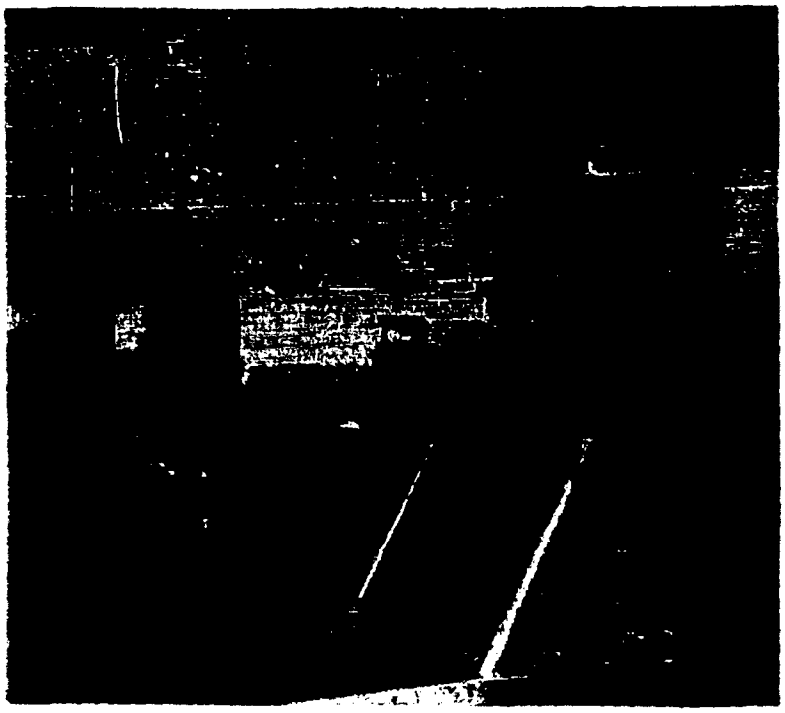

Figure 7.2 Loading Fixture for Use with Prototype Dry Agent Disseminating Store

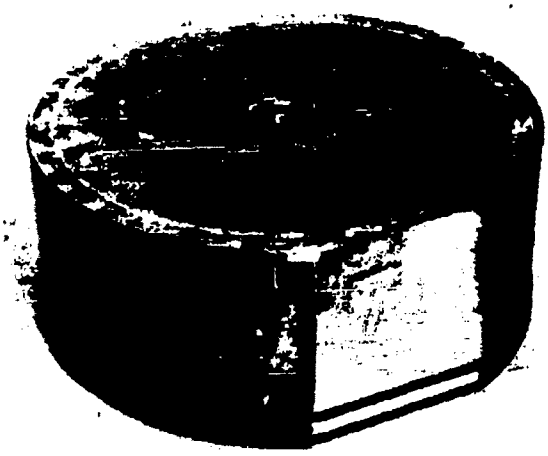

Figure 7.3 Loading Tube Piston

CONFIDENTIAL

3028

A Colson C/U Half-Ton Lifter was purchased and modified to provide a mount for the loading tube and pneumatic controls. The loading tube is supported in a gimbal ring (see Figure 7.2) that can be translated laterally by means of a hand crank. These features facilitate alining the loading tube with the store.

The gimbal is mounted in the lifter arms in such a way that the loading tube can be easily removed as shown in Figure 7.4. This is done so the tube can be positioned vertically for filling, and then the lifter can be moved out of the way.

A pressure regulator, pressure gage, and three-position four-way valve are located on the loading fixture as shown in Figure 7.5. Gas for operating the loader can be supplied to the pressure regulator from either an air compressor or high pressure gas cylinders. The use of dry nitrogen is recommended for use with agents which must be kept dry.

The pressure regulator is required since the two major operations that must be performed require substantially different pressures. The regulator also allows control of the speed of the two operations. Pressure control is most important in the second operation of retracting the inner tube which requires about 6,000 lb force or about 30 psi. As the powder charge moves out of the inner tube, the required force diminishes, and during the course of this operation it is necessary to continually decrease the pressure to maintain a reasonable retracting speed.

7.3 Multiple Sealed Packages

The concept of filling the disseminator with six or eight sealed packages of compacted agent offers many advantages as compared to the use of an auxiliary loading device. Some of these advantages are:

1) The amount of support equipment required would be reduced significantly.

2) The loading plant facilities would be less elaborate.

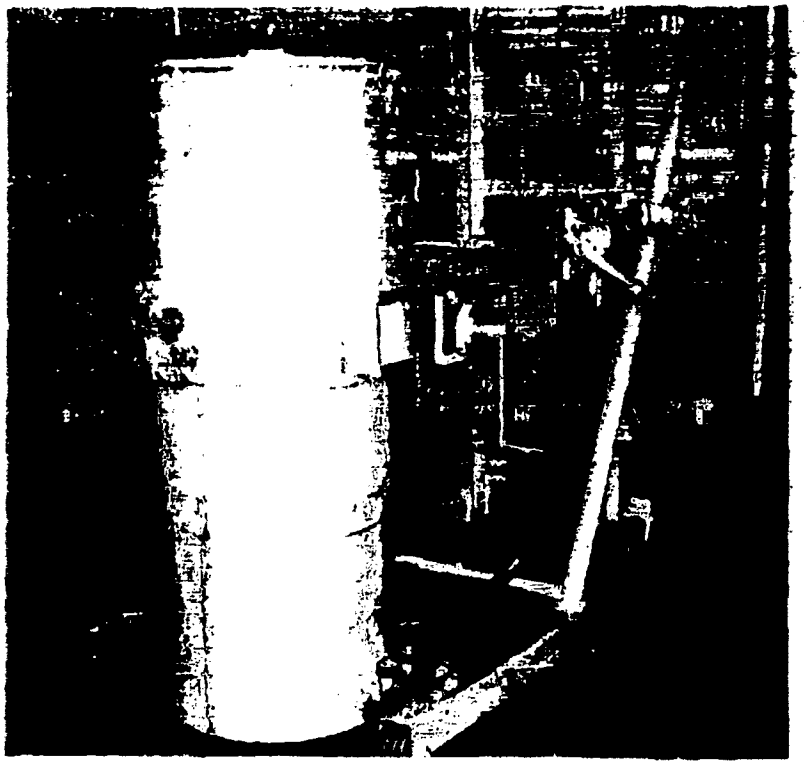

Figure 7.4 Loading Tube Disconnected from Lifter Arms

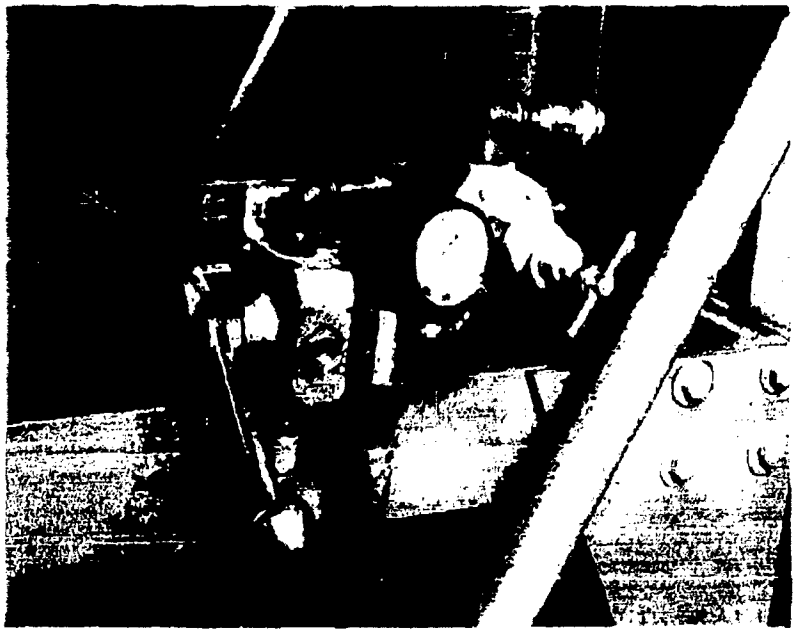

Figure 7.5 Operating Controls for Loading Tube

3) It would be easier to make the filling operations safe for operating personnel.

4) The filling operation could probably be performed quicker.

Unfortunately, the requirement that the package or container must provide a biological seal and yet be capable of being broken up and fed through the disseminator along with the agent presents a formidable problem. Nevertheless, the advantages are attractive enough to warrant the effort that is being expended in an attempt to develop a package meeting the requirements.

In search for a suitable packaging technique three general encapsulating methods are being considered.

The first method is to form a suitable skin by applying the proper substance to the exterior surfaces of a compacted charge of agent. The second is to compact the agent in a container previously prepared from a rigid foam plastic material of the required properties. The third is to compact the agent in a bag made from a plastic film that can be caused to undergo chemical or physical changes inside of the disseminator so the film disintegrates or disperses before the disseminator is operated.

With reference to the first method of encapsulation, two techniques have been tried. One is to spray or paint the substance being investigated directly onto the compacted powder after removing the slug of powder from the mold. The other technique is to apply the encapsulating substance to the interior surface of the mold before introducing the powder and then cause the substance to transfer to the powder after compaction. This latter technique has been accomplished with wax that has been transferred by heating the mold. To date, neither of these techniques has produced a satisfactory encapsulation.

The foam plastic approach uses the blades of the disaggregator within the disseminator to shave off the foam container and the compacted powder simultaneously. The container must be broken into small pieces that will flow through the discharge opening without plugging the hole. To obtain a

gas-tight container, the unicellular type foam was selected. A foam container was fabricated and loaded with compacted talc and then tested in the Second Experimental (disseminator) Unit. The test demonstrated that the unit is capable of digesting a type of foam plastic, but that it will be necessary to incorporate a feature in the disseminator to prevent relatively large pieces of foam from plugging the orifice. The effort on this approach has been toward producing a foam material that was sufficiently strong yet adequately friable. Fortunately, the Chemical Activity of General Mills Central Research Laboratory has had considerable experience in the development of foam plastics. With their cooperation in this particular investigation, we believe some progress was made toward developing a suitable encapsulating material.

The plastic film approach to encapsulation considered the use of a film that would have poor resistance to certain environmental conditions. For instance, if a quantity of agent were compacted into a bag made of film, sealed, and placed in the disseminator, which in turn was sealed, a change of temperature or a change of gas within the disseminator might deteriorate the film so it would crumble or vaporize. Accordingly, a survey of possible films was conducted. The consensus pointed to polypropylene film brought to low temperature (-20°F) at which time the film should become brittle enough to fracture into small pieces. However, samples of polypropylene film which were subjected to cold box tests down to -50°F and -109°F (dry ice temperature) did not react as desired. Other possibilities in this area of disintegrating films are currently being investigated.

8. FLIGHT TESTING OF LIQUID AGENT DISSEMINATING STORE

During the period from August 13 to 29, 1962, GMI provided technical assistance in connection with flight testing of the GMI liquid agent disseminating store by the BW/CW Weapons Group at Eglin Air Force Base, Florida. These tests were conducted to investigate the airworthiness of the store and to evaluate performance of the F-105 and F-100D airplanes with the GMI disseminating store attached. A report covering this test project is being prepared by the BW/CW Weapons Group. On the basis of the verbal reports of the test pilots and the personal observations of GMI representatives, it can be said that the store functioned entirely satisfactorily and the airplanes performed normally with the store attached.

In order to establish the maximum performance conditions for the F-105 airplane to be used in the flight tests, the GMI store was shipped to the Republic Aviation Corporation at Farmingdale, Long Island, New York. Here the store was mounted on an F-105 and flutter and vibration analysis and static stiffness measurements were made. These data were then used to compute the allowable flight conditions for the F-105 airplane with the GMI store attached. This work was accomplished in late July and early August. Upon completion of the measurements at Farmingdale, the GMI store was shipped to Eglin Air Force Base for flight testing.

Two flights were made with the disseminator on the F-105 airplane. For the first flight the unit was mounted at the left inboard wing station. The centerline station was used on the second flight. The airplane was flown at 400 knots indicated air speed and manuevered at altitudes of 5,000 and 30,000 feet. The disseminator was filled with dyed water that was disseminated at 200 feet. The dissemination was photographed from an F-100D chase plane. Personnel in the chase plane reported that the aerosol stream was separated from the bottom aft of the airplane by a space of approximately one foot.

One flight was made with the disseminator mounted on the inboard wing station of an F-100D airplane. This airplane was flown at 300 knots indicated air speed and maneuvered at altitudes of 5, 000 and 30, 000 feet. Dissemination was made at 200 feet. This flight was also covered by photography from a chase plane.

The disseminator was filled with water containing methylene blue dye so the airplanes could be examined for contamination after each flight. The F-105 was found to be free of contamination after the first flight, but on the second flight a small amount of dye was found on the lower ventril (fin). No contamination was found upon examining the F-100D after operating the disseminator on this airplane.

9. SUMMARY AND CONCLUSIONS

Work has progressed on our broad program of research and development on the dissemination of solid and liquid BW agents. Each area of work which is summarized in the following paragraphs is discussed in detail in the section referenced at the end of the paragraph.

Applied stresses and energies required for compaction of powders have been successfully measured using an improved piston-cylinder device in an Instron test machine. Values for the constants k and m in the equation $\sigma = k \cdot p^m$ have been determined for talc, saccharin, and cornstarch. Previously reported difficulties with the triaxial shear test have been overcome by using a sample preparation procedure that does not require the use of the rubber membrane which prevented natural shear failure of the sample. Effort has been directed toward determination of the tensile shear strength of powders as well as compressive shear strength using the triaxial technique. The bulk tensile strength of saccharin, cornstarch, powdered milk, Sm, and talc has been measured as a function of compressive load and distance from the piston to the fracture plane. The bulk density of talc (Mistron Vapor) has been determined as a function of compressive load and distance from the piston (Section 2).

Aerosol decay has been investigated for three humidity conditions – less than 5 percent, approximately 50 percent, and greater than 95 percent – for five powders. Saccharin, cornstarch, and powdered milk exhibited decay rates that increased monotonically with increasing humidity; whereas, talc and powdered sugar exhibited decay rates that were higher for the two extreme humidity conditions than for the intermediate condition. It has been demonstrated experimentally that high frequency fluctuations on the light-scattering records have significance and are not merely system noise. A formula for the fluctuation has been derived mathematically. A new swirl disperser has been used to introduce powders into the aerosol decay chamber, and the aerosols thus produced were found to be more stable than those obtained with the rupturing-diaphram disperser (Section 3).

The high-speed wind tunnel dissemination studies have shown that the maximum bulk density to which Sm can be compacted and yet be aerosolized efficiently by the aerodynamic breakup mechanism is about 0.58 g/cm^3. This limiting density was the same for both Mach numbers 0.5 and 0.8. It is believed that any dependence upon Mach number is far overshadowed by the rapidly increasing strength of the compacted Sm as the bulk density is raised above this value. Tests of compacted Sm which had been stored at a low temperature for ten weeks indicate that when compacted material is to be stored for long periods, the maximum allowable density will be lowered to about 0.55 g/cm^3. In making this determination a new technique was used wherein the change in concentration of the fine portion of the aerosol was measured. A wind tunnel study of the ejection tube shroud using a scale model has produced a design which is expected to eliminate contamination of the store (Section 4).

A powder flow rate of 53 lb/min has been achieved with the full-scale experimental feeder using talc compacted to a density of 0.65 g/cm^3. The second experimental unit, which is a prototype of the airborne disseminator, has been completed and this unit has been operated with uncompacted talc. A sample of talc initially compacted to 0.55 g/cm^3 has been collected from the discharge of the full-scale feeder and subsequently disseminated satisfactorily in the high-speed wind tunnel at Mach number 0.5 using the GMI-3 fixture (Section 5).

Design and fabrication of the first-generation dry agent disseminating store progressed from the design study stage to actual fabrication and procurement of the various components. An order has been placed with the Fletcher Aviation Company of El Monte, California for fabrication of the main structural parts of the store. The speed-selection portion of the rotary actuator assembly has been tested. A cockpit control panel has been designed. The high-pressure vessel and associated valves and pressure regulator for the dry nitrogen system have been ordered from Tavco, Inc. of Santa Monica, California, who are specialists in this type of equipment. The cascading method, using 6000-psi nitrogen cylinders for "topping-off", has been selected for filling the nitrogen system (Section 6).

A loading fixture has been fabricated for the purpose of inserting charges of compacted powder into the dry agent disseminating store. The material is first compacted into a cylindrical tube in the loading fixture and is then transferred to the store. As an alternate method of loading, an investigation has been started with the objective of perfecting a method of encapsulating quantities of compacted agent small enough to permit loading the store without the aid of special equipment. The problem is to find an encapsulating material which can be digested by the disseminator (Section 7).

In August the GMI liquid agent disseminating store was successfully flight tested on an F-105 and an F-100D airplane at Eglin Air Force Base. These tests were conducted by the BW/CW Weapons Group at Eglin to determine airworthiness of the store. The tests also demonstrated that there is no contamination of the airplanes when the store is mounted at a wing station. There was minor contamination of the lower ventril of the F-105 when the store was mounted on the centerline station (Section 8).

10. REFERENCES

1) General Mills, Inc. Electronics Div. Report No. 2322. Dissemination of solid and liquid BW agents (U), by G. R. Whitnah et al. Contract DA-18-064-CML-2745. Eighth Quarterly Progress Report (August 22, 1962). Confidential.

2) ----. Report No. 2300. Dissemination of solid and liquid BW Agents (U), by G. R. Whitnah et al. Contract DA-18-064-CML-2745. Seventh Quarterly Progress Report (June 22, 1962). Confidential.

3) ----. Report No. 2322, op. cit., pp. 3-2 and 3-3.

4) Ibid. p. 3-4.

5) Ibid. p. 3-6.

6) Ibid. p. 3-20.

7) Ibid. p. 7-2.

8) General Mills, Inc. Electronics Div. Report No. 2216. Dissemination of solid and liquid BW agents (U), by G. R. Whitnah et al. Contract DA-18-064-CML-2745. Fourth Quarterly Progress Report (August 10, 1961). (AD 325, 247). pp. 62-72. Confidential.

9) ----. Report No. 2264. Dissemination of solid and liquid BW Agents (U), by G. R. Whitnah et al. Contract DA-18-064-CML-2745. Sixth Quarterly Progress Report (Feb. 23, 1962). pp. 5-6 thru 5-19. Confidential.

10) ----. Report No. 2322, op. cit., pp. 7-13 and 7-14.

11) Ibid. pp. 6-1 thru 6-4.

12) General Mills, Inc. Report No. 2300, op. cit., pp. 6-2 thru 6-7.

13) ----. Report No. 2322, op. cit., pp. 7-1 thru 7-12.

14) Ibid. pp. 7-4 thru 7-7.

APPENDIX A

LAYOUT,
EJECTION TUBE SHROUD

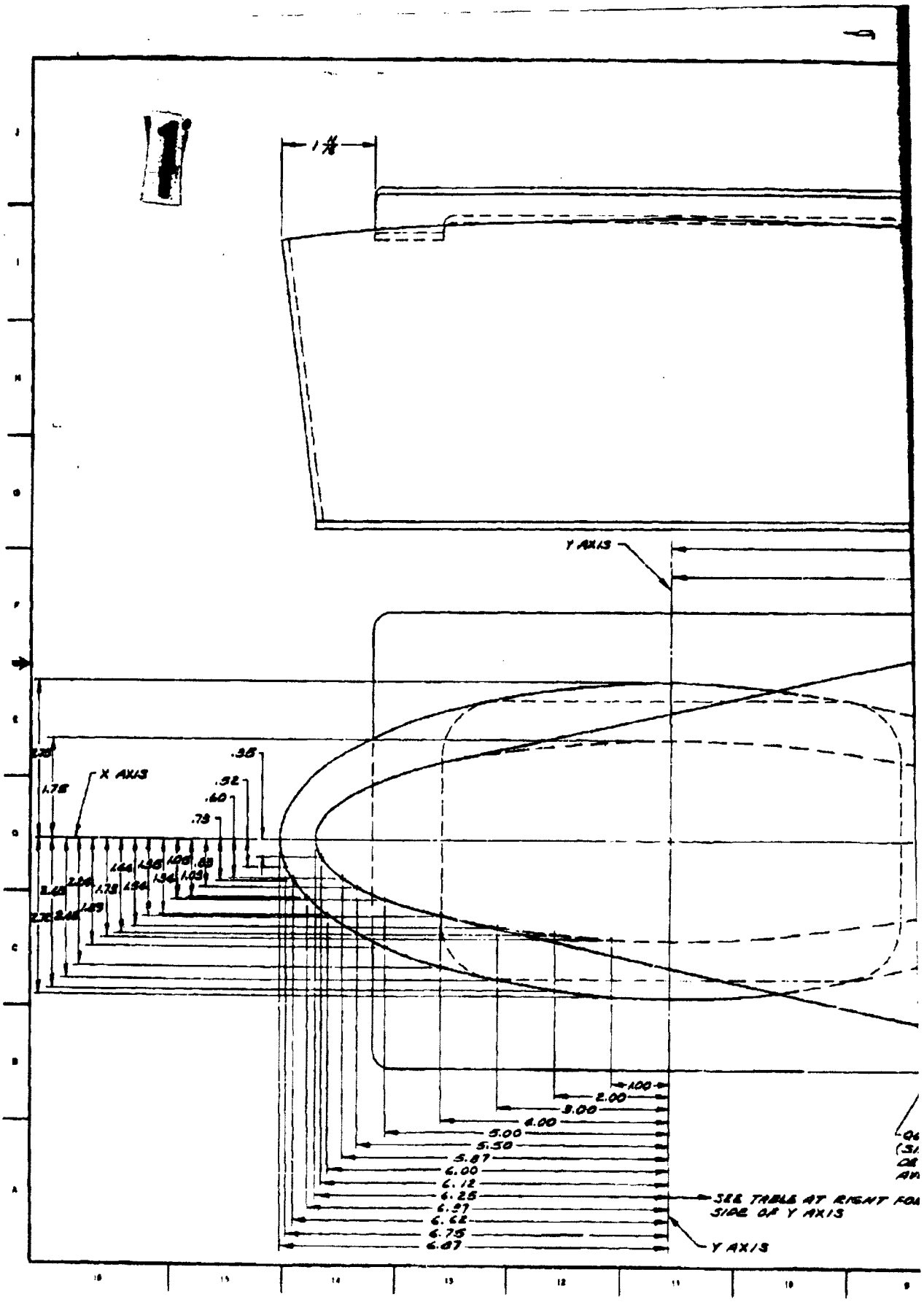

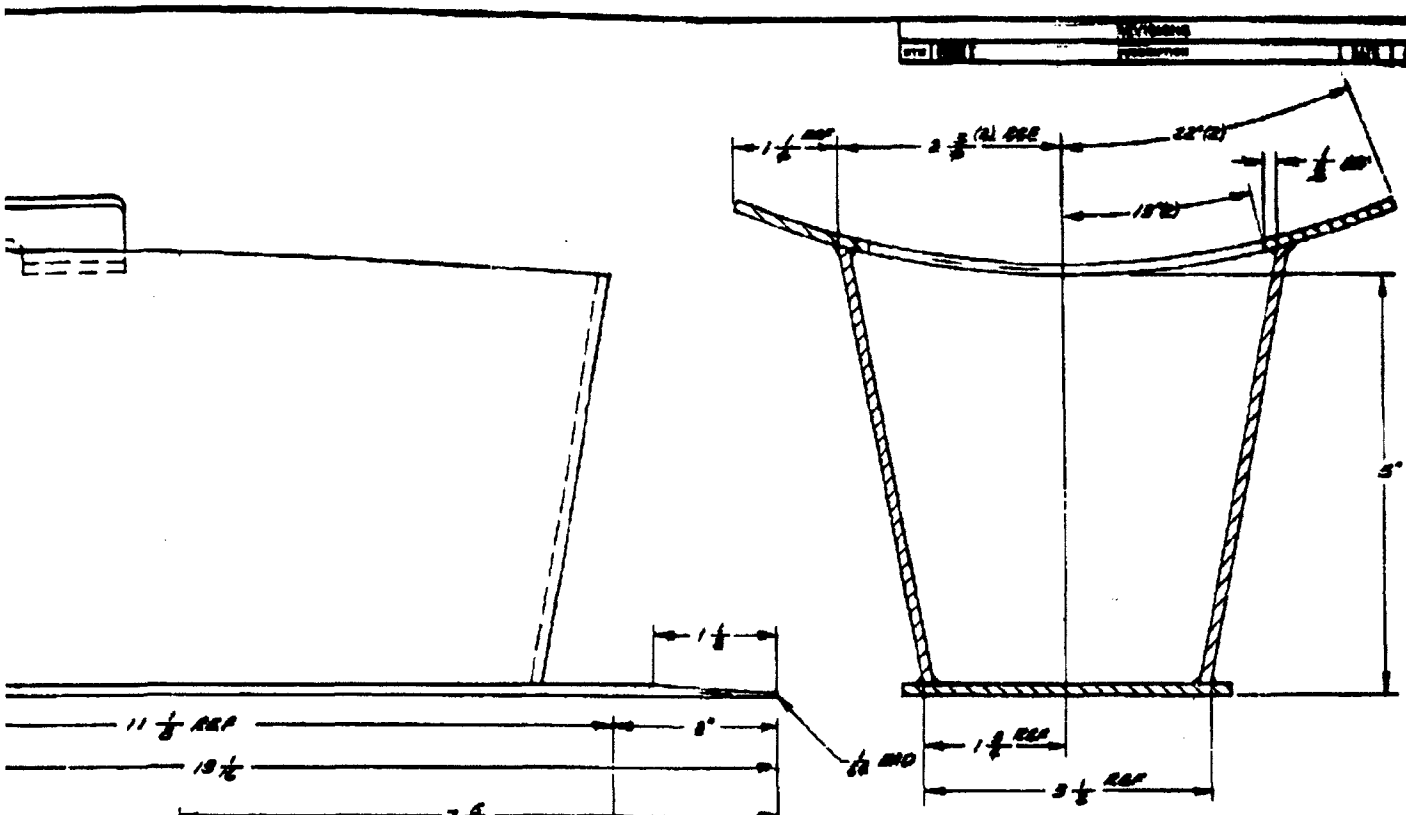

CURVE COORDINATES

X	Y	Y'
1.00	2.78	1.78
2.00	2.68	1.66
3.00	2.48	1.64
4.00	2.24	1.58
5.00	1.98	1.80
6.00	1.70	1.00
7.00	1.39	.78
8.00	1.06	.56
9.00	.72	.31
10.25	.30	.00
11.12	.00	—

CHROMATE PER MIL-C-5541 (GMI 63-P21)	+1/32 ±.03 -1/32 -.03	8-27-62	ELECTRONICS DIVISION
	AL ALLOY, 6061-T6 TEMPER T6, .125 THICK PER QQ-A-327b		LAYOUT, EJECTION TUBE SHROUD (REVISED)
			CODE IDENT NO 98731 · SIZE D · SK 29100-795
			SCALE FULL · SHEET

SK29100-795

APPENDIX B

CONTROL BOX

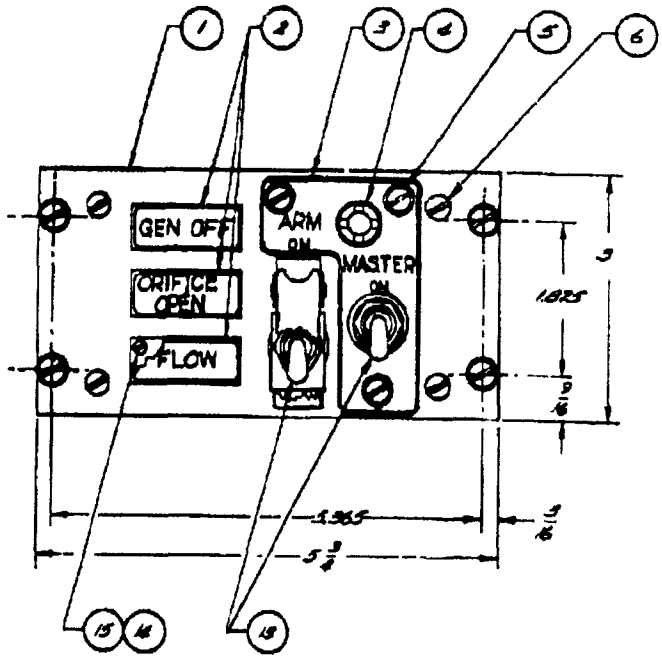

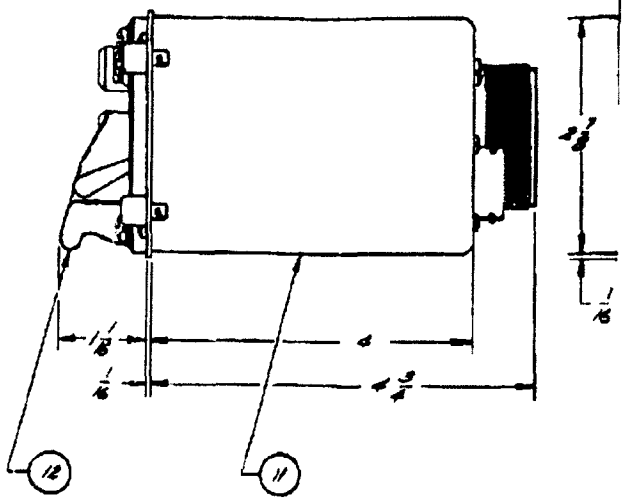

▷ SCREW HEADS MUST HAVE FLAT BLACK FINISH

2 ALL DIMENSIONS ARE FOR REFERENCE ONLY

▷ PART NUMBERS SHOWN IS VENDORS PART NUMBERS

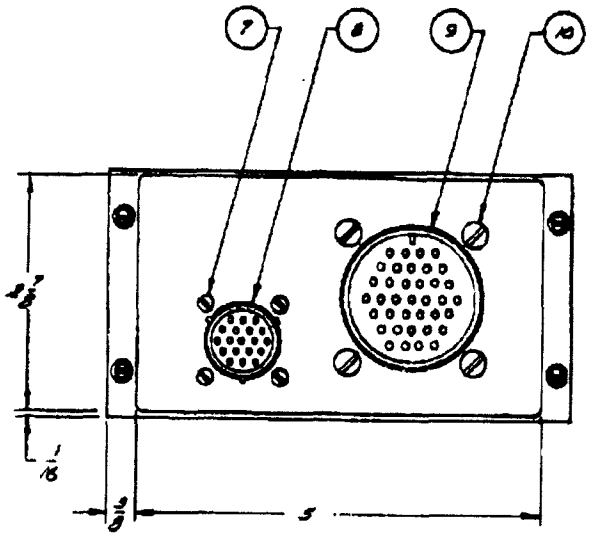

15	6	[illegible]	[illegible]
14	6	MS 35299-44	SCREW - MACH., FLAT HD, [illegible]
13	2	MS 35058-22	TOGGLE SWITCH, SASH
12	1	MS 25224-1	GUARD - TOGGLE SWITCH
11	1	SK 2900-358	COVER - CONTROL BOX
10	4	MS 35299-49	SCREW - MACH., FLAT HD, 6-32 NC-3A x 7/16 LG
9	1	SK 2900-909-5	CONNECTOR - ELECTRICAL, RECEPTACLE
8	1	SK 2900-459	CONNECTOR - ELECTRICAL, RECEPTACLE
7	4	MS 35239-15	SCREW - MACH., PAN HD, 8-32 NC-3A x 3/8 LG
6	4	MS 35225-31	SCREW - MACH., PAN HD, 8-32 NC-3A x 3/8 LG
5	3	MS 35289-29	SCREW - MACH., PAN HD, 6-32 NC-3A x 7/16 LG
4	1	IT 150-5030-67	PANEL LIGHT (DARKLIGHT)
3	1	SK 2900-807	CONTROL PANEL
2	3	L 2900-444	INDICATOR LIGHT (DARKLIGHT)
1	1	SK 2900-808	PANEL - COMPONENT MOUNTING
ITEM	QTY	PART NUMBER	DESCRIPTION

LIST OF MATERIALS

UNLESS OTHERWISE SPECIFIED DIMENSIONS ARE IN INCHES TOLERANCES ON FRACTIONS DECIMALS ANGLES

ORIGINAL DATE OF DRAWING 10-11-62

DRAWN [illegible] CHECKED ENGINEER APPROVED

HEAT TREATMENT MATERIAL

ELECTRONICS DIVISION MINNEAPOLIS MINNESOTA

CONTROL BOX

CODE IDENT NO 98731 SIZE D SK 2900-909

SCALE 1/1 SHEET

DEPARTMENT OF DEFENSE
WASHINGTON HEADQUARTERS SERVICES
1155 DEFENSE PENTAGON
WASHINGTON, DC 20301-1155

MEMORANDUM FOR DEFENSE TECHNICAL INFORMATION CENTER
(ATTN: WILLIAM B. BUSH)
8725 JOHN J. KINGMAN ROAD, STE 0944
FT. BELVIOR, VA 22060-6218

AUG 1 2013

SUBJECT: OSD MDR Cases 12-M-3144 through 12-M-3156

At the request of [redacted], we have conducted a Mandatory Declassification Review of the documents in the above referenced cases on the attached Compact Disc (CD) under the provisions of Executive Order 13526, section 3.5, for public release. We have declassified the documents in full. We have attached a copy of our response to the requester. If you have any questions, please contact Ms. Luz Ortiz by phone at 571-372-0478 or by e-mail at luz.ortiz@whs.mil, luz.ortiz@osd.smil.mil, or luz.ortiz@osdj.ic.gov.

Robert Storer

Robert Storer
Chief, Records and Declassification Division

Attachments:
1. MDR request w/ document list
2. OSD response letter
3. CD (U)

April 26, 2012

[redacted]

Department of Defense
Directorate for Freedom of Information and Security Review
Room 2C757
1155 Defense Pentagon
Washington, D.C. 20301-1155

Sir:

I am requesting under the Mandatory Declassification Review provisions of Executive Order 13291, copies of the following documents. I have tried several times to acquire them through DTIC, but the sites stated they are not available.

I am conducting research into the previous methods used to disseminate biological agents. Many source I use to have access to have been deleted from the internet. On numerous occasions I have been informed that formerly classified information that was declassified, have now become classified again (since 911). My attempts to locate such Executive Orders, regulations, laws, or other changes to this question have not successful nor revealed a specific source. As such I would appreciate any information you can shed on this question.

Documents requested.

AD 348405, Dissemination of Solid and Liquid BW (Biological Warfare)Agents Quarterly 12-M-3144
Progress Report Number 14, 4 Sept - 4 Dec 1963, G. R. Whitnah, February 1964, General Mills Report number 2512, General Mills, Inc., Minneapolis, MN, Contract number DA 18064 CML 2745, 102 pages. Prepared for U.S. Army Biological Laboratories, Fort Detrick, Maryland. Approved by S.P. Jones, Director of Aerospace Research at General Mills. Project No. 82408. General Mills Aerospace Research Division, 2295 Walnut Street, St. Paul 13,Minnesota.
AD 346751, Dissemination of Solid and Liquid BW (Biological Warfare) Agents, Quarterly 12-M-3145
Progress Report Number 12, March 4 - June 4, 1963, G. R. Whitnah, July 1963, General Mills Report number 2411, General Mills, Inc., Minneapolis, MN, Contract number DA 18064 CML 2745. 184 pages. Approved by S.P. Jones, Director of Aerospace Research at General Mills. Project No. 82408. General Mills Aerospace Research Division, 2295 Walnut Street, St. Paul 13, Minnesota.
AD 346750, Dissemination of Solid and Liquid BW (Biological Warfare) Agents, Quarterly 12-M-3146
Progress Report Number 13, 4 June - 4 Sept 1962, G.R. Whitnah, October 1963, General Mills

Report number 2451, General Mills, Inc., Minneapolis, MN, Contract Number DA 18064 CML 2745. 19 pages (?)

AD 332404, Dissemination of Solid and Liquid BW (Biological Warfare) Agents, Quarterly 12-M-3147
Progress Report Number 7, Dec. 4, 1961 - March 4, 1962, by G.R.Whitnah, February 1963, General Mills Report Number 2373, General Mills, Inc., Minneapolis, MN, Contract Number DA 18064 CML 2745. 123 pages.

AD 333298, Dissemination of Solid and Liquid BW (Biological Warfare)Agents, Quarterly 12-M-3148
Progress Report Number 9, June 4, 1962 - Sept. 4, 1962. by G.R. Whitnah, October 1962, General Mills Report Number 2344, General Mills, Inc., Minneapolis, MN, Contract Number DA 18064 CML 2745. 130 (or 150) pages.

AD 332405, Dissemination of Solid and Liquid BW (Biological Warfare) Agents, Quarterly 12-M-3149
Progress Report Number 8, Period March 4, 1962 - June 4, 1962. G.R. Whitnah, August 1962, General Mills Report Number 2322, General Mills, Inc., Minneapolis, MN, Contract Number DA 18064 CML 2745. 198 pages.

AD 329067, Dissemination of Solid and Liquid BW (Biological Warfare) Agents, Quarterly 12-M-3150
Progress Report Number Six, G.R. Whitnah, February 1962, General Mills Report Number 2264, General Mills, Inc., Minneapolis, MN, Contract Number DA 18064 CML 2745. 103 pages. Approved by S.P. Jones, Manager, Materials and Mechanics Research, General Mills Research and Development Office, 2003 East Hennepin Avenue, Minneapolis 13, Minnesota.

AD 327072, Dissemination of Solid and Liquid BW (Biological Warfare) Agents, Quarterly 12-M-3151
Progress Report Number Five, 4 June - 4 Sept 1961. by G.R.Whitnah, November 1961, General Mills Report Number 2249, General Mills, Inc., Minneapolis, MN, Contract Number DA 18064 CML 2745.

AD 325247, Dissemination of Solid and Liquid BW (Biological Warfare) Agents, Quarterly 12-M-3152
Progress Report Number 4, 4 March - 4 June 1961, by J.E. Upton for G.R. Whitnah, Project Manager. February 1963, General Mills Report Number 2216, General Mills, Inc., Minneapolis, MN, Contract Number DA 18064 CML 2745. General Mills Electronics Group, Research Dept., 2003 East Hennepin Avenue, Minneapolis 13, Minnesota. 225 pages.

AD 324746, Dissemination of Solid and Liquid BW (Biological Warfare) Agents, Progress 12-M-3153
Report 3 Juen - 3 Sept. 1960. by G.R. Whitnah, October 1960, General Mills Report Number 2125, General Mills, Inc., Minneapolis, MN, Contract Number DA 18064 CML 2745. 78 pages

AD 323599, Dissemination of Solid and Liquid BW (Biological Warfare) Agents, Quarterly 12-M-3154
Progress Report Number 2, for period 4 Sept - 4 Dec 1960, by G.R. Whitnah, February 1961, General Mills Report Number 2161, General Mills, Inc., Minneapolis, MN, Contract Number DA 18064 CML 2745. 90 pages? Mechanical Division of General Mills, Inc., Research Department, 2003 East Hennepin Avenue, Minneapolis 13, Minnesota.

AD 323598, Dissemination of Solid and Liquid BW (Biological Warfare) Agents, Quarterly Progress Report, for period 4 Dec. 1960 - 4 March 1961, by G.R. Whitnah, May 1961, General Mills Report Number 2200, General Mills, Inc., Minneapolis, MN, Contract Number DA 18064 CML 2745. 95 pages. 12-M-3155

AD 337635, Dissemination of Solid and Liquid BW (Biological Warfare) Agents, Quarterly Progress Report No. 10, period Sept. 4, 1962 - Dec. 4, 1962. G.R. Whitnah, Project Manager, Approved by S.P. Jones, Aerospace Research, February 1963. 247 pages. 12-M-3156

Sincerely